EXPERIMENTALLY DEFORMED CALCITE-CEMENTED SANDSTONES

THE NATURE OF DEFORMATION IN EXPERIMENTALLY DEFORMED CALCITE-CEMENTED SANDSTONES

By

DOUGLAS HENRY UNDERHILL, B.A., M.Sc.

A Thesis

Submitted to the School of Graduate Studies

in Partial Fulfillment of the Requirements

for the Degree

Doctor of Philosophy

McMaster University

May 1972

DOCTOR OF PHILOSOPHY (1972)
(Geology)

McMaster University
Hamilton, Ontario

TITLE: The Nature of Deformation in Experimentally Deformed Calcite-cemented Sandstones

AUTHOR: Douglas Henry Underhill, B.A. (University of Connecticut)
M.Sc. (McGill University)

SUPERVISOR: Dr. Paul M. Clifford

NUMBER OF PAGES: 198

SCOPE AND CONTENTS: An experimental study has been carried out in order to determine the nature of deformation in calcite-cemented sandstones. This work should provide a basis to understand the mechanical behavior of other rock materials which consist of more than one mineral component. Specimens were shortened 2.1 - 19.8 percent, at room temperature, under 1 - 2600 bars confining pressure and at a strain rate of the order of 10^{-4} per second. Specimen strengths, and the development of strain at the macroscopic and microscopic scales were systematically evaluated. The high strength of the rock and the deformational features which develop are shown to result from the mechanical interaction between the weak and/or ductile calcite matrix and the strong, brittle sand grains.

ACKNOWLEDGEMENTS

I would like to thank Dr. P.M. Clifford who not only suggested the research problem, but also provided helpful guidance throughout the work. The efforts of Mr. R.J. Rector, who worked together with the writer to develop the experimental facilities and techniques used in the investigation, contributed much to the completion of the project. Sincere thanks also go to Dr. J.D. Embury who introduced the writer to many concepts used in mechanical metallurgy and through discussion and suggestions helped the writer to apply these concepts in the present work. Drs. B.J. Burley and H.P. Schwartz read the manuscript and offered suggestions. Many other people including the technical staff, professors and students at McMaster University offered aid and suggestions which were instrumental in the completion of this work. My wife, Lin, typed the manuscript and provided technical and moral support throughout the endeavor.

The indispensible financial support was provided by the Mines Branch of the Department of Energy, Mines and Resources(1966-1971), the National Research Council(1966-1971) and bursaries from the Bickell Foundation.

ABSTRACT

Stress-shortening data and the micro- and macro-fabrics of experimentally deformed calcite-cemented graywacke were analyzed in order to understand the nature of deformation in calcite-cemented rocks. Forty-four room temperature triaxial experiments were conducted on the Blairmore sandstone in the range of 2.1 - 19.8 percent shortening, 1 - 2600 bars confining pressure, at strain rates on the order of 10^{-4}/second. Under these condition, the normal transition from longitudinal fracture, at low confining pressure, to limited homogeneous flow, at high confining pressure is observed. The strength $(\sigma_1 - \sigma_3)$ increases from 2.3 kilobars(kb) at 1 kb confining pressure(cp), to 5.9 kb at 2.6 kb cp. At low confining pressures, deformation takes place primarily by brittle fracture of the calcite. At high confining pressures, the calcite deforms primarily by twinning, and the sand grains deform by fracturing parallel to σ_1. The transition in deformational behavior of this rock is similar to the transition observed in orthocalcite rocks. However, in contrast to orthocalcite rocks, (1) strength is enhanced, (2) ductility is markedly reduced, and (3) the brittle-ductile transition is suppressed to much higher confining pressures. The behavior of this rock is analyzed by considering a two-phase model material consisting of a dispersion of strong, brittle particles within a weak and/or ductile matrix. Principles developed through the study of particulate reinforced composite engineering materials indicate that the mechanical behavior of these materials is dependent upon the mechanical interaction of the two phases. The sand grains act to constrain flow of the ductile matrix. Concurrently,

plastic deformation within the matrix results in the development of stress concentrations within the nearly rigid sand grains. These enhanced stresses may result in the initiation and propagation of fractures within the sand grains. Propagation of the fractures is parallel to the maximum principal stress and the fractures characteristicly develop in this manner. Although the inherent physical properties of the individual phases determine the strain development within the individual phases, it is the interaction of the two phases which determines the unique behavior of the composite material. This behavior in turn controls the strength of the material and exerts an important influence on the development of the deformation fabric. The two-phase model not only provides insight into the behavior of calcite-cemented sandstones and other analogous rocks, but also makes it possible to predict how these rocks will behave when factors such as temperature and strain rate are permitted to vary.

TABLE OF CONTENTS

LIST OF FIGURES

LIST OF PLATES

LIST OF TABLES

Chapter 1

INTRODUCTION

General Statement

The experimental study of rock deformation in the laboratory provides a detailed understanding of the fracture and plasticity of rocks and can ultimately be related to field studies in an attempt to understand the behavior of materials within the earth's interior. By varying factors such as the imposed rate of deformation, temperature and state of stress, the macroscopic behavior of materials may be classified. In addition, study of the microstructural features such as crystal structure, grain size, texture and fabric reveal the detailed processes of deformation at the atomic level. It is significant that many of the relationships which have been established through experimental work can also be recognized in the natural environment.

To date, the greatest geologic interest has focused on the brittle and ductile behavior of single phase materials such as limestone and quartzite. There have been few detailed investigations of the mechanisms of deformation of multiphase rocks and the influence of microstructural variables in these systems.

In contrast to rock deformation studies, however, much research into the deformation of multiphase systems has been carried out in the engineering sciences. Theoretical and experimental studies of multiphase materials have been performed for many metallic and ceramic systems in which the microstructural variables are well known.

After considerable experience in the investigation of rock deformation, Griggs and co-workers(1960, p. 104) concluded that their "...(experiemental) results with rocks and rock-forming minerals without exception follow the empirical laws developed in the study of metals. This implies that the vast body of data collected in experiments on metals may be applied in some detail to the interpretation of deformed rocks..." It is therefore not unreasonable to expect that the deformational behavior of multiphase rock materials may be understood in terms of the principles developed during the investigations of multiphase metallic and ceramic systems.

Purpose and Scope of the Investigation

The purpose of the present study was to analyze the deformational behavior of a calcite-cemented sandstone. The analysis of this multiphase rock is based on the relatively well-established deformational properties of the individual phases. The present study deals with both the macroscopic and microscopic aspects of deformation in an attempt to delineate the basic conditions governing both the flow and fracture of calcite-cemented sandstone.

During the period 1966-1969, the investigation required the writer, in conjunction with P.M. Clifford and R.J. Rector, to develop a suitable triaxial testing apparatus, test procedures and data processing methods. Using the techniques developed, a study was carried out to investigate the deformational behavior of calcite-cemented Blairmore sandstone.

Approach Used in the Investigation

Initially, it was hoped that a model two-phase sandstone could be developed. This would permit the experimental control of such variables

as volume fraction and grain size and would facilitate the systematic determination of the effect of these variables. Although some progress was made using sand with a halite matrix, this approach was abandoned because of the lack of sufficient time to develop the necessary techniques.

Subsequently, a naturally occurring calcite-cemented sandstone was selected as the experimental material. Friedman's work(1963) on similar calcite-cemented rocks provides a thorough description of the deformational features and their relation to the operative stress system in these rocks. The present investigation was designed to extend the knowledge of the deformational behavior by systematically observing how the rock deforms over a range of confining pressures.

All together, 44 room temperature triaxial compression experiments were conducted by the writer in the range of 1 - 2600 bars confining pressure, 2.14 - 19.82 percent total shortening, at strain rates on the order of 10^{-4} per second(Appendix B).

Various theoretical analyses are reviewed in order to account for the well-known empirical observation that increasing confining pressure increases strength as well as enhancing ductile behavior. Stress concentrations are considered in order to explain how extension fractures may develop within a material upon which all of the applied principal stresses are compressive. The interpretation of the microfabric is based on the principles of micromechanics and the deformational behavior of composite materials. This is in turn related to the strength and macroscopic behavior of the rock.

Chapter 2

REVIEW OF LITERATURE

Factors Controlling the Deformational Behavior of Rock Materials

Experimental rock deformation studies were initiated by Adams and his associates about seventy years ago. Since that time, numerous experiments have been performed in order to define the fundamental deformational behavior of rock materials. The variables which affect this deformation have in turn been determined.

The factors which affect deformation may be divided into two main types. First, there are the inherent properties of the materials which determine the microscopic aspects of deformation and include the structure, composition, and orientation. The second may be termed the external or macroscopic variables which include the state of stress under which deformation occurs, the imposed strain rate and temperature of deformation.

In assessing the results of any experimental study, it is necessary to consider the effects which result solely from the experimental techniques themselves. This is particularly important in relating the experimental aspects of rock deformation to field observations.

In this section, we will review the more important aspects of deformation. Emphasis will be placed on the deformational behavior of calcite and quartz, at room temperature and under "dry" conditions.

The Dependence of Deformational Behavior Upon Material Properties

The ultimate control of strength and deformational behavior depends upon the mechanical properties of the material itself. A rock

is a polycrystalline aggregate consisting of one or more minerals and the mechanical behavior depends upon the properties of the individual mineral phases and their interaction. The mechanical role of porosity or cracks must also be considered.

The mechanical behavior of the individual phases is determined by the atomic forces of chemical bonding. Brittle strength is then determined by the atomic forces which resist the separation of the solid into two parts(Kelly, 1966). Plastic deformation is also a function of chemical bonding. "Restrictions on bond bending, relevant to dislocation generation and mobility generally increase with increasing covalency. Stronger and more directional bond types resist dislocation motion"(Cagniglia, 1966).

The anisotropic mechanical behavior of minerals is then determined by the variation of bond strength and character along different directions within the crystal.

Additional factors which must be considered for a polycrystal are the dimensions of the individual grains, the nature of grain boundaries and the presence of any porosity or cracks. The fracture strength has been shown to depend on grain size through the Petch relation, $\sigma_{fracture} = kd^{-\frac{1}{2}}$, where k is a constant and d is the grain diameter. This has been shown for limestone(Brace, 1961, 1964), anhydrite(Skinner, 1959) and granite(Houpert, 1966). In each case, the strength is thought to be determined by Griffith flaws which are apparently equal to the grain diameter. Although little is known about the strength of grain boundaries in rock materials, some work has been carried out in order to determine whether fracture in rocks

tends to be intergranular or intragranular(Willard & McWilliams, 1969).

The presence of porosity and cracks is known to lower the strength or rocks(Balakrishma, 1963; Rector, 1970). This is thought to reflect the decrease in effective load bearing cross section, as well as the increase in stresses resulting from stress concentrations in the vicinity of the discontinuities.

Mechanical anisotropy such as a planar fabric or preferred crystallographic orientation have been shown to have a great effect on the strength and deformational behavior of rocks. The role of planar anisotropy is treated by several workers(Donath, 1961, 1964; Jaeger, 1960; McLamore & Gray, 1967). Anisotropy of crystallographic orientation has been shown to have a profound effect on both the strength and ductility of the Yule marble. Strength differences of up to 40 percent are observed between specimens deformed parallel and normal to the rock fabric(Handin & Hager, 1957). This can be related to the anisotropic mechanical behavior of the calcite.

Some work has also been carried out which demonstrates that the state of prestrain has a significant effect on rock strength and behavior. Limestone subjected to a prestrain is found to have a reduced strength under uniaxial test conditions(Donath, 1968). Under confining pressure, the rock is found to have an increased yield strength and an altered stress-strain curve as compared with the undeformed material(Donath, 1968, 1970).

It should be obvious from this brief review that there are many factors which contribute to the mechanical behavior of even a single phase rock such as limestone.

Modes of Deformation

The deformational behavior of solids can be understood in terms of competition between the various modes of local fracture and of shape change. Fracture results in inhomogeneous deformation and is dependent upon local tensile stress development. Shape change or flow is the product of shear strains which result from shear stresses and leads ideally to the homogeneous distribution of strain.

The deformation of rocks can be understood in terms of four fundamental modes; extension fracture, brittle faulting, ductile faulting, and homogeneous flow. Extension fracturing occurs by "...separation of a body across a surface normal to the direction of least principal stress"(Griggs & Handin, 1960, p. 348). This is the most brittle type of behavior. The initial movement is perpendicular to the surface.

Brittle faulting occurs through a shear fracture or a shear zone. Shear fracture is characterized by a single surface of rupture with complete loss of cohesion. The initial movement is parallel to the fracture surface which is normally located at about 30 degrees to the direction of the maximum principle stress. A shear zone consists of a series of closely spaced shear fractures. Shear zones constitute a mode which are transitional between shear fractures and ductile faulting(Tobin, 1966, p. 12).

Ductile faulting and homogeneous flow are types of flow, which is "...any deformation, not instantly recoverable without permanent loss of cohesion"(Handin& Hager, 1957, p. 3). Ductile faulting is macroscopically discontinuous flow confined to a zone(Donath & Parker,

1964, p. 48). Homogeneous flow is macroscopically continuous and is the most ductile behavior of all modes.

Flow is defined in terms of three microscopic mechanisms: (1) Cataclastic flow is the granulation, breaking and crushing of grains which accompanies the movement of grains relative to one another; (2) gliding flow is the intragranular deformation of grains by twin or translation gliding along preferred crystallographic planes; and (3) recrystallization is the rearrangement of material through local melting, solid diffusion or solution and redeposition(Griggs & Handin, 1960, p. 348).

It is important to note that the term homogeneous deformation as commonly used in rock deformation studies has a special meaning. In order to understand permanent rock deformation, "We must take into account the local discontinuities in deformation that have no part in classic strain theory. However, provided the nature and distribution of local discontinuities in deformation are statistically the same in all representative samples of the body, deformation of a fabric may be regarded as statistically homogeneous and statistically continuous." (Turner & Weiss, 1963, p. 366; See for further discussion.) It is on this basis the term homogeneous is used in contrast to the strictly homogeneous strain of classic theory.

The Effect of the Major External Variables on Deformation

The external variables which have the most significant effect on the competition between the various modes of deformation are the state of stress, temperature, the strain rate and the interstitial environment. These factors and their effects are discussed in more detail in

the following section.

(a) Definitions -- Stress, Strength. Stress is defined as force per unit area. The fundamental unit of stress is the bar. One bar equals 10^6 dynes per centimeter^2 by definition(1 bar = 1.02 kg/cm^2 = 14.50 p.s.i.). The kilobar = bars x 10^3 and will be abbreviated kb. For any stress array, it is possible to define a new coordinate system which has axes perpendicular to the planes on which the maximum normal stresses act, and on which no shearing stresses act. The shear stress is defined as the tangential force per unit area applied to any plane. The planes are called the principal planes, and the stresses normal to these planes are called the principal stresses. For a three dimensional system there are three principal stresses disposed in an orthogonal array. Throughout this discussion, the principal stresses will be labelled σ_1, σ_2 and σ_3. Compressive stresses are taken as positive, and $\sigma_1 > \sigma_2 > \sigma_3$. The principal shear stresses are defined as the stresses which lie symetrically disposed to any two principal stresses. Magnitude of the shear stresses is equal to $(\sigma_m - \sigma_n)/2$ as shown in Figure 1, where σ_m and σ_n are the two principal stresses.

Mohr devised a graphical method for representing the state of stress at a point on any oblique plane through the point. Figure 2 is a Mohr diagram for a two-dimensional state of stress. Principal stresses are plotted along the x axis, and shear stresses along the y axis. The angle between σ_1 and the plane designated is θ, and is shown as 2θ in the Mohr diagram.

Furthermore, it can be shown that a triaxial state of stress, defined by three principal stresses can be represented by three Mohr's

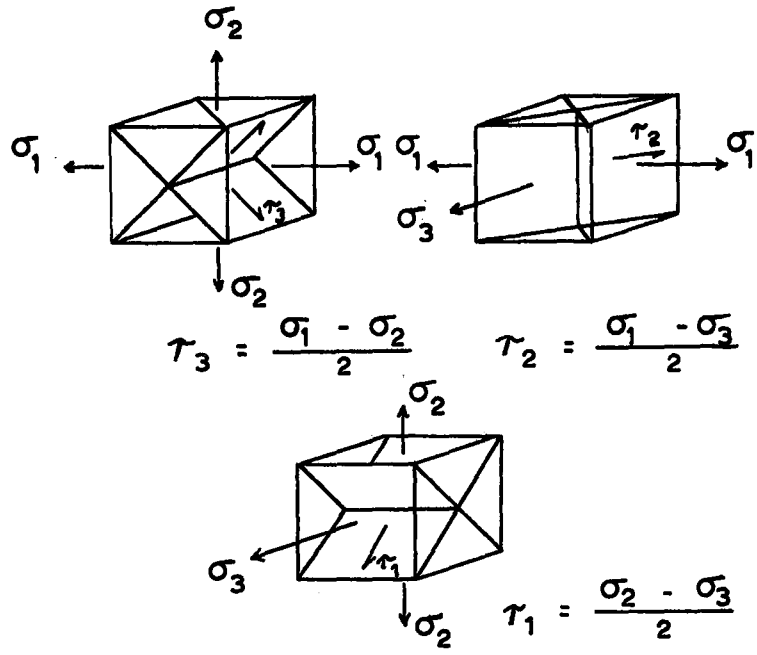

(a)

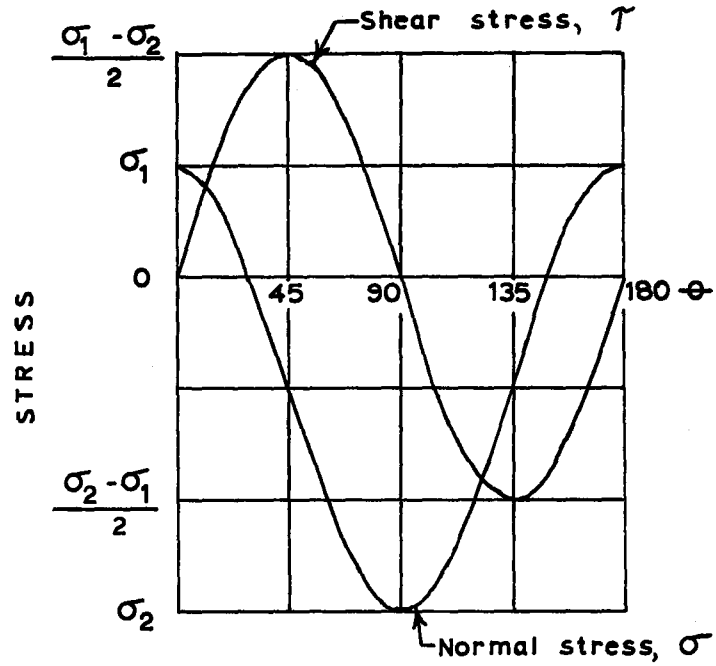

(b)

Fig. 1. (a) Sketch showing the orientation of the three principal shear stresses symmetrically disposed at 45° to the principal normal stresses. (b) Orientation and relative intensity of the normal shear stresses within the plane defined by the principal stresses σ_1 and σ_2.

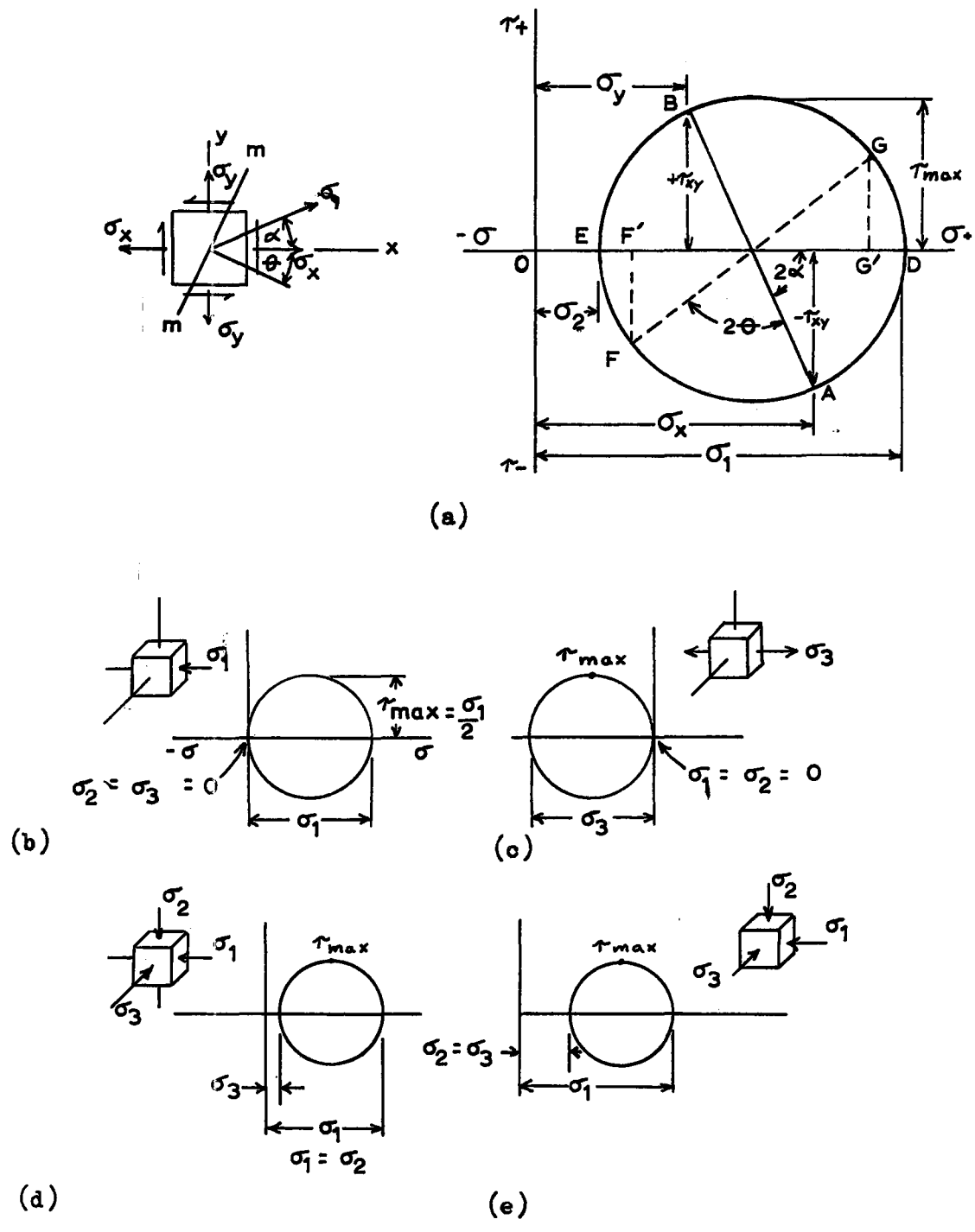

Fig. 2. Mohr's circle for various states of stress. (a) General relations; (b) uniaxial compression; (c) uniaxial tension; (d) triaxial compression; (e) triaxial extension.

circles(Nadai, 1950).

In experimental rock deformation, the state of stress at the surface of the test specimen is primarily determined by the type of test apparatus and the experimental procedure. Because of symmetry of loading and deformation, the principal stresses normally are symetric with regard to the test specimen. A summary of the sense and relative magnitudes of the principal stresses of the more common types of tests is included in Table 1.

The strength of a rock has been defined as the resistance to failure -- continuing flow or fracture(Handin, 1960). Unless otherwise noted, strength is taken as the differential stress($\sigma_1 - \sigma_3$) at a given value of σ_3 throughout this work. The ultimate strength is taken at the maximum coordinate on the stress-shortening record.

The term shortening has been used in preference to the term strain because of the inhomogeneous nature of the distribution of deformation in many of the present experiments. It is defined as is longitudinal strain, which is the ratio of change in length to the original length. Other terms will be defined as needed.

(1) Effect of Stress on Strength and Deformation

The magnitude and sense of the principal stresses profoundly affect the strength and deformational behavior of rock materials. Wuerker(1956) found that under uniaxial conditions the ratio of compressive strength to tensile strength varied between 3 and 110 among 13 rocks investigated. More commonly, the ratio is found to lie between 5 and 15(Brace, 1961; Jaeger & Cook, 1969).

The important variable, confining pressure, is introduced through

	Principal stresses		
	σ_1	σ_2	σ_3
Uniaxial compression			
$\sigma_y = \sigma_z = \tau_{xy} = 0$	σ_x	0	0
Uniaxial tension			
$\sigma_y = \sigma_z = \tau_{xy} = 0$	0	0	$-\sigma_x$
Triaxial compression			
σ_x; $\sigma_y = \sigma_z$; $\tau_{xy} = 0$	$\sigma_x = \sigma_x + p^*$	p	$p = \sigma_y = \sigma_z$
Triaxial extension			
σ_x; $\sigma_y = \sigma_z$; $\tau_{xy} = 0$	$p = \sigma_y = \sigma_z$	p	$\sigma_x = p - \Delta\sigma_x$

p^* = confining pressure

Table 1. Summary of the states of stress developed in homogeneous elastic specimens for the more common types of tests.

the triaxial test. The effect of increasing confining pressure is dependent upon the nature of the behavior of the material under study. Increasing confining pressure results in a very significant increase in the strength of brittle materials. A similar, but less significant increase in strength is observed in materials undergoing flow. Furthermore, increasing confining pressure is responsible for the transition from brittle to ductile behavior in many materials.

For materials, such as quartz single crystals, quartzite and pyrex glass, which behave in a very brittle manner at room temperature, increasing confining pressure results in significant increase in the fracture strength(Griggs & Bell, 1938; Griggs et al., 1960; Handin & Hager, 1957; Handin et al., 1967). Although a paucity of data makes it difficult to compare the fracture strength of brittle materials under conditions of triaxial extension and triaxial compression, there is some indication that the compressive strengths are 8 to 12 times the strengths in extension(e.g. pyrex glass, Handin et al., 1967, p. 633) under equivalent confining pressure. Other materials such as dolomite and fine-grained limestone, which behave in a brittle manner at low to moderate confining pressures and at room temperature, give compressive strengths which are 4 or more times, the strengths in extension(Handin, et al., 1967).

For materials such as limestone, which are not strictly brittle, increasing confining pressure causes the material to undergo a brittle-ductile transition. With the onset of the transition, the material is observed to undergo non-recoverable deformation and the amount of deformation before failure increases with increasing confining pressure.

At the same time, there is an increase in strength. However, the relative increase is less than the observed strength increase for brittle materials under a similar confining pressure increase.

Paterson(1967) notes that an increase in confining pressure normally increases both the level and the slope of the stress-strain curve for rocks undergoing deformation by flow. In order to better define the effect, Paterson proposed comparing the values of σ_1 and σ_3 at a constant amount of strain which he chose as 5 percent, in order to avoid uncertainties at very low or very high strains.

The slope of the Mohr envelope is designated tan a, where

$$\tan a = \frac{\tan \psi}{2(1 + \tan^2 \psi)^{\frac{1}{2}}} \qquad (2\text{-}1)$$

and tan ψ is the slope of a plot $\sigma_1 - \sigma_3$ at 5 percent strain against σ_3 the confining pressure.

Paterson indicates that there are two extreme cases for the pressure sensitivity. Ductile materials such as some metals, as well as calcite and marbles have a small tan a, on the order of .01. In contrast, granular materials such as sandy soil, quartz sands or poorly bonded sandstones which undergo uniform, cataclastic deformation represent the other extreme and have a relatively large tan a, on the order of .3 to 1.0.

The low values of tan a associated with ductile materials is thought to reflect the generalization that deformation by crystallographic slip or twinning is only slightly pressure sensitive, whereas deformation by frictional sliding has a high pressure sensitivity. It will also be shown that the propagation of fracture which is necessary

for cataclasis also has a high pressure sensitivity(Chapter 5).

(a) Effect of Stress on the Orientation of Planes of Failure or Deformation

The orientation of planes of failure or deformation are found to be dependent upon the state of stress under which they form. In fact, the four fundamental modes of rock deformation are in part defined with regard to the orientation of the operative principal stresses. It is generally agreed that extension fractures form normal to the direction of least principal stress. Most workers feel that extension fractures may only form if the least principal stress is equal to zero or is tensile(Brace, 1964; Jaeger & Cook, 1969; Bombolakis, 1964; Hoek & Bieniawski, 1965). Griggs and Handin(1960) feel that the tensile principal stress makes a special case which should be called tension fracturing. They further state that extension fractures may form even though all macroscopic stresses are compressive. They suggest, however, that the failure may be caused by the "wedging action" associated with microscopic surface cracks or flaws. Brace(1964) concludes that extension fractures which form under compressive stresses are intrusion fractures resulting from injection of jacketing material into surface cracks. This injection causes local tensile stress concentrations.

Brittle faulting under triaxial compressive conditions develops through shear fractures or shear zones. These surfaces or zones are characteristically oriented at between 20 and 40 degrees to σ_1. The angle is commonly 25 to 30 degrees at low confining pressures and increases toward 40 degrees with increasing confining pressures. Increases in ductility bring about an increase toward 45 degrees

(Handin, et al., 1967).

Materials undergoing homogeneous flow may show the development of minor shear zones distributed over the surface of the specimen. These zones are inclined at 45 degrees to the maximum principal stress, and are apparently similar to Luders bands which develop during the plastic deformation of metals. They have been described for various geologic materials which undergo homogeneous deformation(e.g. limestone, Paterson, 1958; gypsum, Boyd & Currie, 1969).

(b) Effect of the Intermediate Principal Stress, σ_2

Nearly all of the triaxial rock deformation experiments have been carried out with two of the principal stresses being equal(i.e. either $\sigma_1 = \sigma_2$, or $\sigma_2 = \sigma_3$). More recently, experiments have been designed to observe how varying all three principal stresses will affect rock behavior. This work has led to the following observations: (1) Failure under triaxial compression in which two of the principal stresses are equal is a special case, and not generally applicable to more general stress states(Mogi, 1971b). (2) The effects of σ_2 on strength are small relative to those of the extreme principal stresses(Handin, 1969). (3) The magnitude of the effect of σ_2 varies from rock to rock, but increasing σ_2 results in increased strength, and decreased ductility (Handin et al., 1967; Mogi, 1971a, b). (4) The stress drop at fracture increases with increasing σ_2(Mogi, 1971b). (5) Fractures always form parallel to the direction of σ_2(Mogi, 1971b).

(2) Effect of Temperature

The effect of temperature changes on deformational behavior varies considerably for different materials. However, increasing temperature

generally results in increased ductility and decreased strength(Handin & Hager, 1958). The effect is small for materials undergoing brittle deformation. For materials undergoing flow through intracrystalline processes such as twinning or translation gliding the effect may be rather great. This is also true under conditions where recrystallization is occurring. The temperature dependence of twinning and translation gliding is well documented for calcite(Turner et al., 1954).

Donath(1968) suggests that temperature changes will have little effect on a material undergoing cataclastic flow. It has generally been found that trivial changes in temperature in the range of 25° C. have little effect on the deformational behavior of most rock materials.

(3) Effect of Strain Rate

The effect of strain rate on the strength and deformational behavior of rock materials is of great importance, as it introduces the fundamental geological variable, time, into the experiments. Strain rate is generally referred to as the amount of change of length per second. Thus, 10^{-1} per second is 10 percent shortening(or lengthening) per second, while 10^{-4} per second is .01 percent per second.

Experimentalists have shown that slower strain rates result in increased ductility and decreased strength. This has been demonstrated for calcite rocks(Heard, 1963), and for both quartz single crystals and quartzites(Heard & Carter, 1968). However, the effect has only been observed at high temperatures for quartz(i.e. above 300 to 500° C.) and is only of moderate importance at room temperature for calcite rocks.

Donath(1968) has shown that there is little effect on the strength

for strain rate changes between 10^{-3} and 10^{-7} per second for a brittle sandstone deforming cataclastically at room temperature. He concluded that "...the strength and ductility of cataclastically deformed rock is independent of the rate of deformation at rates slower than 10^{-3} per second"(Donath, 1970). Donath(1970) found the strength of a limestone decreased by 19 percent when the strain rate was decreased from 10^{-3} to 10^{-7} per second. Heard(1963) found a similar variation for the Solenhofen limestone.

Other workers have shown that a change of one order to magnitude of strain rate near the rate 10^{-4} per second will probably have a negligible effect(Wuerker, 1959; Watstein, 1953) or at the greatest a 5 percent change(Perkins et al., 1970) on the strength of brittle rock and/or concrete. The effect of small changes in strain rate will have little effect on the behavior of rock materials under the conditions of the present study.

(4) Effect of Interstitial Fluids

The effects of pore fluids are relatively well known. Brace(1968) summarizing the evidence, concludes that "...the stress at which fracture occurs is determined not by confining pressure alone, but rather by the effective confining pressure." The effective confining pressure equals confining pressure minus the pressure of pore fluids.

Recent work has shown that the chemistry of pore fluids has a significant effect on the strength and ductility of sandstones(Swolfs & Logan, 1970). The relative effect was found to vary for different chemical species and is most significant for low pore pressures(less than 100 bars).

The effect of small amounts of pore moisture is less well known, although there is evidence that it must be considered. Colback and Wiid(1965) found that specimens dryed over dessicants may have strengths which are twice the strengths of saturated specimens. Similarly, Price(1966) shows that air dryed test cores may have strengths which are only 50 percent as great as oven dryed cores.

Griggs and Blacic(1965) have shown that presence of even small amounts of water may drastically reduce the strength of quartz. As little as 0.1 percent by weight of water was found to reduce the strength of quartz from tens of kilobars to a few hundred bars at 500° C. Griggs and Blacic suggest that the water acts to hydrolyze the silicon-oxygen bonds and thereby catalyzes plastic deformation. This effect has not been observed below 300° C. The effect has only been observed in synthetic quartz crystals(Griggs & Blacic, 1965; Heard & Carter, 1968).

It is apparent that even a small amount of moisture may have a significant effect on the strength of rock materials, even under conditions which are normally thought to be "dry".

Effects of Experimental Technique on Rock Deformation

Various aspects of experimental technique involving the properties of the experimental apparatus, the shape and characteristics of the test specimen and the jacketing madium, may act to influence the strength and/or deformational mode of the test specimen.

Because of the difference in mechanical properties between the rock specimen and the anvils through which the load is applied, the question of what effect stress concentrations and frictional restraint will have on rock strength and deformational behavior must be considered.

Brace(1964) has shown that standard cylindrical test specimens having a length/diameter ratio of 2, may give strengths which are as much as 20 percent less than strengths for "dogbone" shaped specimens which are designed to eliminate stress concentrations arising from end restraint. However, the increased strengths and somewhat more consistent results which are achieved by the use of the "dogbone" specimens is generally not thought to be sufficient to warrant the added cost in time and money which is required to prepare specimens of this type.

It has been shown that the ideal length/diameter ratio for cylindrical rock samples is 2.5. This ratio minimizes end effects while not exceeding a ratio for which bending moments become important(Mogi, 1966). Mogi has shown, however, that although the length/diameter ratio affects failure strength under 1 bar . confining pressure, under high confining pressure, the strength is less sensitive to this ratio.

Jaeger and Cook(1969) propose that the anvils may be responsible for the longitudinal fractures which develop in specimens deformed under atmospheric test conditions. Under confining pressure, the effect of frictional constraint on specimens deforming in a homogeneous manner is responsible for the typical barrel shape. No completely satisfactory method of overcoming this drawback has been developed.

Additional effects result from the anvils when the apparatus so constrains the anvils that they must follow coaxial paths during the deformation of the specimen. Donath(1968) has pointed out that coaxial constraint of the anvils results in the development of symmetric features, such as conjugate faults, during deformation. Specimens deformed in an apparatus where lateral motion of the anvils is not

constrained normally develop only one fault.

Jacketing materials have long been known to affect the strength of experimentally deformed rocks. Corrections may be made for strong jackets by subtracting the added strength of the jacket. Brace(1964) has shown that in certain cases the jacket material may intrude into the specimen causing decreased strength. This "intrusion" fracturing mechanism may be recognized as it results in the formation of longitudinal fractures. By selecting thin walled, low strength jackets which do not form intrusion fractures, it is possible to minimize the effects of jacketing.

It is only recently that the role of the modulus of the test apparatus has been defined in rock deformation. The elastic behavior of the testing apparatus has been shown to affect both the shape of the stress-strain record, and the deformational behavior of brittle rocks.

Jaeger and Cook(1960, p. 167-171) discuss the effect which the stiffness of a testing machine may have on the stress-shortening record of a rock. The stiffness, k, of an elastic member is defined as the force, per unit displacement, or

$$k = P/x. \qquad (2\text{-}2)$$

where x is the displacement produced by P along the direction in which it acts. The amount of energy stored in an elastic member and recoverable from it, as P is decreased to zero is

$$S = P^2/2k. \qquad (2\text{-}3)$$

A rock specimen of area A, length L, and Young's modulus E has a stiffness

$$k_R = AE/L. \qquad (2\text{-}4)$$

In the same way, the test apparatus will undergo an elastic elongation which is expressed as k_M.

When the load on a test specimen is decreased to zero, the specimen and apparatus relax in an elastic manner and the energy stored by the stiffness of the machine is recovered. The elastic energy stored in the system consisting of specimen plus apparatus is

$$S_s = P^2(1/k_R + 1/k_M)/2 \qquad (2\text{-}5)$$

as each part is subjected to the same load P.

Jaeger and Cook point out the k_R is commonly around 4×10^6 lb per inch(0.11×10^6 bars per centimeter) and that k_M is typically about one-fourth of this value. The test apparatus then stores about four times as much energy as the specimen. When failure of the specimen occurs, the energy given by (2-5) is released in the process of fracture, and this is influenced by the large quantity of energy released by the testing machine.

If a load-displacement diagram is studied, it is possible to understand the effect. The stiffness of the soft machine is represented by the flat line, k_1, and the complete stress-strain curve for the rock is shown. The region around the point where the complete load-displacement curve of the specimen is tangent to k_1 is shown in an enlarged scale in Fig. 3. The effect of a small additional compression, Δx, near the point of tangency decreases the ability of the rock specimen to resist the applied load by an amount $\Delta P_R = dP/dx\Delta x$. It also results in a decrease in the load applied by the machine of $k\Delta x$, provided energy is neither added nor withdrawn to the system. If $|dP/dx| > |k|$, as is the case with k_1, the ability of the specimen to resist the load at $x + \Delta x$ is less

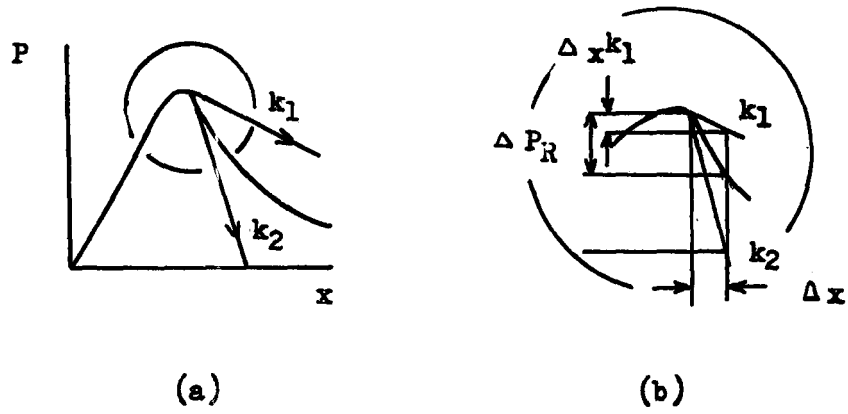

Fig. 3 (a) A complete load displacement curve for a rock specimen with lines showing the behavior of soft, k_1, and stiff, k_2, testing machines. (b) An enlargement of the peak of the load-displacement diagram showing the loss of specimen strength, ΔP_R, and machine load, $k\Delta x$, for an incremental compression, Δx (After Jaeger & Cook, 1969, p. 169).

than the load applied to it by the testing machine in this part. This results in the violent failure which has been found to be characteristic of brittle materials under these conditions.

Experimental work has demonstrated that the effects which influence rock strength can be effectively eliminated as long as specimens of uniform shape and controlled surface conditions are employed. Although in the past, most experimentalists have employed cylindrical specimens with a length/diameter ratio of 2.0, work by Mogi(1966) indicates that a ratio of 2.5 may be a somewhat better ratio. Effects such as barreling and the development of symmetric faults reflect the effects of anvil constraint and must be accounted for. The effect of machine stiffness on specimen behavior and deformation record is now understood and must be considered. With proper design, jacketing effects may be essentially eliminated.

Criteria of Failure

Failure criteria relate the load at yielding or failure(yield strength or fracture strength) to the other stresses, $\sigma_1 = f(\sigma_2, \sigma_3)$. The criteria of Coulomb, Mohr and Griffith have most commonly been referred to, and have generally been thought to give the best fit of experimental data.

(1) Coulomb Criterion

Coulomb suggested that for shear failure that the shear stress leading to failure across a plane is resisted by cohesion of the material and by the product of a constant times the normal stress across the plane. The criterion is expressed by

$$S_o = |\tau| - u\sigma \quad \text{where } \sigma = \text{normal stress across the plane} \qquad (2\text{-}6)$$

τ = shear stress across the plane

S_o = constant regarded as the inherent shear strength of the material

u = coefficient of friction

Experimental results under triaxial conditions generally follow this relationship. A plot of σ_1 against σ_2 gives a linear relation for brittle materials. If the angle between σ_1 and the failure plane changes, then the relation is non-linear.

The co-efficient of internal friction (u) can be defined by the angle of internal friction (ϕ)

$$u = \tan \phi \qquad (2\text{-}7)$$

where ϕ is the angle between the "Mohr envelope" and the abcissa of

the Mohr diagram(see discussion on Mohr criterion). The Coulomb criterion predicts that the direction of shear fracture is inclined at an acute angle to the direction to the maximum stress and can be determined by the expression

$$\theta = (1/2)\tan^{-1}(1/u) \text{ or } \theta = \frac{90 - \phi}{2} \qquad (2\text{-}8)$$

where θ is the angle between the maximum principal stress and the fracture plane.

The theory predicts two conjugate failure planes disposed at θ degrees to σ_1.

(2) Mohr Criterion

Mohr generalized the Coulomb criterion by extending it into three dimensions and by allowing for a variable co-efficient of internal friction(Handin, 1969). The Mohr hypothesis postulates that material properties are a function of the state of stress and that shear failure occurs on those planes for which the shearing stress (τ) is at a maximum and the normal stress (σ) is at a minimum.

Experimentally determined values of the normal stresses at failure(σ_1, σ_2, σ_3) can be used to draw a series of "Mohr circles" in shear and normal stress space. The Mohr's envelope, the tangent to the family of Mohr circles, defines the yield surface of the solid under combined stress conditions. Failure will not take place if values of σ and τ are below the envelope, but failure will occur if values of σ and τ just touch or lie above the envelope.

The many implications and interrelations between these and other criteria are discussed in more detail by Jaeger & Cook(1969, p. 83-101).

(3) The Griffith Criterion

The Griffith theory of brittle fracture is the only mechanistic theory of rock strength. It was developed in order to rationalize the observation that the cohesive strength of materials calculated from a theoretical basis of molecular structure exceeds the actual strength by as much as three orders of magnitude. Griffith(1921) proposed that this discrepancy can be accounted for by considering the inherent defects in the structure caused by the presence of microscopic and submicroscopic cracks. These cracks act to produce stress concentrations of sufficient magnitude so that the theoretical cohesive strength is reached in localized regions at an average applied stress which is well below the theoretical value.

Inglis(1913) gives the analytical solution for the stress concentration around a small elliptical hole in a plate. The

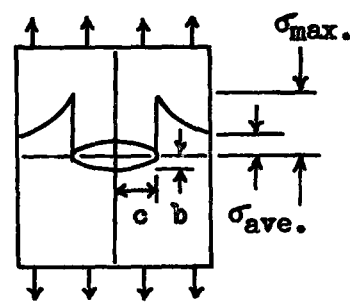

Fig. 4 Sketch showing the stresses associated with a small hole in a plate.

required to extend the crack wall. Then

$$\sigma = \left[\frac{2E(\gamma + p)}{\pi c}\right]^{\frac{1}{2}} \simeq \left[\frac{Ep}{c}\right]^{\frac{1}{2}} \qquad (2\text{-}14)$$

For metals, the surface energy term can be neglected as the plastic-work term is probably 10^5 to 10^6 ergs/cm^2, compared with values of γ of 1,000 to 2,000 ergs/cm^2. The important element of this hypothesis is that if a material is not completely brittle there is an increase in fracture strength, and the increase for a very ductile material is very large.

While the above solution is for tensile conditions, Griffith (and others) have shown that even when the applied stresses are compressive, some of the stresses associated with each flaw will be tensile. The strength

$$(\sigma_1 - \sigma_3) = 8\,\sigma_{tensile}(\sigma_1 + \sigma_3) \text{ if } \sigma_1 + 3\sigma_3 > 0$$

and $$\sigma_3 = -\sigma_{tensile}, \text{ if } \sigma_1 + 3\sigma_3 < 0. \qquad (2\text{-}15)$$

The theory predicts that the uniaxial compressive strength will be 8 times the uniaxial tensile strength. An equation where

$$\tau^2 = 4\sigma_{tensile}(\sigma + \sigma_{tensile}) \qquad (2\text{-}16)$$

may be used to define a parabolic failure envelope.

McClintock and Walsh(1962) modified the theory to account for friction between the crack surfaces which occurs when high pressures act to close the cracks. Jaeger and Cook(1969) point out that this does not alter the Griffith envelope at uniaxial conditions or at low pressures. However, at higher pressures the frictional effect becomes important and the theory becomes identical with the Coulomb theory and gives a linear stress-strain curve and a linear Mohr

required to extend the crack wall. Then

$$\sigma = \left[\frac{2E(\gamma + p)}{\pi c}\right]^{\frac{1}{2}} \simeq \left[\frac{Ep}{c}\right]^{\frac{1}{2}} \qquad (2\text{-}14)$$

For metals, the surface energy term can be neglected as the plastic-work term is probably 10^5 to 10^6 ergs/cm^2, compared with values of γ of 1,000 to 2,000 ergs/cm^2. The important element of this hypothesis is that if a material is not completely brittle there is an increase in fracture strength, and the increase for a very ductile material is very large.

While the above solution if for tensile conditions, Griffith (and others) have shown that even when the applied stresses are compressive, some of the stresses associated with each flaw will be tensile. The strength

$$(\sigma_1 - \sigma_3) = 8\,\sigma_{tensile}(\sigma_1 + \sigma_3) \text{ if } \sigma_1 + 3\sigma_3 > 0$$

and $$\sigma_3 = -\sigma_{tensile}, \text{ if } \sigma_1 + 3\sigma_3 < 0. \qquad (2\text{-}15)$$

The theory predicts that the uniaxial compressive strength will be 8 times the uniaxial tensile strength. An equation where

$$\tau^2 = 4\sigma_{tensile}(\sigma + \sigma_{tensile}) \qquad (2\text{-}16)$$

may be used to define a parabolic failure envelope.

McClintock and Walsh(1962) modified the theory to account for friction between the crack surfaces which occurs when high pressures act to close the cracks. Jaeger and Cook(1969) point out that this does not alter the Griffith envelope at uniaxial conditions or at low pressures. However, at higher pressures the frictional effect becomes important and the theory becomes identical with the Coulomb theory and gives a linear stress-strain curve and a linear Mohr

envelope.

Both mathematical and photoelastic investigations have been carried out in order to study the development of fractures from model "Griffith flaws".

Hoek and Bieniawski(1965) found that in uniaxial tension, fracture may initiate from a single flaw and propagation of the fracture parallel to σ_1 will lead to total failure within a matter of milli-seconds.

Under conditions of uniaxial compression(Bombolakis, 1964) and biaxial compression(Hoek & Bieniawski, 1965) isolated critically oriented cracks(i.e. inclined at between 20 and 40 degrees to σ_1) initiated fractures near their ends. The fractures propagate less than one or two crack lengths following a curved path into a position parallel to σ_1 which is then stable. Propagation ceases within this orientation as the stress at the ends of the crack are no longer tensile. Under uniaxial compression, Hoek and Bieniawski found that it was necessary to increase the applied load to more than three times the load at primary initiation in order to continue propagation.

This work led to the conclusion that a single Griffith crack cannot account for the failure of a specimen in a compressive field unless the ratio of applied principal stresses is less than or equal to zero(i.e. in uniaxial compression or when one principal stress is tensile).

For biaxial compression, shear fractures most probably develop from an overlapping array of closely spaced, en echelon cracks, which coalesce to form the macroscopic shear fracture(Bombolakis,

1964; Hoek & Bieniawski, 1965).

The status of the Griffith theory is still unsettled. As recently as 1967, Jaeger wrote that "from the theoretical point of view, the most important event of the past few years has been the trend towards replacing the older phenomenological theories(of rock failure) by the Griffith crack theory"(1967, p. 4). Uncertainties arising from tests of predictions of the Griffith theory(for example, that the compressive strength will be 8 times the tensile strength), detailed study of crack initiation and crack propagation, and detailed study of rock failure have left other workers more skeptical. They conclude that the behavior of rocks as now known cannot be explained in terms of the Griffith theory, but will require a more complex mathematical formulation(Price, 1970; Wawersik & Fairhurst, 1970).

Perhaps the argument advanced by Hawkes and Mellor(1970) is in the best agreement with what is known about rock behavior. They propose that Griffith theory must be interpreted as the criteria for the onset of cracking, which, while representing irreversible deterioration of the rock, does not necessarily represent failure. Furthermore, the actual failure resulting from continued cracking and the coalesence of small fractures is a more complex process which is not accounted for by the Griffith theory.

The Deformational Behavior of Quartz and Calcite and Rocks Consisting of These Minerals

Quartz and calcite are two of the most common rock forming minerals. For this reason, considerable attention has been devoted to determining the deformational behavior of these materials.

1. Quartz and Quartzite

Natural quartz is one of the strongest common substances. All attempts to render quartz ductile by high confining pressure at room temperature have failed(Griggs & Blacic, 1965).

It has been found that quartz single crystals can sustain a differential stress of 20 kilobars even at 500°C. and that only at this stress level does ductile deformation occur(Heard & Carter, 1968, p. 26). The onset of water-weakening observed in synthetic quartz crystals does not occur below a temperature of 300°C.(Griggs & Blacic, 1965; Heard & Carter, 1968).

At room temperature quartz behaves as an elastic-brittle substance which has a Young's modulus of 1.00×10^6 bars(Birch, 1966).

Various workers have performed experiments to determine the strength of both quartz single crystals and quartzite. Results given in Table 1, indicate that quartz single crystals have a strength in excess of 20 kilobars when loaded in compression, at atmospheric confining pressure and at room temperature. Similar tests carried out under 2.5 kilobars confining pressure give compressive strengths between 36 and 54 kilobars. Under compressive conditions, failure occurs along shear fractures inclined at about 35° to σ_1. Although

Temperature °C	Confining Pressure kb	Differential Stress kb	
(Compressive tests)		(Parallel to C_v)	
25	1 Atm.	21.0	
25	1 Atm.	23.6	
25	1 Atm.	30.0	
25	2.5	54.6	
25	2.5	36.4	
25	2.5	48.1	All from Griggs, Turner & Heard, 1960.
(Tensile tests)		(Normal to C_v)	
25	1 Atm.	1.08	Sosman, 1927
		(Parallel to C_v)	
25	1 Atm.	0.813	Sosman, 1927
(Extension tests)		Sioux quartzite in halite envelope	
25	5.0	3.8	Griggs & Handin, 1960.

Table 2. Summary of the strength of quartz and quartzite.

there are relatively few data, quartz is from 1/19th to 1/26th as strong in tension as in compression.

Working with the Cheshire quartzite, Brace(1964) found that the uniaxial compressive strength is 4.60 kb, which is 16.5 times the uniaxial tensile strength of .28 kb. Hoek(1965) found that the Witwatersrand quartzite has a compressive strength of 1.93 kb which is 9.3 times the uniaxial tensile strength of 0.207 kb.

One may conclude that quartz is a very strong and brittle material whose strength in compression is 10 or more times its strength in tension or extension under test conditions at room temperature and strain rates of the order 10^{-4}/second.

2. Non-cemented Quartz Sands

A systematic study of the deformational behavior of non-cemented quartz sands was carried out by Borg and co-workers(1960) and by Borg and Maxwell(1956). Quartz sands with a grain size between 100 and 300 microns were subjected to both triaxial compression and extension at room temperature and at confining pressures between atmospheric and 2.00 kb.

It was found that the application of confining pressure resulted in compaction of the sand. This was accompanied by a reduction in porosity, grain size and pore size. Numerous fractures were developed within the individual grains during the application of confining pressure. The fracture index[1] was found to be between 191 and 268

---

[1]Based on fracturing in 200 grains per specimen as follows: Per cent unfractured grains x 1, plus percent of grains with 1-3 fractures x 2, plus percent of grains with 4-6 fractures x 3, plus percent of grains with more than 6 fractures x 4, plus percent of demolished grains x 5, x 100(Borg et al., 1960). Index may vary from 100 to 500.

within samples subjected to confining pressure alone.

Application of differential stress resulted in further deformation and an increase in the number of fractures(i.e. fracture indices between 247 and 382 were determined for strains of between 3 and 23 percent). Strengths were generally low, as the sands were able to sustain about .50 kb differential stress after 5 percent shortening under 1.00 kb confining pressure, or about 1.60 kb differential stress at 5 percent shortening under 2.00 kb confining pressure.

Fractures developed within the quartz grains were described as conjugate or consisting of a series of parallel planar breaks which have joined to produce a single discontinuity. "Fractures frequently radiate from points of contact of neighboring grains. Sets of parallel trending fractures are rare, and as many as six breaks trending in different directions can be viewed"(Borg & Maxwell, 1956).

Studies of the orientation of the fractures indicate that the fractures develop at essentially all inclinations to the principal stresses. There is a tendency, however, for the fractures to be inclined at less than 45 degrees to σ_1.

The fracture behavior of the quartz sands was explained in terms of the Herzian solution for the stress distributions in two spherical elastic bodies in contact. The points of contact are points of stress concentration associated with the contact stresses. The resultant fractures were thought to represent both tensile and shear fractures. More recently, following the study of photoelastic models, Friedman(one of the original investigators) and co-workers concluded that the fractures which develop within grains of non-cemented granular aggregates are most frequently extension fractures(Gallagher, et al., 1970).

3. Calcite and Calcite Rocks

(a) Introduction

In 1957, Handin and Hager noted that the deformational behavior of limestone had received more attention than any other rock. Since then, several investigators including Brace(1961; 1964), Heard(1960; 1963), Paterson(1958), Donath(1964), Tobin(1966) and others have carried out work which provides an additional insight into the nature of deformation in calcite-rocks under a wide variety of conditions.

Experimental results indicate that at atmospheric confining pressure, limestones fail in a brittle manner after undergoing small amounts of elastic strain. In contrast, tests carried out under confining pressure indicate that calcite rocks behave in a ductile manner. In fact, most limestones and marbles may sustain more than 10 percent shortening without fracturing or faulting, under a confining pressure as low as 1.00 kb. At this point, we will review the deformational behavior of calcite rocks and define the factors which are thought to control this behavior.

(b) Brittle Behavior

With the exception of properly oriented single crystals of calcite, which deform by ductile twinning(Griggs, 1938), calcite and calcite rocks can sustain only limited amounts of elastic strain(generally less than one percent). The specimens then fail by brittle rupture at room temperature, under uniaxial test conditions(Handin & Hager, 1957; Handin, 1966). The theoretical Young's modulus of calcite is $.85 \times 10^6$ bars (Brace, 1961).

In order to investigate the factors which control the strength of monomineralic calcite rocks, Brace(1961;1964) carried out uniaxial compressive tests on the very fine grained Solenhofen limestone and a coarse grained marble. He proposed that a direct test of the Griffith theory of brittle strength could be made by comparing the uniaxial strength, $C_o = 8(2E\gamma/\pi a)^{\frac{1}{2}}$. For two different rocks consisting of the same material, Young's modulus, E and the surface energy, γ, are material constants, and should not differ for the two rocks. The flaw size, defined by "a", is then the only remaining variable.

Brace concluded from consideration of various studies that the flaws associated with the length of a grain boundary are the most probable source of the "Griffith flaws". By carefully measuring the grain size of the two rocks under study, he defined the potential flaw size.

In order to test the hypothesis of control by Griffith flaws, he then calculated the compressive strength of the two rocks and compared it to the experimentally determined values. He found that the Griffith crack length corresponds to the maximum grain size in the two rocks. Furthermore, the strength relationship to grain size follows the form $C_o = k(D)^{-\frac{1}{2}}$ as predicted by theory(Fig. 5). As a result of the agreement, Brace concluded that the Griffith theory does predict the strength of limestones and some other monomineralic rocks.

Uniaxial compressive strengths for limestones and marbles of known grain size are given in Fig. 5 for comparison with the experimentally determined strength curve of Brace. The strength of these

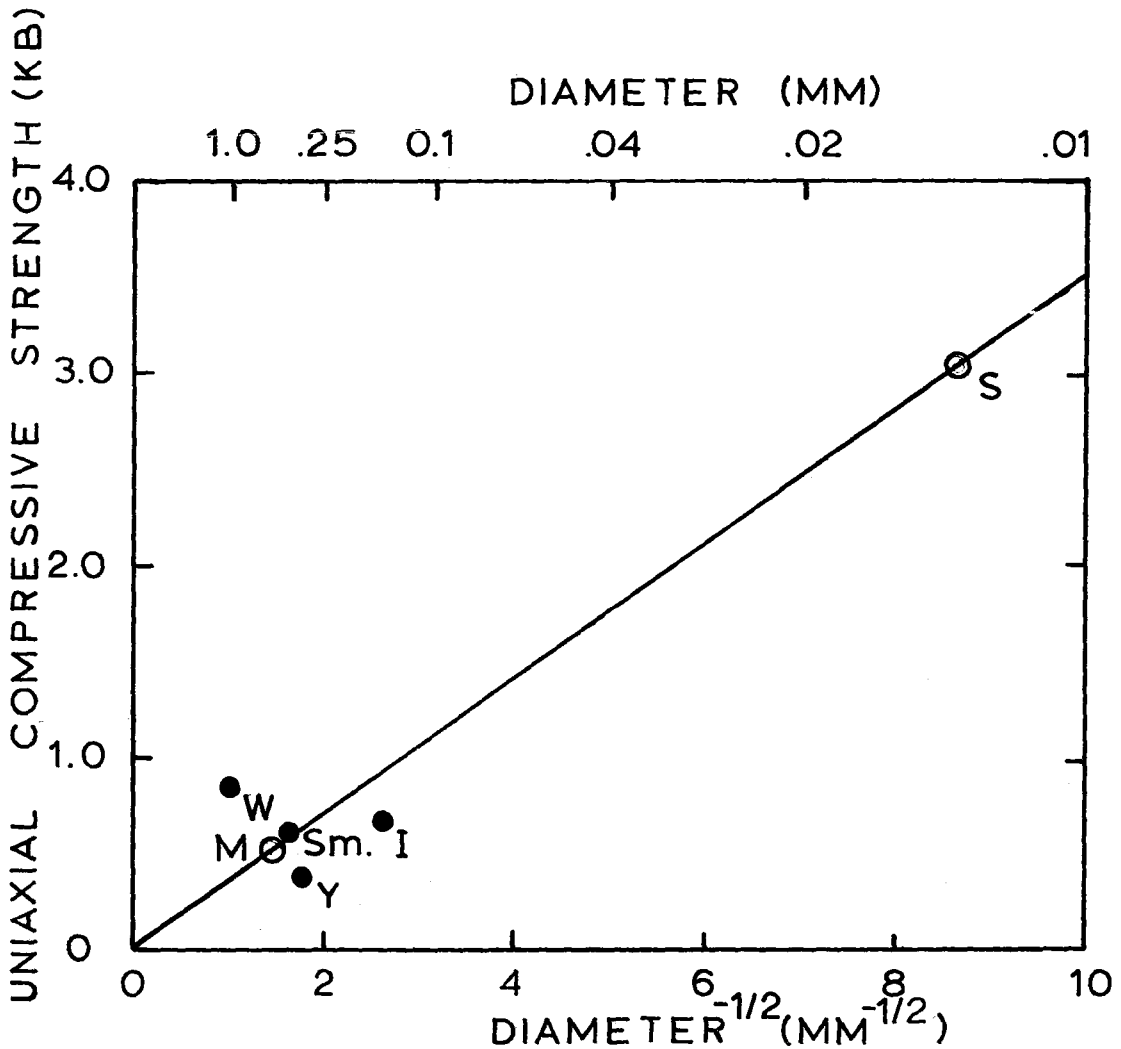

S Solenhofen limestone (Brace, 1964)
M Marble (Brace, 1964)
W Wombeyan marble (Paterson, 1958)
Sm. Schermerhorn marble (Donath, 1964)
I Indiana limestone (Hardy, 1970)
Y Yule marble (Handin & Hager, 1957)

Figure 5. Graph showing the relation between grain size and uniaxial compressive strength of marbles and limestones. The experimentally determined curve from Brace(1964) is shown with other rocks of known grain size from the literature.

rocks vary from a low of about 400 bars to a high of near 3000 bars. Strengths which fail below the curve are most commonly for rocks with relatively high porosity(i.e. more than 2 to 3 percent), and this is thought to be the principal reason for low strengths. Rock strengths lying significantly above the line such as for the Wombeyan marble can not be accounted for with the available information. In general, the uniaxial compressive strengths of limestones and marbles show moderate agreement with strengths predicted by the Griffith theory.

(c) The Brittle-Ductile Transition

The effect of increasing confining pressure on the deformational behavior of calcite and calcite rocks is well established. In contrast to quartz which remains brittle, calcite undergoes a brittle-ductile transition.

Paterson(1958) carried out an experimental investigation in order to study the macroscopic nature of the brittle-ductile transition in the Wombeyan marble. The transition from longitudinal fractures at atmospheric confining pressure to well defined shear fractures followed at higher confining pressures by shear zones with increasing width and finally the development of homogeneous deformation throughout the test specimen at 450 bars confining pressure is well documented. Similar behavior has been observed in the Solenhofen limestone(Heard, 1960) and in the Crown Point limestone and "Schermerhorn" marble (Donath, 1964).

Recognition of the various types of macroscopic behavior as

defined by the appearance of the test specimens and the shape of the stress-strain records led to the definition of different modes of behavior -- extension fractures, fault and uniform flow as defined by Griggs and Handin(1960).

Tobin(1966) pointed out that the qualitative nature of the macroscopic characteristics were not readily related to similar rocks which had been subjected to natural deformation. In order to better define the nature of the deformation of limestones, Tobin compared microscopic characteristics to macroscopic features of the experimentally deformed Crown Point limestone. Tobin(1966, p. 7) found that the deformational behavior could be defined in terms of three major microscopic modes of deformation -- lack of deformation or undeformed grains, faulting or development of fractures and slip surfaces, and homogeneous flow represented by the development of visible lamellae.

The microscopic characteristics can be used to define four groups of indicative categories -- homogeneous flow mode, ductile faulting mode, a transitional mode, and the brittle faulting mode. The study showed that ductile deformation of the Crown Point limestone takes place through plastic deformation of the individual grains. Ductile faulting was characterized by substantial amounts of fractures and slip groups. Brittle faulting is characterized by a predominance of fractures and slip groups, with an associated number of undeformed grains. There is a general lack of lamellae development in the brittle faulting group.

Tobin's study showed that the transition from brittle to ductile behavior in the Crown Point limestone can be viewed as the gradual suppression of fracturing and faulting and the more general development

of plastic deformation throughout the specimen.

(d) Ductile Deformation of Calcite

Intensive investigations have been carried out in order to determine the ductile deformation mechanism of both calcite single crystals (Turner, Griggs & Heard, 1954) and the polycrystalline Yule Marble(Borg & Turner, 1953). Results of these studies led to the unique identification of the active glide systems.

Flow in calcite can be understood in terms of three mechanisms.

1. twin gliding $\{01\bar{1}2\}$, parallel to the edge $(01\bar{1}2):(10\bar{1}1)$ -- designated e-twinning;
2. translation gliding on $\{10\bar{1}1\}$, parallel to the edge $(10\bar{1}1):(02\bar{2}1)$; designated r-translation;
3. translation gliding on $\{02\bar{2}1\}$, parallel to the edge $(10\bar{1}1):(02\bar{2}1)$; designated f-translation.

The deformation mechanisms of twinning and translation gliding in calcite may be understood in terms of the development and movement of dislocations(Keith & Gilman, 1960).

Various workers(Turner, Griggs & Heard, 1954; Carter & Raleigh, 1969) point out that at temperatures below about 600°C., favorably oriented calcite deforms predominately by twin gliding on one or more of the e planes. Within the host crystal, the upper layers are displaced toward the c-axis with respect to the lower layers. This is by definition a positive sense of shear(Turner, Griggs & Heard, 1954; See Fig. 7).

Single crystals or grains so oriented that twin gliding may not occur, deform by some alternative mechanism.

The work of Borg and Handin(1967) resulted in the determination of the apparent resolved shear stress for e-twinning, r-translation and f-translation at room temperature -- 50, 1500 and 2200 bars respectively.

The predominance of the development of e-twins can then be accounted for by the low shear stress required for the development of twins as compared with other mechanisms.

Turner and Ch'ih(1951, p. 904) stated that for the Yule marble deformed dry at 10,000 atmospheres, "Even where experimental deformation has been carried out under conditions favoring profuse development of visible glide lamellae, we are forced to conclude that some other type of intracrystalline movement, leaving no visible trace of its activity, has played a part in deformation".

(e) Heterogeneous Versus Homogeneous Deformation in Calcite Rocks

An important part of Handin and Griggs'(1951) work on the deformation of the Yule marble involved a test of two alternative hypotheses of deformation. The "heterogeneous" hypothesis "...assumes that individual grains deform in response to the external stress field with negligible or minor restriction on their freedom of motion by neighboring grains".(Handin & Griggs, 1951, p. 864). The hypothesis of "homogeneous" deformation "...assumes, ...that each grain is completely restricted by contact with its neighbors so that, 'Each grain suffers exactly the same strain as the surrounding material in bulk' "(Taylor, 1938).

Comparison of experimentally developed fabrics with model fabrics generated by assuming either heterogeneous or homogeneous deformation led Turner and Griggs to conclude that the homogeneous hypothesis gave much closer agreement.

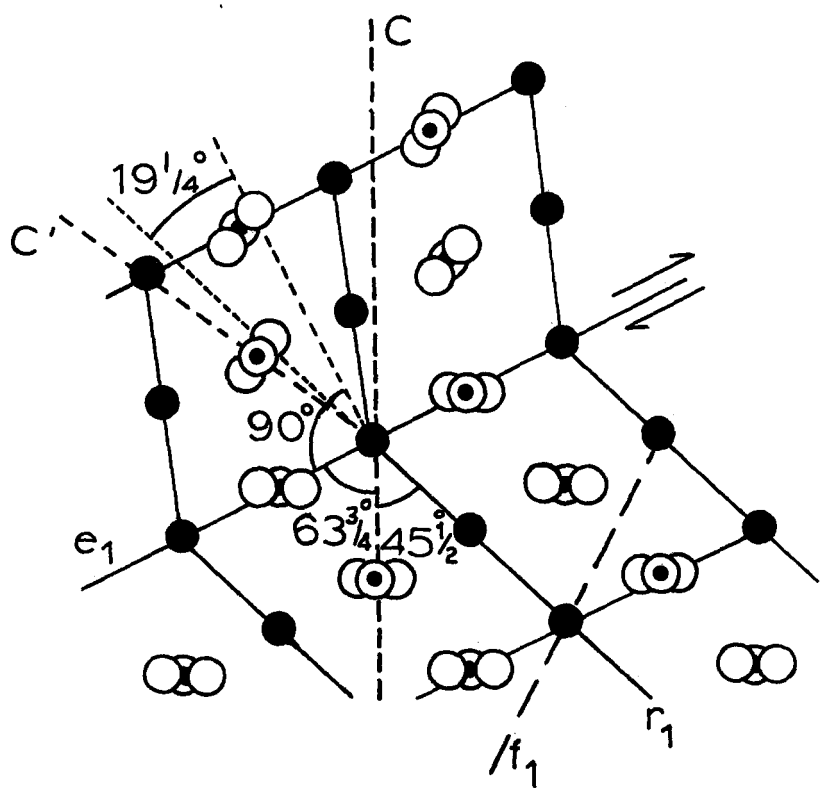

Fig. 6. Calcite lattice (diagrammatic) to illustrate twinning on $\{01\bar{1}2\} = e_1$. Section normal to the zone axis a_2. CO_3 groups, indicated by grouped circles, are greatly reduced in size. Solid large circles are Ca ions. Lattice above the line marked e_1 is twinned on e_1. Note the change of orientation of $[000\bar{1}]$ from c to c'(After Williams & Cahn, 1964).

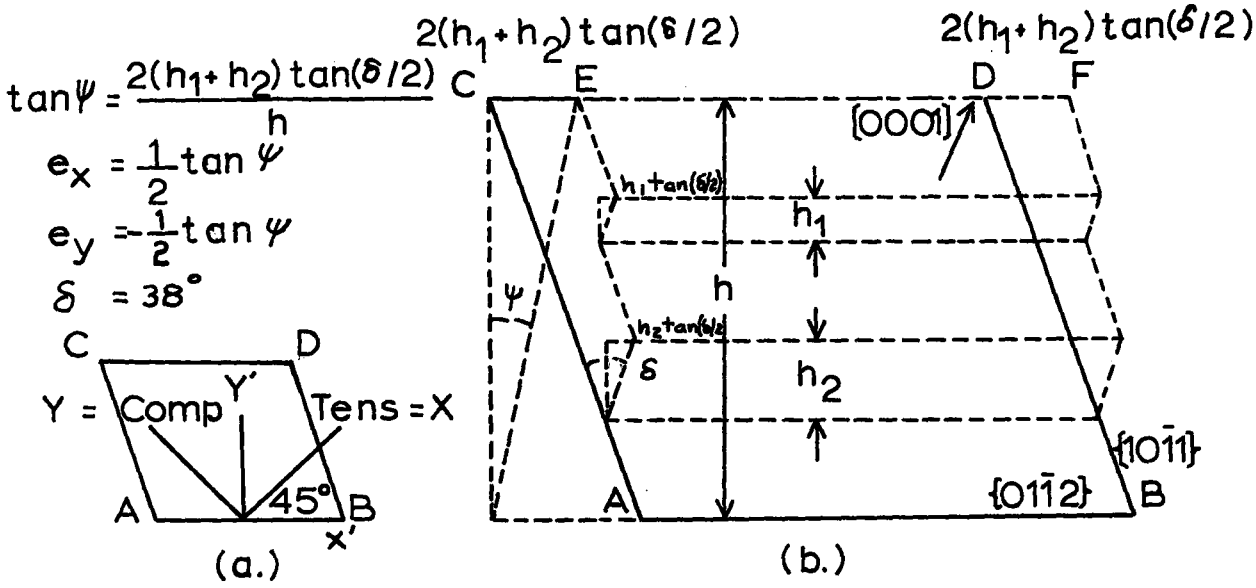

Fig. 7. Illustration of strain due to mechanical twinning on {01$\bar{1}$2} in calcite. (a) Orientation of the principal axes of strain in twinning relative to the plane of the shear. x' and y' axes are those to which engineering shear strain in the grain is referred, x, y the principal axes associated with the deformation. (b) Geometry of the twinning strain. Tan ψ is the engineering shear strain associated with twinning. (After Conel, 1962).

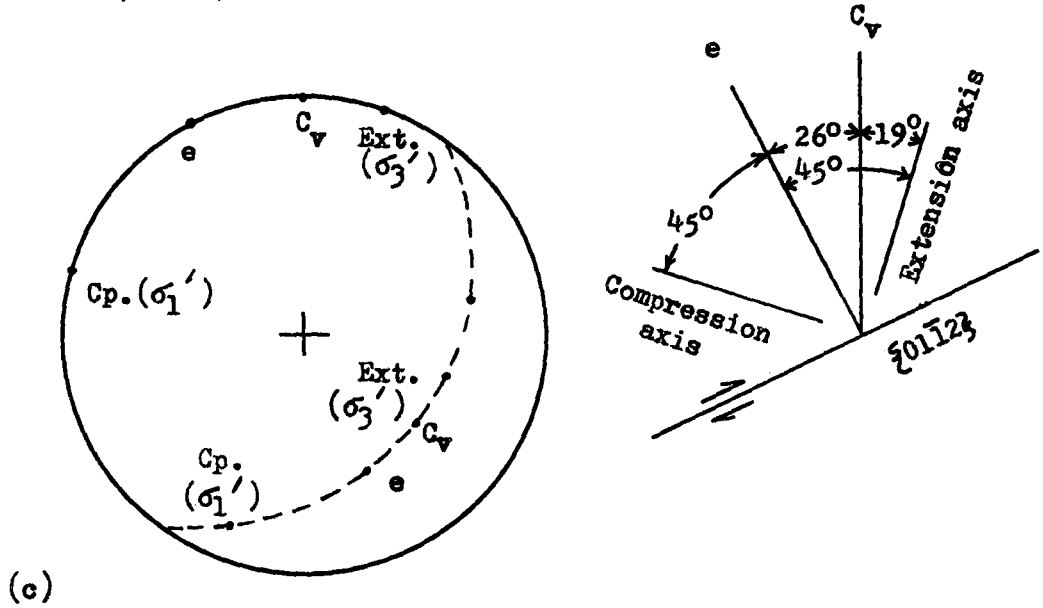

(c) Diagrams illustrating position of compression (σ_1') and extension (σ_3') axes that would be most effective in causing observed e twin lamellae in a calcite crystal. Section is normal to e plane and contains glide direction and optic axis (C_v)(After Friedman, 1963).

In order for a crystal to undergo a general homogeneous strain by slip, five independent slip systems are necessary as demonstrated by von Mises(1928). Paterson(1969, p. 370) points out that earlier workers have recognized that five independent slip systems are necessary, but not sufficient for ductile behavior in polycrystalline materials. Reviewing the known slip systems in calcite, he concludes that e-twinning alone is insufficient to satisfy von Mises' criteria. However, the activation of slip on any two of the translation slip systems, or the combination of twinning with any one slip mode will be sufficient to satisfy the criteria. Other modes of deformation such as cataclasis or kink-band formation may also take place under certain circumstances and thereby contribute to the development of homogeneous deformation.

It is therefore not surprising to find indications of deformation through mechanisms other than twinning, even though a majority of the grains are favorably oriented for twin development. Conversely, it is unreasonable to expect that all strain will be accounted for through twin development.

(f) Twin Lamellae Development

Lamellae developed parallel to $\{01\bar{1}2\}$ lie at an angle of $26\frac{1}{4}^{\circ}$ to the c axis. Two types of lamellae are commonly developed within both naturally and experimentally deformed calcite. Those lamellae which are broad enough to have clearly recognizable symmetrical differences in optical behavior of adjacent lamellae within a grain were designated as <u>twin lamellae</u>(Borg & Turner, 1953, p. 1345). The second category were designated as <u>nontwinned lamellae</u>, for the lamellae appear under the microscope as planar partings of such thinness that

it is impossible to determine whether the material(if any) within the parting is twinned or not.

Conel(1962) carried out work which he indicated gave proof of the true twinned nature of these lamellae. He therefore proposed that the term nontwinned lamellae be replaced by the term microtwinned lamellae. His results indicate that the lamellae in the rocks which he studied had a thickness on the order of 1 to 10 microns.

Garber(1947) describes observations on the mechanism of twinning in calcite which are thought to deal with structures resembling microtwinned lamellae. He recognized four distinct stages in the process of twinning in calcite; (1) elastic deformation of the crystal, (2) formation of "elastic" twins, twins which disappear when the load is removed, (3) formation of stable twin layers, (4) thickening of the twin layers. Similar observations have also been made by Williams and Cahn(1964).

(i) The relation of stress and twinning

As mentioned earlier, twin gliding is dependent upon the resolved shear stress on the twin plane. It is also essentially independent of normal stress across the twin plane(Turner, Griggs & Heard, 1954, p. 889). It was shown by Turner and Ch'ih(1951, p. 899-900) that for the experimentally deformed Yule marble the greatest amount of twinning(shown by the relative number of twins developed) occurs on the e-plane(designated e_1) on which the shear stress, or the resolved shear stress coefficient(S_o)[1], is highest. Turner(1953)

---

[1] $S_o = \sin x_o \cos y_o$ where x_o = angle between load axis and glide plane and y_o = angle between load axis and glide line.

developed a technique for the dynamic interpretation of calcite twin lamellae which is based on the petrofabric technique of locating the mutually perpendicular directions of compression and extension that most favored development of the observed twin lamellae. Handin and Griggs (1951, p. 866-869) first explained the geometry of these relationships.

(ii) Strain resulting from twin development

Conel(1962) outlines the method of calculation of visible strain due to twinning. Twinning of calcite results in a shearing strain and the amount of strain depends on the degree of twinning. The twinning is characteristically heterogeneous. This occurs as most grains are only partially twinned, and contain completely twinned layers separated by layers of the untwinned or host crystal. The deformation is homogeneous within each twinned band as a result of the atomic movements involved in the twinning process. The plane of shear in twinning is perpendicular to the twin plane and includes the twinning direction. A twinned crystal is in a state of plane strain parallel to the shear plane in twinning, provided only one set of lamellae is developed in the crystal(Jaswon & Dove, 1960)

"In a given partially-twinned grain, the average shear strain induced by partial twinning is computed by thinking of the deformation as uniformly distributed throughout the grain. The situation is depicted diagramaticly in figure 7a. An original rhombehedral shaped crystal ACDB viewed in the $(1\bar{2}10)$ plane, of height $\underline{h}$ is deformed by twinning on layers of thicknesses $\underline{h}_1$ and $\underline{h}_2$ into the shape shown in dashed lines AEFB. The average engineering shear strain in the plane

of the drawing referred to the Cartesian axes $\underline{x}$ and $\underline{y}$ is

$$\gamma = \tan\psi = \frac{2(\underline{h}_1 + \underline{h}_2)}{\underline{h}} \quad \tan(\delta/2) \qquad (2\text{-}17)$$

where $\delta/2$ is one-half the angle between r(1011) in the host and r'(1011) in the twinned crystal, and equal to 19° 08.5' in calcite. In order to compute the average shear strain in a grain due to mechanical twinning, it is only necessary to measure the relative lengths of twinned and untwinned crystal traversed along a line normal to the operative twin plane.

For infinitesimal γ, the principal axes of strain for twinning lie at 45° to the twinning plane as shown in Figure 7a, and the magnitudes of the principal strains along these axes are,

$$e'_{\underline{x}} = \tfrac{1}{2}\tan\psi$$

$$e'_{\underline{y}} = -\tfrac{1}{2}\tan\psi$$

$$e'_{\underline{z}} = 0$$

where $\tan\psi$ is given in Equation 2-17." (Conel, 1962, p. 56-57)

Strain may develop by (1) increasing the number of twin lamellae or (2) by broadening the existing twin lamellae. Turner and Ch'ih (1951, p. 898) found that for the Yule marble defined dry at 10,000 atmospheres, the strain develops by increasing the number of lamellae rather than by broadening of the individual lamellae. They found that the mean spacing index increases in a linear manner as deformation proceeds. Their results also indicated that grains favorably oriented for lamellae development showed a higher intensity of development than less favorably oriented grains.

4. Calcite-cemented Sandstone

Friedman(1963) carried out the only systematic study of experimentally deformed calcite-cemented sandstones. He investigated deformed specimens of sand crystals(i.e. single crystals of calcite that poikilitically enclose detrital grains) as well as the Tensleep and Supai sandstones. These rocks were deformed under a variety of experimental conditions including extension and compression, at confining pressures between 1 kb and 5 kb, at temperatures between 150° and 300°C., and at a strain rate on the order of 10^{-4}/second.

Tests carried out at the lower confining pressures and temperatures terminated as failure occurred along a plane oriented at about 30 degrees to σ_1, after strains of 6 percent or less were obtained. The ultimate strength in compression at 1.00 kb confining pressure was about 4.70 kb. Tests carried out at higher confining pressures and temperatures gave strains as high as 22 percent. While specimens subjected to 1.00 kb confining pressure alone showed no signs of deformation under the microscope, examination of the deformed cores subjected to differential stress indicated that in most cases, both the calcite cement and the detrital grains deformed in a manner similar to monomineralic aggregates such as marbles and quartz sands. The most conspicuous deformation feature in calcite were abundant twin lamellae parallel to e{01$\bar{1}$2}. The number of lamellae increases with increasing strain. The orientation of the principal stresses determined by the orientation of the lamellae is in good agreement with the experimental orientation.

As might be expected, the detrital grains deformed in a brittle

manner. Microfractures developed within the detrital grains, and a majority of the microfractures were oriented perpendicular to σ_3. The orientation of the microfractures was found to be nearly independent of mineralogy and crystallographic control.

Analysis of the experimental results lead Friedman to conclude that "...the calcite-cement in the sandstones tends to be 'protected' by surrounding detrital grains in contact. Twinning occurs in the calcite only after the detrital grains begin to fracture. The grains fracture under relatively small loads on the aggregate as a whole, because the stress concentrations at points of contact are very large." (p. 34). Friedman also noted that "perhaps surprisingly, the fractures do not radiate from points of contact, but form as if each grain reacted to the forces applied to the aggregate in bulk". In recognition of this relation, Friedman further commented, "Stresses must be transmitted to the individual grains of a sand aggregate through grain contacts. Borg and Maxwell(1956) found that microfractures tended to radiate from point contacts in deformed unconsolidated sand, but in the cemented materials, the microfractures are principally of the extension type and tend to transect grains. They are clearly related to the known principal stress axes across the whole rock rather than to local stress concentrations at grain contacts"(p. 33). Friedman implies that all of the microfractures originate as the result of stress concentrations developed at the point of grain to grain contact, but he also suggests that the orientation of the fractures is somehow dependent upon the orientation of the principal stresses themselves.

At the time of the 1963 paper, Friedman wrote that a majority of the microfractures were extension fractures, but he also concluded that fractures with normals inclined between 20 and 40 degrees to σ_3 were probably shear fractures. Turner and Weiss(1963, p. 437) refer to the microfractures in the quartz grains of Friedman's specimens as "demonstrable shear fractures" and make no reference to extension fractures. More recently, investigation of two-dimensional photomechanical model studies led Friedman and co-workers(Gallagher et al., 1970) to conclude that "...only extension rather than shear and extension fractures form in grains of deformed sandstones, sand and rock discs".

The Mechanical Behavior of Engineering Composite Materials

Considerable effort has been expended by the engineering disciplines in order to design and fabricate materials with improved mechanical properties such as greater stiffness, toughness and high-temperature strength. The most successful method of producing a high strength material is to fabricate a composite material. Composite materials are formed when a material of one phase is distributed within a second phase. The dispersed phase is usually harder or stronger than the matrix phase(Krock & Broutman, 1967). We will review what is known about some high strength man-made materials in order to gain some insight into the behavior of two-phase rock materials.

Three basic types of composite materials exist; dispersion-strengthened, particle-reinforced, and fiber-reinforced composites. The particle-reinforced materials are of most interest as they have the greatest similarity to rock materials. These materials have a dispersoid size greater than 1.0 micron, and a dispersoid concentration of greater than 25 percent. In contrast, dispersion-strengthened materials have a dispersoid which is less than 0.1 micron, and a volume-concentration of less than 25 percent. Fiber-reinforced materials contain dispersed particles which have one long dimension (Krock & Broutman, 1967).

(1) General Behavior

The general mechanical behavior of composites has been summarized by Van Vlack(1968, p. 17).

"Deformation of a two-phase microstructure provides an example of

behavior that does not follow additive mixture rules. The total response of the material depends on an interaction between the various phases. If, for example, a load is placed on a composite, the elastic behavior of each grain or phase is influenced by the load carried by the adjacent material. In the absence of fracture or plastic deformation, one grain cannot receive more strain than the next grain. This means, of course, that the part of the material with the higher modulus of elasticity will have a proportionately higher tensile stress, with consequent shear stresses along grain and phase boundaries. Stress distributions are further complicated by differences in Poisson ratios, so that during service complex triaxial stress patterns develop on a microscopic scale in most ceramic products."

2. Strength of Brittle Matrix Composites

Experimental work has been carried out to determine what factors control the fracture strength of a brittle material consisting of a glass matrix containing a dispersion of strong inclusions. Hasselman and Fulrath(1966, 1967) proposed that the strength of such materials is related to the presence of flaws within the glass matrix which act as "Griffith cracks". An etching technique was used to determine the inherent flaw size of the matrix-forming glass. This flaw size was found to control the strength of the glass. It was hypothesised that the second phase inclusions could limit the average flaw size. The flaw size would then be controlled by the mean free path between the inclusions.

In order to calculate the mean free path, mfp, between the part-

icles, Hasselman and Fulrath used the relation

$$mfp = \frac{4R(1 - V)}{3V} \quad (2\text{-}18)$$ where R = radius of uniform spherical particles

V = volume fraction

Nivas and Fulrath(1970) extended this work to include systems which have two sizes of inclusions or a distribution of sizes about a mean. A measuring technique suggested by Underwood and others(1968) was used to determine the mean free path.

Results of both studies indicate that; where the mean free path is less than the length of the Griffith flaws normally found in the matrix, the mean free path is controlling. Where the mean free path is greater than the flaws found in the matrix, the strength is independent of the presence of the second phase inclusions.

(3) Deformational Behavior of Ductile Matrix Composites

In general, ductile matrix particulate composites may be divided into two categories based on their deformational behavior. The categories depend on whether the dispersed particles deform under load or do not deform, and merely strengthen by being harder than the matrix phase in which they are dispersed. "From a knowledge of whether or not the dispersed particles deform under load, we can make fair predictions of the dependence of volume concentration dispersoid on elastic modulus, yield strength, ultimate tensile strength and fracture elongation"(Krock, 1967, p. 460).

In both types of composite, the onset of yielding starts with plastic deformation of the softer matrix phase marked by the appearance

of either slip lines or twins. Normally a short range of deformation accompanied by very high strain hardening is observed. In this initial phase, the dispersoid deforms elastically.

In composites with a deformable dispersed phase extensive plastic deformation can occur. The stress necessary to impart extensive ductility to the composite is identical to the flow stress of the dispersed phase under the stress state present in the composite(reduced applied stress and triaxial compression in the tensile test which is normally employed in engineering studies). For materials with a deformable dispersoid, the stress initiating gross plastic flow is independent of the volume concentration of the dispersed phase and the mean free matrix separation. The entire flow curve is dependent and governed by the flow properties of the despersed phase. Such factors as temperature dependence of deformation is primarily controlled by the temperature dependence of the dispersed phase(Krock, 1967; Krock & Shepard, 1963).

An alternative type of behavior occurs in those composites in which the dispersed phase does not deform in a ductile manner. These materials are found to have limited ductility. In contrast to composites in which the dispersed phase deforms, the mechanical properties are found to be dependent upon the volume fraction of the dispersed phase. The yield strength, tensile strength, and fracture elongation are found to depend on the mean free matrix separation(Krock, 1967). For composites with a non-deforming dispersed phase, the nature of the dispersoid becomes unimportant. For example, the ductility versus

volume fraction curve is the same for some copper matrix alloys whether the second phase consists of holes, alumina, chromium or something else(Edelson & Baldwin, 1962).

In this type of material, the particulate reinforcement is thought to occur because the presence of the particles in the matrix blocks, restrains, or in some other way controls phemomena otherwise responsible for either extensive plastic deformation or fracture. The matrix is the primary load carrying element in the composite and the function of the particles is to increase the local resistance of the alloy to slip and undergo large plastic deformation.

While this acts to increase the strength, the ductility is thought to be decreased as the particles act to concentrate strain within the matrix. For this reason, the stress-strain record rises much more rapidly than for the matrix when it is free from inclusions and the fracture strain is reached at a low external strain(Edelson & Baldwin, 1962).

Most deformational studies of engineering materials are carried out under tensile conditions. In experiments with composites containing a non-ductile dispersed phase, failure normally occurs through ductile rupture. Investigation has shown that initial cracks or void develop within the composite either near the ends of the dispersed particles or by fracture of the particle itself(Gurland & Plateau, 1963). Under tensile conditions, total failure occurs through the growth and coalesence of holes as strain progresses(Drucker, 1966; McClintock, 1968).

Cracks are thought to form in, or adjacent to, the particles, because of the stress concentrations which develop at these sites with the onset of plastic deformation within the matrix. If the stress exerted upon the particle by the plastically deforming matrix is sufficient, then the particle will fracture, otherwise a void may form at the interface between the matrix and particle along the axis of maximum extension. The fracture is a tensile fracture and is oriented normal to σ_3(Gurland & Plateau, 1963). In these materials, the ultimate strength is essentially determined by the fracture strength of the dispersed phase.

Although many engineering tests are carried out under uniaxial tensile conditions, results of experiments by Gangulee and Gurland (1967)(also discussed by Drucker, 1966) provide evidence that similar behavior is observed under compressive conditions. In this study, a rectangular beam consisting of an elastic-plastic matrix(aluminum) containing a small volume fraction of brittle inclusions(silicon particles) was subjected to pure bending(Fig. 8).

During bending, the outside of the beam is subject to tensile forces while the inside is subjected to compressive forces, and a neutral surface is present near the median line of the beam. With the onset of plastic deformation within the matrix, the brittle inclusions become stressed elastically. The first inclusions to undergo failure are located near the outside edge of the beam where the tensile strains are the greatest. The fractures which develop are oriented normal to the long axis of the beam. With increasing

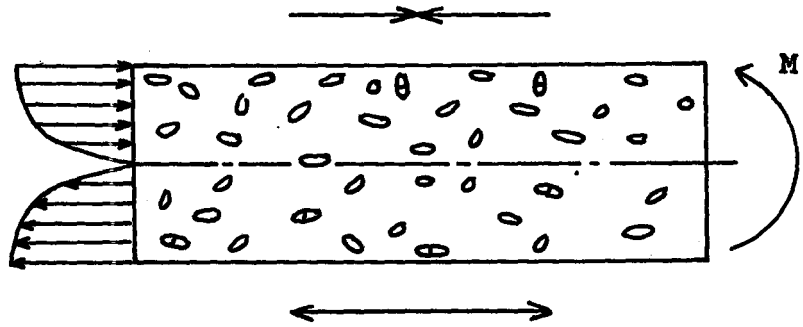

Fig. 8 . Diagrammatic sketch showing the orientation of fracture development within brittle inclusions dispersed in a ductile matrix undergoing ductile deformation during bending(After Drucker, 1966).

amounts of strain, inclusions closer to the neutral surface undergo fracture. At some point during the bending, fracture also occurs within inclusions on the side of the beam undergoing compression. In contrast to the fractures formed within inclusions on the tensile side, the fracture of these inclusions are oriented parallel to the long axis of the beam. The fracture of these inclusions is thought to result from the transverse tensile stress concentration which develops around the particles within the side of the beam undergoing compression.

(4) Summary

Experimental investigations of two-phase engineering materials consisting of a hard or strong phase dispersed within a second phase of lower strength provide a general understanding of the strength and deformational behavior of two-phase materials. The behavior of these materials can be categorized into two different classes, depending on

whether the dispersed phase deforms or remains rigid during the deformation of the composite.

Composites which have a dispersed phase which undergoes deformation may have considerable ductility, while maintaining high strength. The strength and ductility is primarily determined by the behavior of the dispersed phase.

Composites containing a non-deforming dispersed phase are characterized by high strength and limited ductility as compared with the normal behavior of the matrix. The strength and ductility is related to the volume fraction of the dispersed phase which in turn controls the mean free matrix separation.

The strength of brittle composites is controlled by size of flaws which occur within the matrix. The strengths are high if the flaw size is limited by the distance between the dispersed particles. The high strength and limited ductility of ductile composites with a non-deforming dispersed phase is thought to occur because the presence of the particles in the matrix blocks, restrains or in some other way controls phenomena otherwise thought to be responsible for extensive plastic deformation.

The interaction of the ductile matrix and the dispersoid results in stress concentrations which effectively alter the state of stress acting upon, and within, the immediate vicinity of the dispersed particles. These stress concentrations act to effectively control the initiation and orientation of fracture development which is frequently observed to occur within or immediately adjacent to the hard inclusions.

Chapter 3

DESCRIPTION OF THE CALCITE-CEMENTED BLAIRMORE SANDSTONE

Petrography

The calcareous Blairmore sandstone(Lower Cretaceous, Red Deer River, Alberta) is a massive, very-well sorted, fine to very fine grained calcite-cemented submature, subgraywacke.[1] The non-oriented block used in this study was collected on the north side of the Red Deer River Highway about 2.7 km. east of the Hunter Valley Ranger Station, Alberta.

The effective porosity is 1.6 percent.[2] The saturated bulk density of the rock was determined to be 2.71 grams per cubic centimeter(Rector, Pers. comm.). The modal composition was determined by point counting. Results based on 509 points on a grid with a 1 millimeter spacing interval are given in Table 3.

The feldspar is comprised of twinned and untwinned plagioclase, as well as potassium feldspar. The individual grains of feldspar vary from fresh and unaltered to highly altered. Rock fragments include volcanic and shale varieties.

A chemical analysis was carried out by Mr. J. Muysson of the Rock Analysis Laboratory at McMaster University in order to determine the composition of the carbonate cement in the rock. Determination

---

[1]The discussion of sedimentological parameters will follow Folk(1961) except where noted.

[2]Porosity determination by Core Laboratories Canada Ltd., Edmonton, Alberta.

COMPONENT	PERCENT (by volume)
Calcite	39.4
Feldspar	24.7
Quartz	11.3
Rock fragments	10.7
Chert	8.3
Mica	0.8
Other	5.1
	100.3

Table 3. Mode determination of the calcite-cemented Blairmore sandstone based on 507 points.

by atomic absorption was carried out on the portion of the powdered sample which dissolved in hot hydrochloric acid.

Results from two different samples indicate that the samples consisted of 17.8 and 1.0 weight percent CaO and MgO respectively.

The low porosity, lack of deformation features, and poikilitic texture of the calcite cement indicate that the calcite was recrystallized following deposition of the rock. Calcite formed at less than 200 degrees Centigrade normally contains not more than 1 percent MgO (Deer, Howie & Zussman, 1962). The remainder of the MgO would be expected to form about 1 percent of dolomite within the carbonate cement. Staining for dolomite indicated tha presence of traces of dolomite within the rock.

Only five percent of the calcite occurs as a cryptocrystalline cement. The remaining 95 percent is comprised of microcrystalline grains which have a mean size of about 0.5 millimeters. Grains between 0.3 and 0.6 millimeters in maximum diameter are the most common. The maximum observed grain size was 1.5 to 2.0 millimeters. It is difficult to make precise determinations of the calcite grain size as the grains have irregular shapes and, frequently, completely surround one or more detrital grains forming a poikilitic texture. In general, the cement consists of medium to coarse grained calcite.

The mean free path(i.e. the distance between detrital grains) within the calcite cement was found to be .068 mm. using the technique outlined by Underwood and co-workers(1968). Linear traverses with orientation parallel and normal to, as well as at an inclination of 22.5, 45 and 67.5 degrees to the bedding plane, were made across a thin section of the starting material. The number of particles

intersected per length of traverse was determined for a total of 860 particles intersected over a traverse length of 146.5 mm. The mean free path was determined from the relation.

$$mfp = \frac{1 - V}{N_L}$$

where V = volume fraction of the dispersed phase

N_L = average number of particles intersected per unit length of line

Size and Shape of the Detrital Grains

During the determination of the modal composition of the undeformed rock, the detrital grains were also examined and measured. The maximum diameter, defined as the longest intercept across the grain, was measured. The minimum diameter, defined as the longest intercept at right angles to the maximum diameter was measured(Middleton, 1962).

The standard statistical parameters were then calculated using the method of moments with the aid of a computer program designed specifically for the analysis of thin section data(Parkash, 1968).

The size of each grain was calculated from the formula

$$\phi = -\log_2 k \quad ab$$

where

ϕ = grain size in phi units
a = maximum grain diameter in thin section
b = minimum grain diameter in thin section

and where a and b are measured in eyepiece micrometer units and k is a factor to reduce the units to millimeters.

In the analysis, the sorting is expressed in terms of one standard deviation about the mean grain size. Sphericity is measured by the

ratio b/a. The roundness was determined by comparison with standard roundness charts.

Determination of the characteristics has been made both for the detrital grains as a group, and for the quartz grains alone.

The results of the analysis of the detrital grains are given in Table 4.

There is little difference between the size and shape of the quartz grains and the other detrital grains. In general, the detrital grains are elongate and are angular to subangular. They have between 2.1 and 2.6 contacts per grain. These contacts are touching points or surfaces -- but no interpenetrative or silica-cemented contacts were observed.

Petrofabrics

The block from which experimental cores were drilled is essentially massive. However, an indistinct bedding lamination is apparent upon close examination. The anisotropy is more apparent in thin section where it is defined by the subparallism of the long axes of the detrital grains.

A histogram showing the angular relationship between the long axis of 100 quartz grains and the inferred bedding direction is given in Fig. 9.

Only 48 percent of the quartz grains have their long axis inclined at less than 30 degrees to the bedding plane(Rector, 1970, p. 34).

Two thin sections of the undeformed material were cut at right angles to the bedding lamination and to each other(Slides 413-D and

PROPERTY	ALL DETRITAL GRAINS	QUARTZ GRAINS	GENERAL CHARACTER
Mean grain size-			
phi units	2.73	2.75	fine to very-fine sand
millimeters	.150	.148	
Sorting-			
1 standard deviation in phi units	.24	.22	very well sorted
Sphericity			
short axis/long axis	.61	.58	elongate
Roundness[1]	.33	.29	angular to subangular
Contacts per grain	2.6	2.1	

[1]The roundness determination is based on the visual estimate of the degree of roundness of each grain as compared with standard charts using a scale of 0.1 to 1.0(from very angular to very well rounded).

Table 4. Grain size and shape characteristics of the detrital grains as determined in thin section.

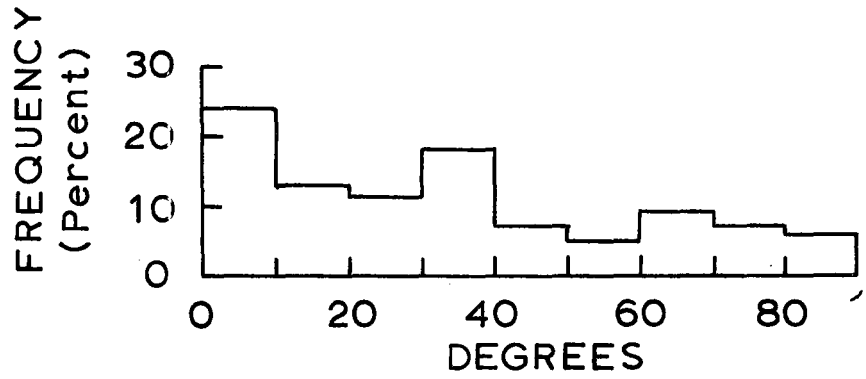

Fig. 9. Histogram showing the angular relation between the long axis of 100 quartz grains and the apparent bedding plane in the calcite-cemented Blairmore sandstone(From Rector, 1970, p. 34).

414-D2U).

Orientations of the optic c-axes of calcite grains distributed uniformly throughout the two slides were determined. A composite stereoplot of all of the c-axes is shown in Fig. 10.

The distribution of the points in Fig. 10 indicates that although the c-axes in the rock do not have a completely random orientation, the degree of preferred orientation is not great, and grains do occur which have orientations over most of the net.

Of the 95 percent of the calcite cement which is sufficiently coarse grained for petrofabric study, 67 percent contain no visible twin lamellae. The remaining 33 percent contain twin lamellae(25 percent contain one orientation and 7 percent contain two). A majority of these lamellae have orientations characteristic of e-lamellae (the poles to the lamellae lie at approximately 26 degrees to the optic c-axes). The lamellae are of the non-twinned(Borg & Turner, 1953) or micro-twinned type(Conel, 1962). They are developed to only a very limited extent, as the lamellae spacing index for the most intensely developed set is only 32.[1]

---

[1]The lamellae spacing index is based on the number of lamellae per millimeter when viewed on edge and measured along a line normal to the lamellae planes.

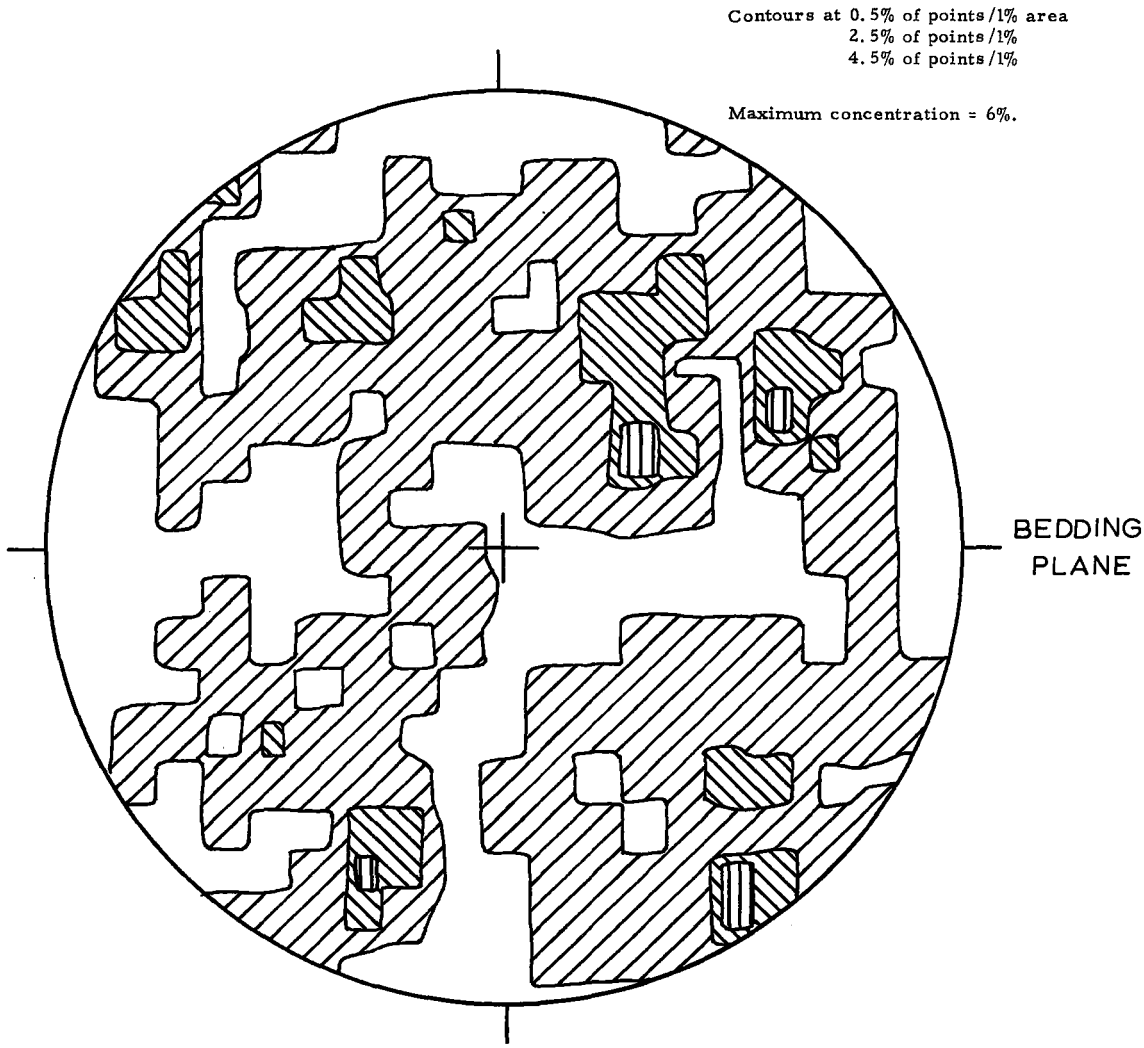

FIG. 10 COMPOSITE DIAGRAM SHOWING THE NEAR RANDOM ORIENTATION OF 100 C_v IN CALCITE CEMENT. PLANE OF DIAGRAM IS NORMAL TO BEDDING PLANE AS INDICATED.

Chapter 4

EXPERIMENTAL RESULTS

Introduction

Forty-four cylindrical specimens of the calcite-cemented Blairmore sandstone were subjected to between 2.14 and 19.82 percent shortening. The experiments were carried out dry at room temperature in a triaxial test apparatus at strain rates on the order of 10^{-4} per second and over the range of confining pressure between atmospheric and 2.60 kilobars(kb). A summary of the test results is given in Table 5, and the complete results are given in Appendix B.

In this section, we will first examine the macroscopic experimental results -- the strength behavior as reflected by the stress-shortening records and the appearance of the deformed specimens. We will then examine the microscopic features of the deformed specimens.

Macroscopic Aspects

(1) Stress-Shortening Records and Strength

The strength of a rock is a measure of the rock to withstand differential stress. In this section, we will consider the strength of the calcareous Blairmore sandstone as recorded by stress-shortening records of the experimental study. All strengths are expressed as differential stress($\sigma_1 - \sigma_3$). In particular, we will examine the yield strength at one percent shortening, the ultimate strength and the ductility and observe the effect of varying confining pressure on these variables.

Number of Tests	44
Temperature(°C)	21
Water Content	none
Confining Pressure(kb)	0 to 2.60
Total Shortening(percent)	3.13 to 22.06
Permanent Shortening(percent) (atmospheric)	2.14 to 19.82
Shortening Rate(prior to ultimate strength)	approx. 10^{-5}/second
Shortening Rate(average rate for test duration)	10^{-4}/second
Loading Rate	6.5 bars/second

Table 5. Summary of test data for deformed specimens used in this study. See Appendix B for a complete listing of data for each specimen.

Figure 11 shows the average stress-shortening curves for all confining pressures investigated. These curves represent the average results of the individual tests and were produced as explained in Appendix A.

2. Yield Strength, Ultimate Strength and Ductility

The point at which deformation is no longer elastic, but plastic, is that stress at which the slope of the stress-strain curve deviates from the elastic modulus. Precise determination of this point is very difficult and it is therefore necessary to use some approximation. The differential stress at 1.00 percent shortening is adopted for this study. This value is selected as it may be readily compared with other published data.

The ultimate strength is defined as the greatest stress difference $(\sigma_1 - \sigma_3)$ the material can withstand under the conditions of deformation and is taken as the maximum ordinate on the stress-shortening record.

For the purpose of this study, ductility is defined as the amount of shortening in percent, corresponding to the ultimate strength. This coincides with the development of fractures(i.e. the fracture strength) under brittle conditions, for confining pressures of up to 1.00 kb, and with the initiation of ductile faulting at higher confining pressures.

The yield strength, ultimate strength, and ductility for most of the test are shown in Fig. 12. Yield strengths for experiments performed at 1.0 kb or less are not shown as they differ little from the ultimate strengths. The effect of increasing confining pressure is

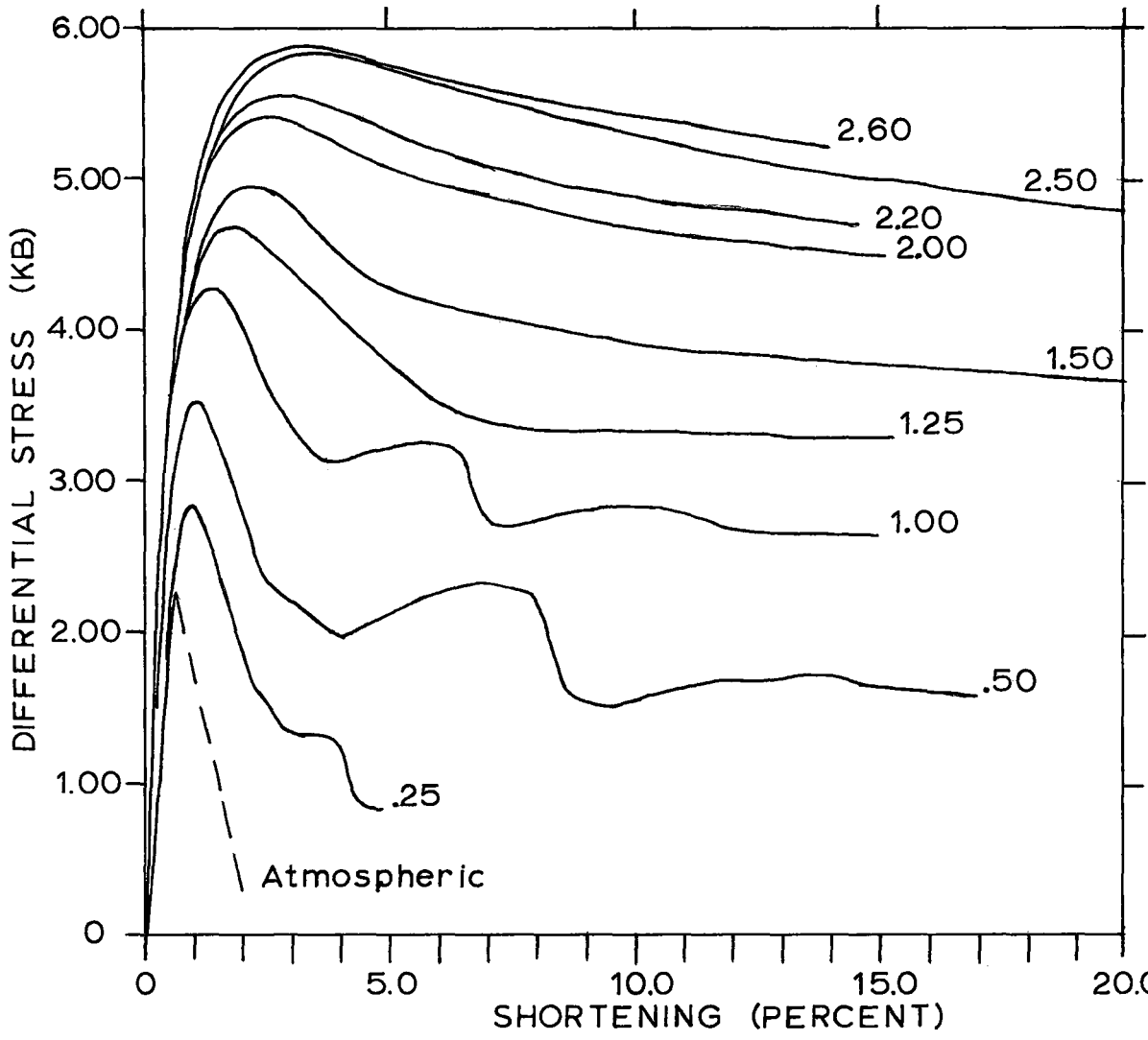

FIG. **11** AVERAGE STRESS-SHORTENING CURVES FOR THE CALCAREOUS BLAIRMORE SANDSTONE DEFORMED AT 21°C., AT A STRAIN RATE OF THE ORDER OF 10^{-4} PER SECOND. CONFINING PRESSURE IN KILOBARS SHOWN AT THE RIGHT OF EACH CURVE.

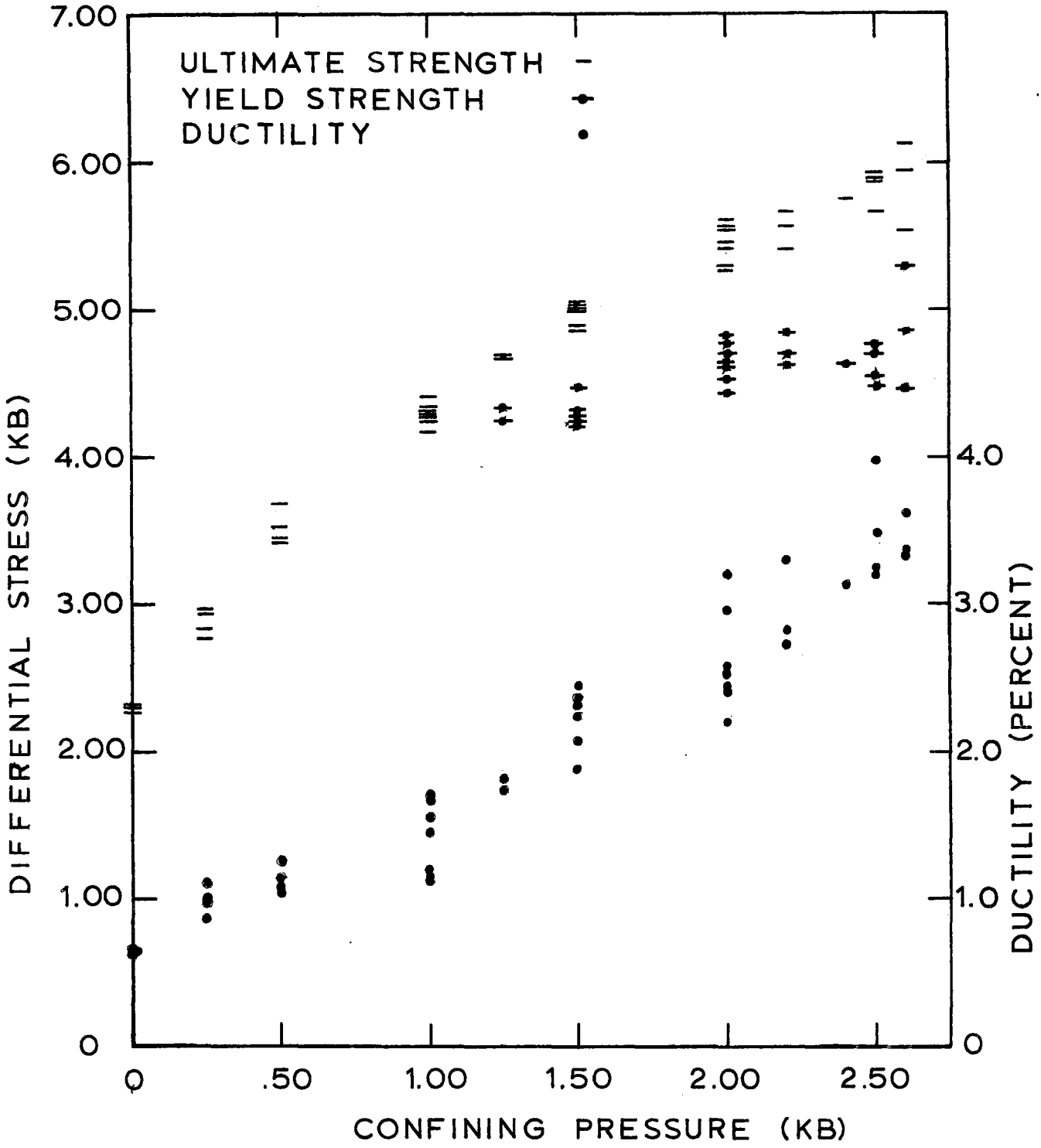

Fig. 12. Graph showing the yield strength(1.00 percent), ultimate strength, and ductility for the calcite-cemented Blairmore sandstone. Yield strengths at 1.00 kb confining pressure and below are not shown as they differ little from the respective ultimate strengths. All strengths given as differential stress, $\sigma_1 - \sigma_3$.

to increase the yield strength, ultimate strength and ductility of the rock. While the yield strengths and ultimate strengths do not differ very much for tests carried out below 1.00 kb confining pressure, above this level, the ultimate strength increases more rapidly than the yield strength.

Between atmospheric and 1.00 kb confining pressure, the ultimate strength is reached after shortening of 1.7 percent or less. Once the ultimate strength is reached, there is a sudden drop in the stress-shortening record associated with the development of fractures.

Additional shortening following the development of the initial fracture is accompanied by an increase in stress, followed by a second marked drop in stress associated with the development of a second shear fracture.

Over the range of confining pressure between 1.25 and 2.60 kb, the stress continues to rise once the yield strength is reached. However, in contrast to lower confining pressures, the stress-shortening record shows no marked drop once the ultimate strength is reached. Instead, the record follows a gradual downslopeing path, and the specimen maintains the ability to sustain a load which is equivalent to 70 percent or more of the ultimate strength even after shortening of as much as 15 to 20 percent.

In general, there is a uniformity of ultimate strength at any given confining pressure. With the exception of the three tests carried out at 2.60 kb confining pressure which have a spread of plus or minus 4.4 percent about the mean ultimate strength, all of the other tests vary less than plus or minus 3.0 percent about the mean ultimate

strength.

Comparison of the ultimate strengths at different confining pressures indicate that the strength increases approximately 240 bars for every 100 bars increase in confining pressure up to about .50 kb confining pressure. The magnitude of this effect decreases with increasing confining pressure and the ultimate strength increases about 90 bars for every 100 bars increase in confining pressure in excess of 2.00 kb confining pressure.

(3) Macroscopic Deformational Modes

The macroscopic deformational behavior of the calcareous Blairmore sandstone is characterized by a transition from very brittle at atmospheric confining pressure to ductile at 2.00 kb confining pressure. Plate 1 shows photographs of representative specimens deformed to different amounts of shortening over the range of confining pressures of this study. Figure 13 is a deformation mode plot summarizing the deformational behavior of all specimens of this study.

At atmospheric confining pressure, the deformation occurs through the development of two or more somewhat irregular failure planes inclined at an angle between 4 and 20 degrees to the core axis. The failure surfaces join to form wedge shaped fragments. Cohesion is lost and the specimen has no ability to support a load.

At confining pressures between .25 and 1.00 kb, failure occurs along a single shear fracture which develops at an average inclination of 30 degrees at low confining pressures(i.e. as low as 20 degrees at .25 kb)and greater than 30 degrees at 1.00 kb(e.g. up to 38 degrees). Shortening occurs primarily through displacement which takes place

Plate 1

Deformed specimens of the calcite-cemented Blairmore sandstone showing the characteristic appearance(x 1.5). The specimens are placed on a diagram which indicates the amount of shortening which each specimen has sustained, and the confining pressure at which each experiment was performed. A key for identification of each specimen is given below.

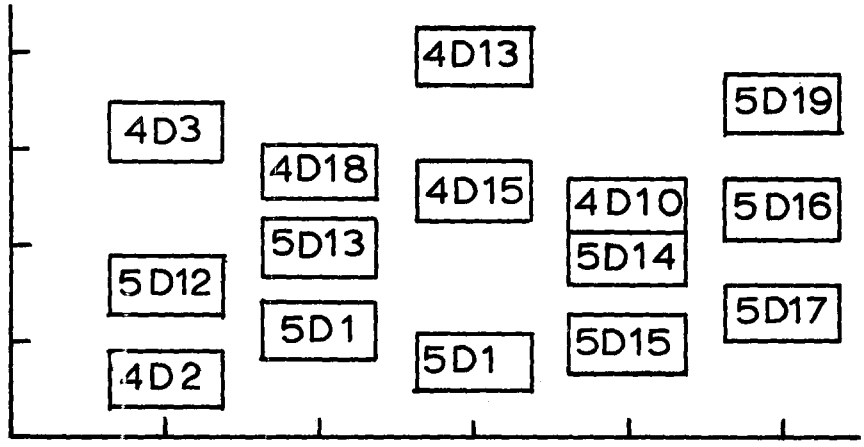

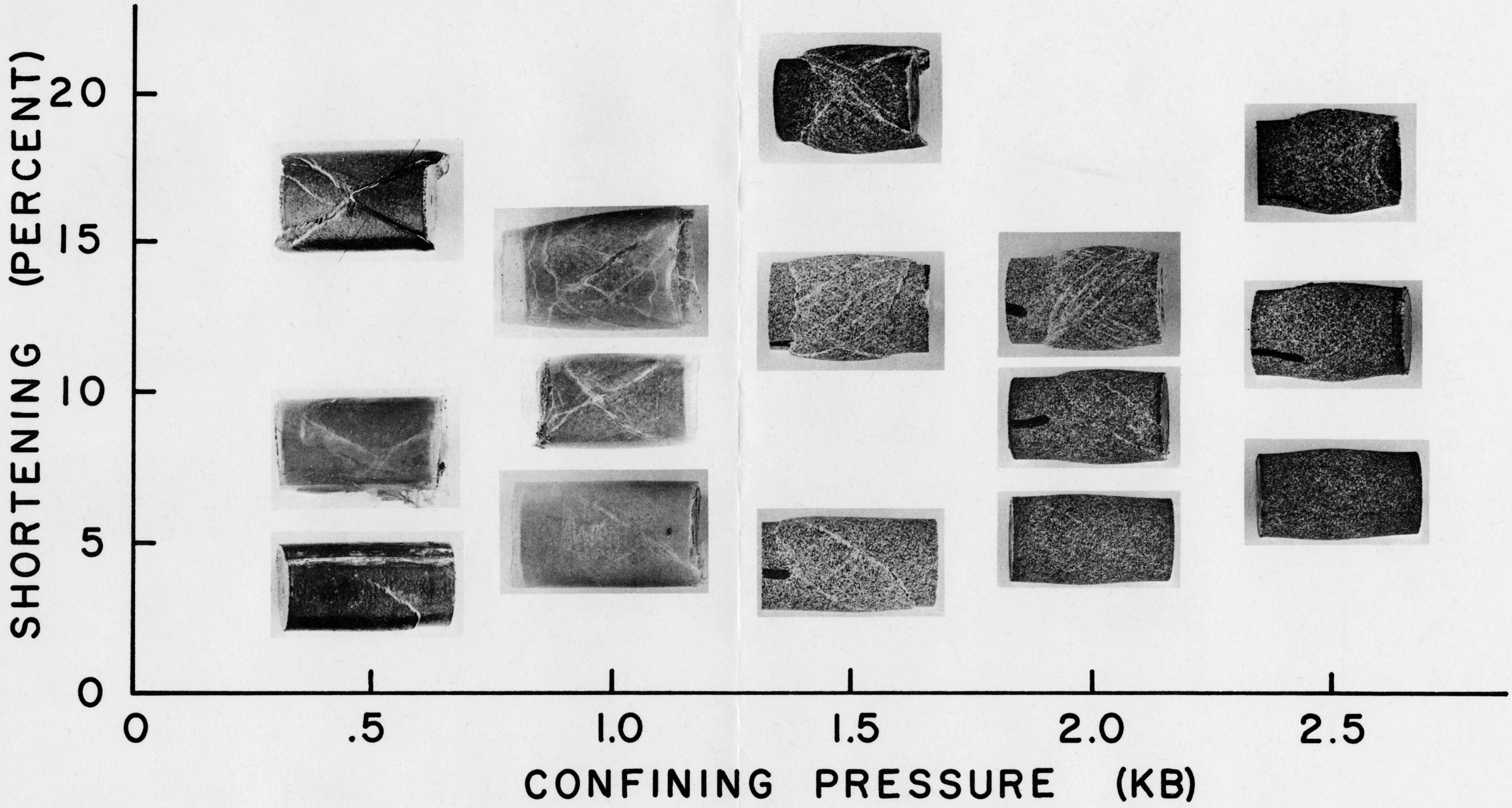
SHORTENING (PERCENT)
0
5
10
15
20
0
.5
1.0
1.5
2.0
2.5
CONFINING PRESSURE (KB)

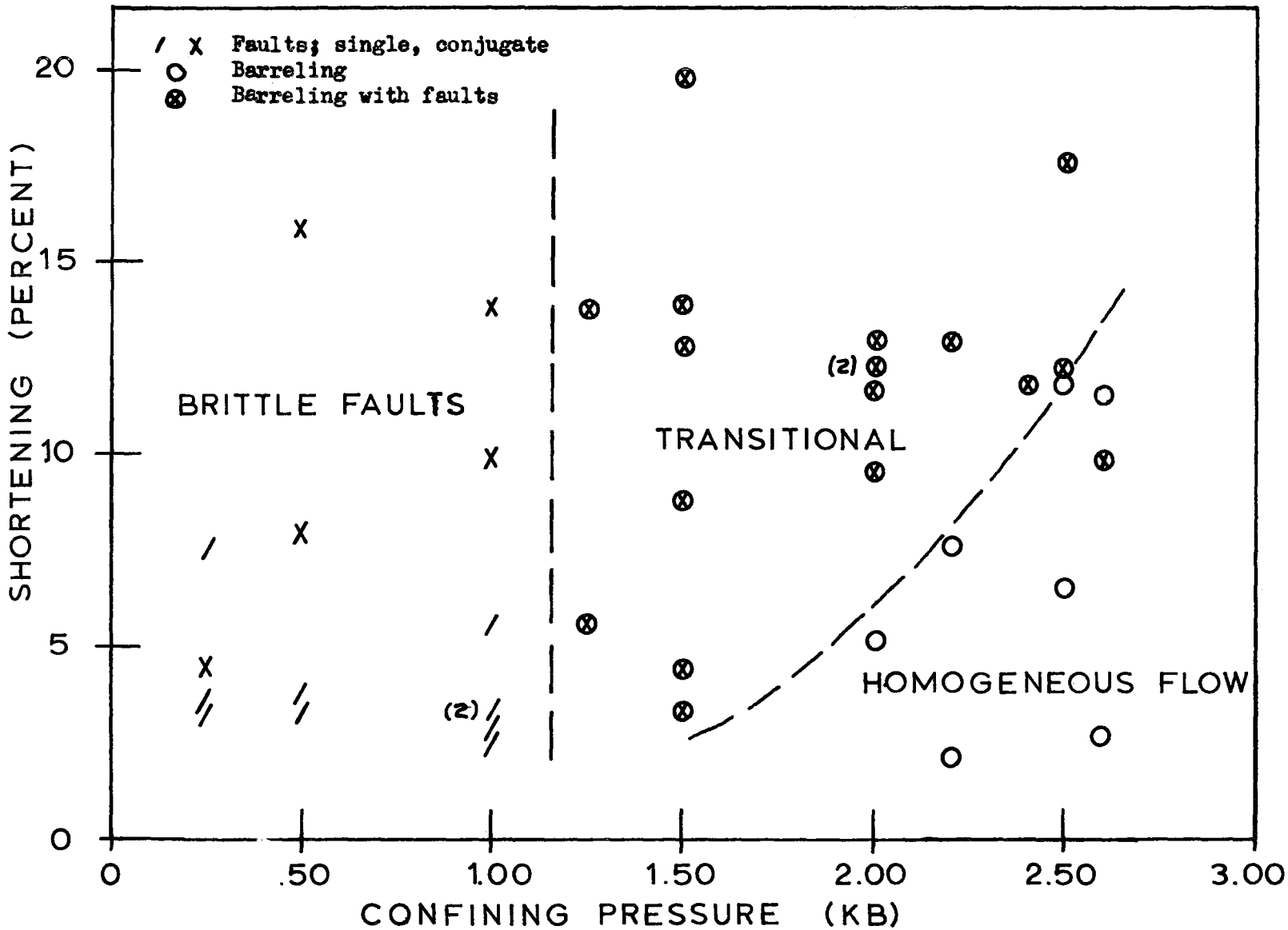

Fig. 13 Macroscopic deformation mode plot of the calcareous Blairmore sandstone, deformed at 21°C., and at a strain rate on the order of 10^{-4} per second.

along the shear surface, and the core maintains the form of a right circular cylinder which is offset along the failure surface.

Further shortening is accompanied by the development of one or more additional shear fractures which are inclined at about 30 degrees to the core axis. These shear fractures tend to intersect the earlier developed fracture along a line parallel to the diameter of the core.

At confining pressures of 1.25 and 1.50 kb, the initial displacement occurs along a zone which is marked near the specimen surface by two or more shear surfaces. The surfaces have an inclination between 28 and 40 degrees to the core axis. Examination under the microscope indicates that shear fractures do not form a single throughgoing surface, but rather diminish within the interior and pass into a central zone where no visible planes of slip are developed.

With increased shortening, additional surfaces or zones develop. The core surfaces are marked by the trace of the shear surfaces or zones and parts of the specimens develop uniform bulging characteristic of ductile behavior. Meanwhile, the central portion of the core develops a slightly schistose appearance which is oriented normal to the core axis. No clearcut shear surfaces are observed to pass through this region.

At confining pressures of 2.00 kb and above, the initial shortening of between 2.5 and 5 percent is accomplished by the near uniform distribution of strain over the specimen. Shortening in excess of 5 percent at 2.00 kb, or about 12 percent at 2.5 kb confining pressure, is accompanied by the development of non-uniform bulging, and minor shear surfaces become apparent.

Microscopic Deformational Behavior

(1) Method of Study

Microscopic examination of deformed specimens was carried out in order to define how deformation occurs within individual grains of a calcite-cemented sandstone. Description involved the determination of the types of features present, their frequency of occurrence and their orientation with respect to the applied load.

(a) Preparation of thin sections

Specimens were selected and thin sections were cut parallel to the long axis of the epoxy impregnated cores near a plane containing the diameter. In those cases where shear fractures or shear zones were developed, the thin sections were cut normal to the plane(s) of the zone(s). In other cases, the thin sections were cut in a random plane parallel to the long axis of the core.

(b) Microscopic study

The microscopic study of the thin sections was arranged so that ten traverse lines were established normal to the long axis of the core, with an interval of 1.5 mm. between the lines. The spacing of individual points along each line was at a 1.0 mm. interval. Thus, 100 points were observed which were distributed over an area of 1.0 cm. by 1.5 cm., within the central portion of the deformed core. As a result, the region within 1 mm. of each edge of the core, and the region within about 5 mm. of each end of the core were excluded from this study.

(c) Features observed

The following observations were made directly at, or adjacent

to, each point on the grid. One grain of quartz was examined and the number of microfractures was recorded. In practice, some clear unaltered feldspar was inadvertently included in this sample. One grain of feldspar was examined and the number of microfractures was recorded.

The nearest grain of calcite to the point under the cross hairs was also examined. In practice, this would represent the closest volume of calcite within a region between detrital grains, as many of the individual calcite grains in the starting material completely enclose one or more detrital grains to form a poikilitic texture. The presence or absence of lamellae was noted for each volume. The presence of through-going fault surfaces, through-going microfractures, and/or granulation was also noted.

The final result is a compilation of the type of deformation features within cement, quartz and feldspar grains distributed uniformly over the central portion of each deformed specimen. The actual record for each specimen was recorded on a grid which forms a map of the specimen. The map shows the relative distribution of the observed features with regard to such macroscopic features as shear fractures or zones.(See Fig. 14 for example) From this map, it is possible to ascertain whether microscopic features are more or less uniformly developed or are concentrated within certain parts of the deformed specimen.

(d) Orientation studies

The orientations of microfractures in detrital grains and twin lamellae within the calcite matrix were measured within selected specimens. Orientation measurements were made with the aid of a

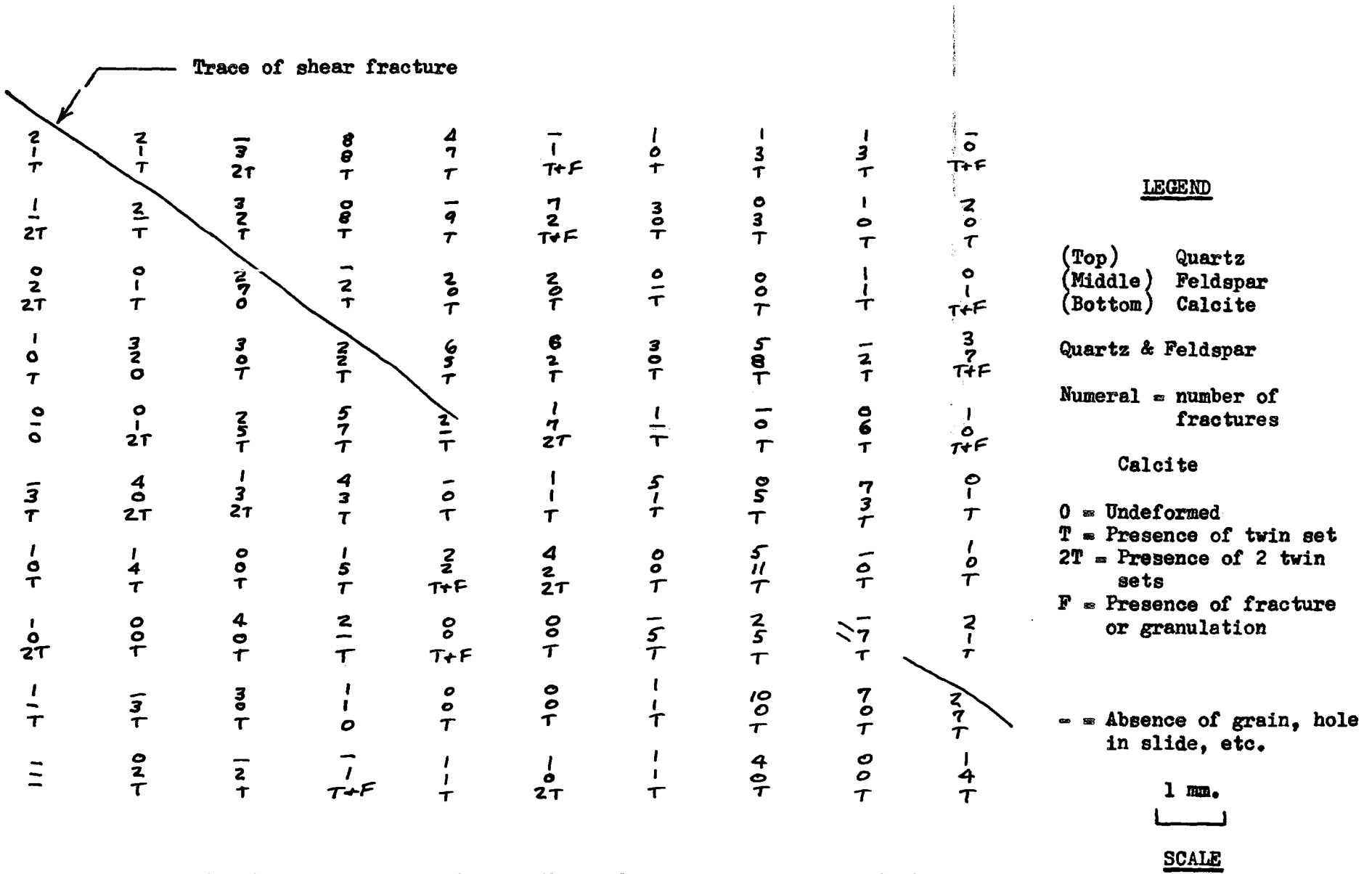

Fig. 14. Example of a map showing the number and distribution of microscopic deformation features of a deformed specimen. Map shown is for Specimen 4D11, shortened 4.22 percent at 1.50 kb confining pressure.

petrographic microscope equipped with a 4 axis Zeiss universal stage.

All orientation data (c_y attitude, calcite twin lamellae, and microfracture surfaces in quartz grains) are plotted stereographically on the lower hemisphere projection of Lambert-Schmidt equal-area nets.

(2) Observations

Comparison of the microscopic appearance of the undeformed calcareous Blairmore sandstone with experimentally deformed specimens of the same rock provides ready indication that deformation under the experimental conditions has a profound effect on the microscopic texture of the rock. The detrital grains deform in a brittle manner through microfracture development. The calcite grains of the matrix commonly exhibit profuse twin lamellae development. Fractured calcite grains are also present in some specimens. It is therefore evident that calcite deforms through both brittle and plastic mechanisms.

A summary of the results of the microscopic study is given in Table 6.

(a) Brittle fracture of detrital grains

Detrital grains of the undeformed Blairmore sandstone are essentially free of fractures; grains in the deformed specimens are not. In general, no matter which type of grain is observed, fresh or altered feldspar, quartz, chert or rock fragment, a large number of the grains contain one or more microfractures.

Some microfractures are irregular, but a majority are predominately planar to slightly curving. Where more than one fracture is developed within a detrital grain, they frequently occur in nearly parallel sets.

Fractures develop under three apparently different sets of

Specimen Number	Confining Pressure (kb)	Shortening (%)	Average number of fractures per quartz grain	Average number of fractures per feldspar grain	Percent of Calcite grains: Undeformed	Lamellae Bearing	Fractured	Twin lamellae index for most well developed twin set[3]	Fracture index for quartz grains[1]	Fracture index for quartz grains[2]
413	nil	nil	0.43	0.04	67	30	0	32	137	128
5D3	.25	3.18	0.94		39	50	11		152	150
4D2	.50	3.18	1.67		15	69	15		183	169
5D12	.50	7.91	2.29		9	68	23		197	186
4D3	.50	15.95	2.48		4	69	27		240	162
3D7	1.00	2.64	1.73		14	81	5		173	168
5D1	1.00	5.54	2.51		1	92	7		211	190
5D13	1.00	9.90	2.78		4	76	20		226	181
4D11	1.50	4.22	2.02	1.87	4	77	9		198	171
4D15	1.50	12.83	3.54	3.11	2	80	18		228	197
5D15	2.00	5.09	2.96		3	92	5	225	258	198
4D10	2.00	12.36	3.63		0	96	4		275	212
3D18	2.20	2.14			21	78	0			
5D17	2.50	6.50	2.39		0	97	3	323	204	178
5D19	2.50	17.57	3.58		0	95	5		237	202
3D10	2.60	2.64	1.30	1.69	11	89	0	188	176	168
3D19	2.60	11.49	3.85	3.71	3	87	10		254	217

[1]Based on fracturing in about 100 grains per specimen as follows: Percent unfractured grains x1, plus percent of grains with 1-3 fractures x2, plus percent of grains with 4-6 fractures x3, plus percent of grains with more than 6 fractures x4, plus percent of demolished grains x5, x100(Borg et al., 1960).

[2]Based on fracturing in about 100 grains per specimen as follows: Percent of unfractured grains x1, plus percent of grains with 1-5 fractures x2, plus percent of grains with 6-10 fractures x3, plus percent of grains with more than 10 fractures x4, plus percent of demolished grains x5, x100(Friedman, 1963).

[3]Based on the number of lamellae per mm. when viewed on edge and measured along a line normal to the twin planes.

Table 6. Summary of the microscopic deformation features of the calcite-cemented Blairmore sandstone.

circumstances. Most commonly, fractures transect grains and end at sites of grain-grain contacts. Fractures may also have one or more end which apparently corresponds to a portion of the grain boundary where adjacent grains are close to, but do not touch, the fractured grain. In the third case, fractures are present in grains which appear to "float" in the cement. In this case, there are no obvious touching or nearly touching grain-grain contacts. In a somewhat analogous case, fractures may develop within grains, in parts of the grain which are remote from the contact point(Plate 2).

Although elongated grains appear to be cut by more fractures, fractures are also commonly developed in grains which are essentially equant. Individual fractures may appear to be confined to the detrital grains, or they may be continuous with fractures within the calcite cement.

(b) Microfracture development within quartz grains

In order to carry out a more systematic study of the frequency and orientation of microfracture occurrence, it was decided to examine the microfractures which occur within only quartz grains. Quartz was selected for the study as the microfractures within the quartz grains are readily studied under the microscope, and furthermore, quartz has relatively well known, uniform properties which make it amenable to theoretical analysis. In addition, comparison of the average number of microfractures within quartz grains and feldspar grains of specimens 4D11, 4D15, 3D10 and 3D19 given in Table 6 indicate that the frequency of microfracture development is essentially equivalent in these two phases.

(a)

(b)

(c)

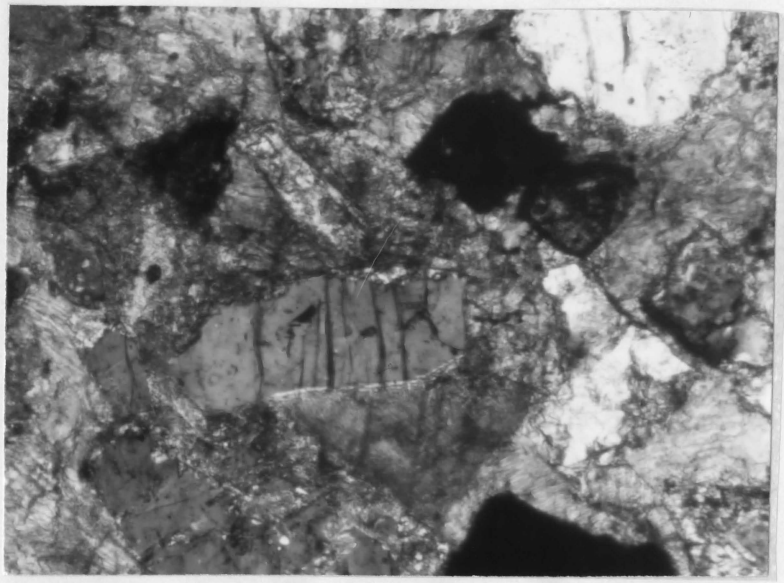

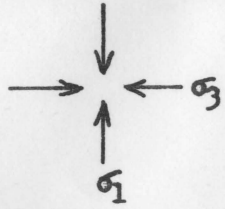

Applied Stress

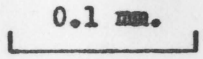

Scale

Plate 2. Photos showing microfractures within detrital grains and the various circumstances under which they develop. (a) Fracture formed at point of grain-to-grain contact. (b) Fractures formed at site of grain-to-grain contact and in non-contact portion of grain. (c) Fractures formed in detrital grain "floating" in calcite matrix. (All from Spec. 5D17).

The study of the frequency of microfracture development in quartz grains is based on the examination of approximately 100 grains per specimen using the method discussed on page 79. Histograms were prepared showing the frequency of grains versus the number of fractures per grain(Fig. 15).

As the undeformed calcareous Blairmore sandstone is comprised of 71 percent of the quartz grains having no fractures and 19 percent with one fracture(and most of these are cracks which cut only part way through the grain), it is clear that any significant increase in the number of fractures within quartz grains must be associated with deformation.

(i) Shortening of between 2 and 4 percent -- As little as 2.64 percent shortening is accompanied by a significant increase in the number of fractured grains. The percentage of quartz grains with no fractures is reduced from 71 percent in the starting material to 50 percent in specimen 5D3 deformed under .25 kb confining pressure. At confining pressures between .50 and 2.60 kb, the number of grains with no fractures is between 29 and 36 percent.

The total number of fractures per grain is generally less than five, and the average number of fractures per grain is between .94 and 1.73, as compared with an average of .43 fractures per grain in the starting material.

(ii) Shortening of between 4 and 6.5 percent -- Shortening of between 4 and 6.5 percent results in a further development of fractures in the quartz grains. The number of unfractured grains is reduced to between 12 and 25 percent at confining pressures between

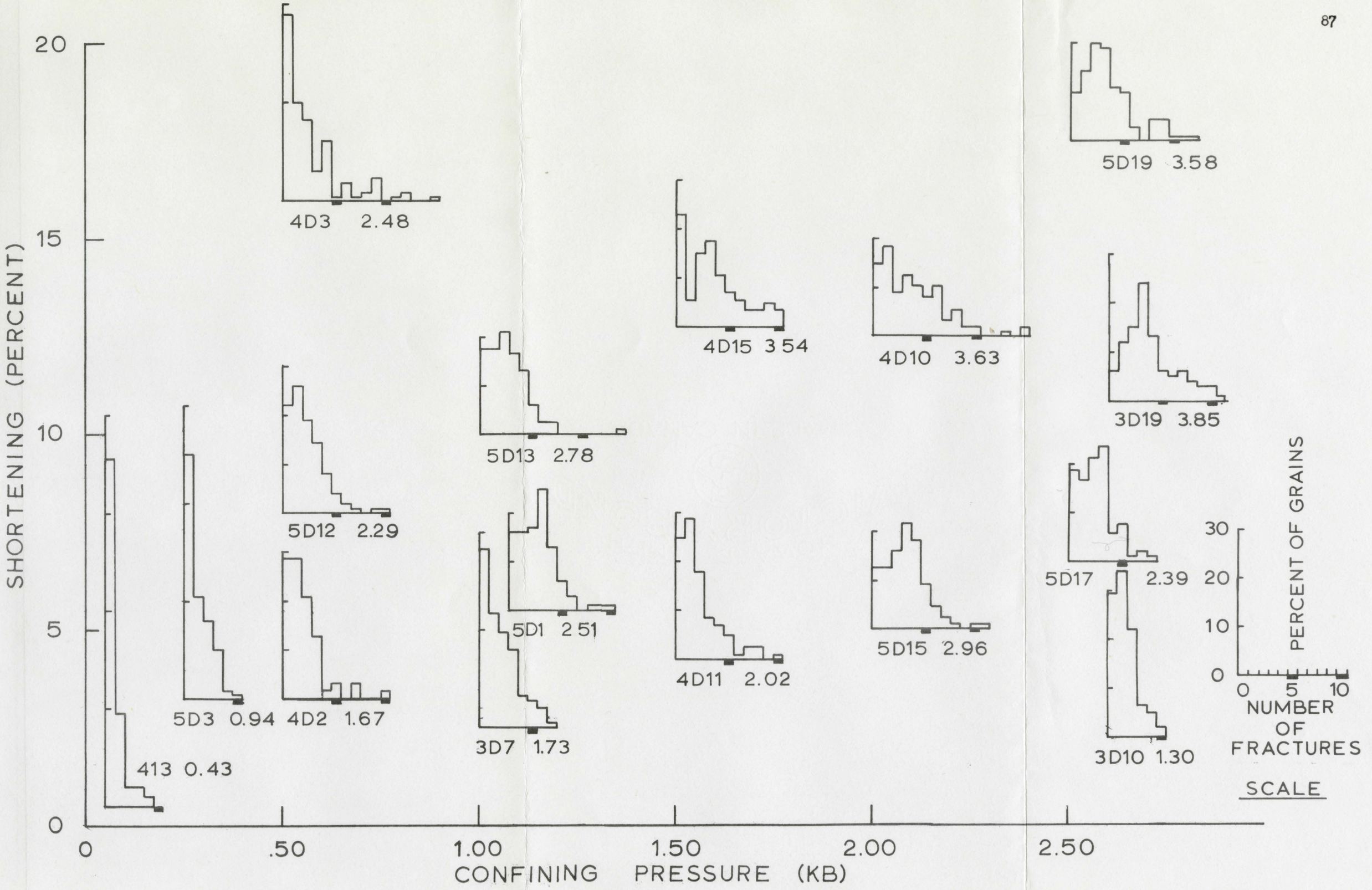

Fig. 15. Histograms showing the relative number of microfractures within quartz grains of the deformed specimens of the calcareous Blairmore sandstone. The arithmetic mean of the number of fractures per grain is also given with each specimen. The histogram near the origin shows relative number of fractures per quartz grain in the starting material.

1.0 and 2.6 kb inclusive. The number of fractures per grain is most commonly between 1 and 10, and the average number is between 2.02 and 2.96 fractures per grain.

(iii) Shortening of between 6.5 and 18 percent -- For confining pressures between 1.0 and 2.6 kb, the average number of fractures per grain is between 2.78 and 3.85. The number of unfractured grains is between 6 and 23 percent. A somewhat different pattern is evident for specimen 4D3, shortened nearly 16.0 percent at .50 kb confining pressure. The average number of fractures per grain is only 2.48, and 36 percent of the grains remain unfractured.

(c) Relative effects of confining pressure and shortening

Results of this investigation indicate that the frequency of microfracture development is dependent on both the amount of deformation and the confining pressure under which the deformation takes place. The effect of the two variables is shown in Fig. 16.

At confining pressures of .50 kb or below, quartz grains are not as intensively fractured on the average as at higher confining pressures. This contrast would be even greater if the few very highly fractured grains which occur within shear fractures were excluded from the average. In general, the specimens deformed at confining pressures of .25 and .50 kb have a relatively large number of grains with between zero and three fractures.

At higher confining pressures, fewer grains are left undeformed, and the average number of fractures and the amount of shortening is not linear. During the initial stage of deformation, shortening of

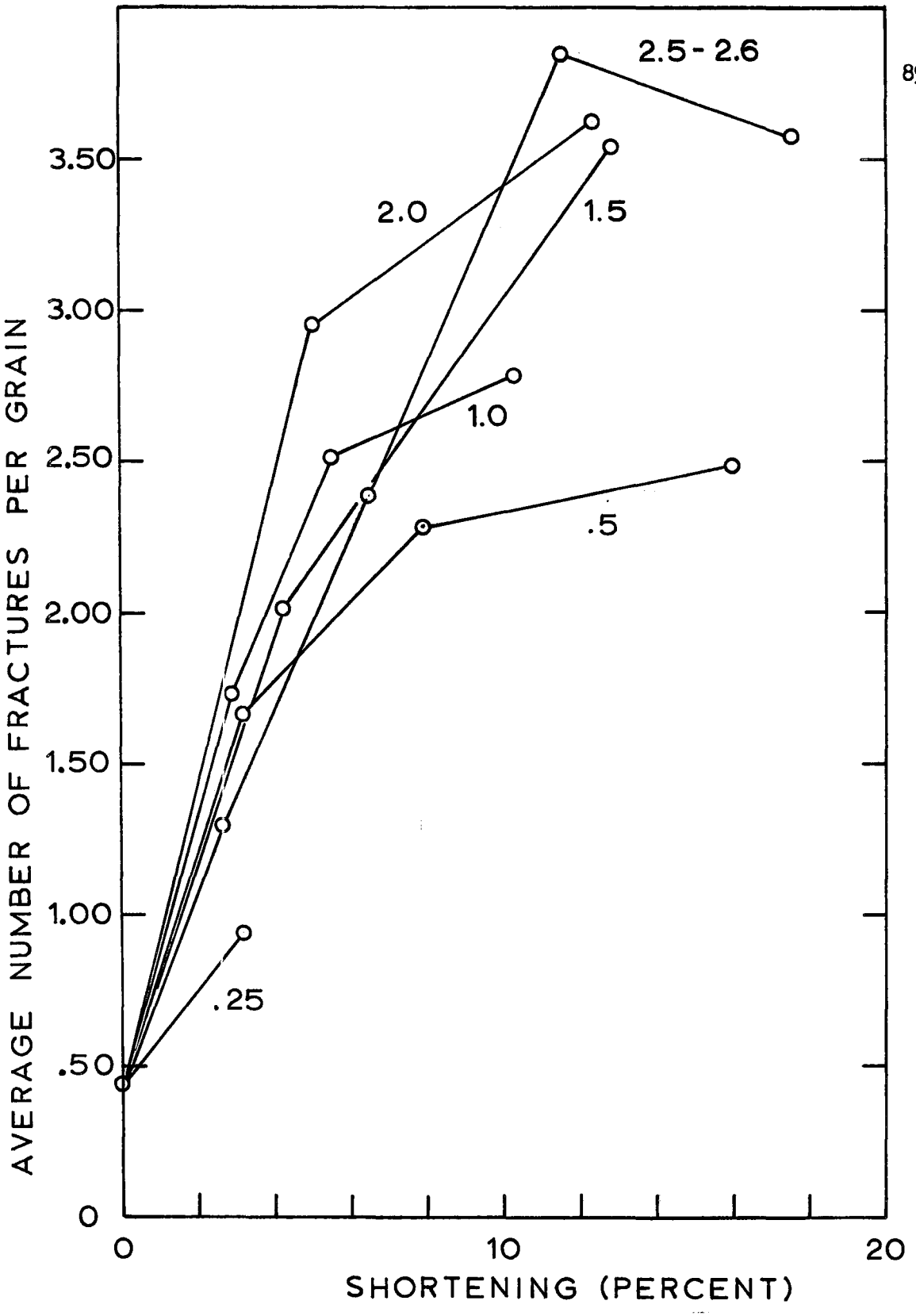

Fig. 16 Graph showing the relation between the numerical average of the number of microfractures per quartz grain and the amount of shortening for deformed specimens. Confining pressure, in kilobars, is indicated for each set of data.

about 5 percent results in the development of approximately 2.5 fractures per grain. A further increase in shortening to between 10 and 17 percent, however, results only in an increase to about 3.5 fractures per grain. It is apparent that the rate of fracture development is highest during the initial stages of shortening(i.e. up to about 5 percent) and decreases significantly above this level.

(d) Orientation of microfractures

It is readily apparent to even the casual observer that the microfractures developed within detrital grains have a high degree of preferred orientation. The universal stage was used to measure the orientation of sets of 2 or more parallel microfractures within quartz grains of specimens 4D11, 4D15, 5D17 and 5D19(Fig. 17). In addition, histograms showing the angular relationship between σ_1 and the poles to microfractures were prepared for each of these specimens (Fig. 18). It must be remembered that although the stereograms indicate that the poles plot as a point maxima, this is in fact part of a continuous girdle whose normal coincides with σ_1. This is because there is a central blind spot so that fractures inclined at less than 45° to the stage are not visible(Borg, et al., 1960).

Results of this study indicate that essentially all of the microfractures are oriented within 20 degrees of σ_1. Furthermore, between 68 and 80 percent of the microfractures are inclined at less than 10 degrees of σ_1.

Comparison or results from specimens 4D11 and 5D17, with specimens 4D15 and 5D19 indicates that there may be a somewhat greater spread associated with increased shortening, however the relative

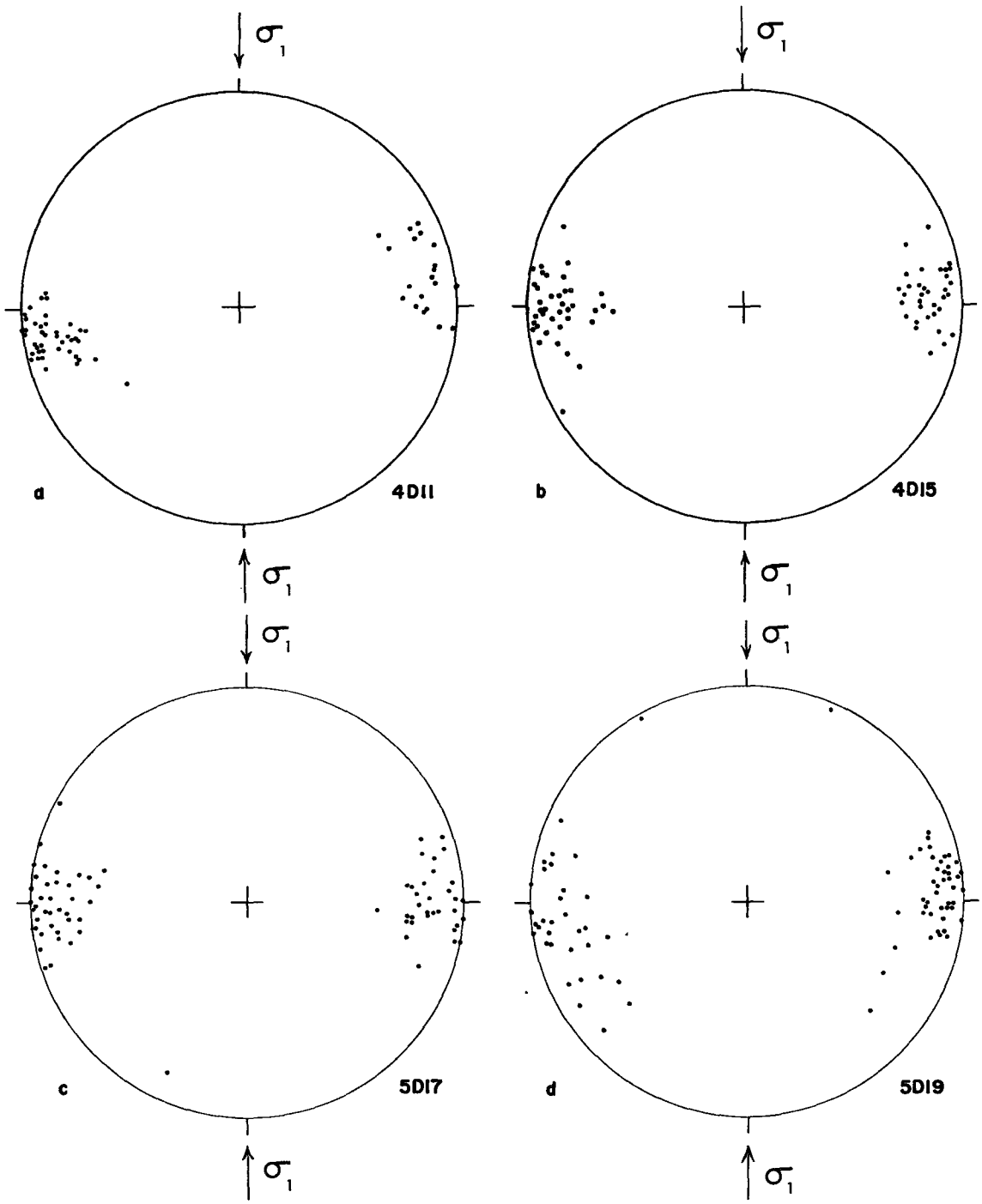

FIGURE 17. DIAGRAMS ILLUSTRATING ORIENTATION OF MICRO-FRACTURES WITHIN QUARTZ GRAINS WITH RESPECT TO LOAD AXIS. PLANE OF EACH DIAGRAM IS PARALLEL TO THE LONG AXIS OF DEFORMED CORE. a. SPEC. 4D11, POLES TO 61 SETS; b. SPEC. 4D15 POLES TO 73 SETS; c. SPEC. 5D17 POLES TO 69 SETS; d. SPEC. 5D19 POLES TO 75 SETS.

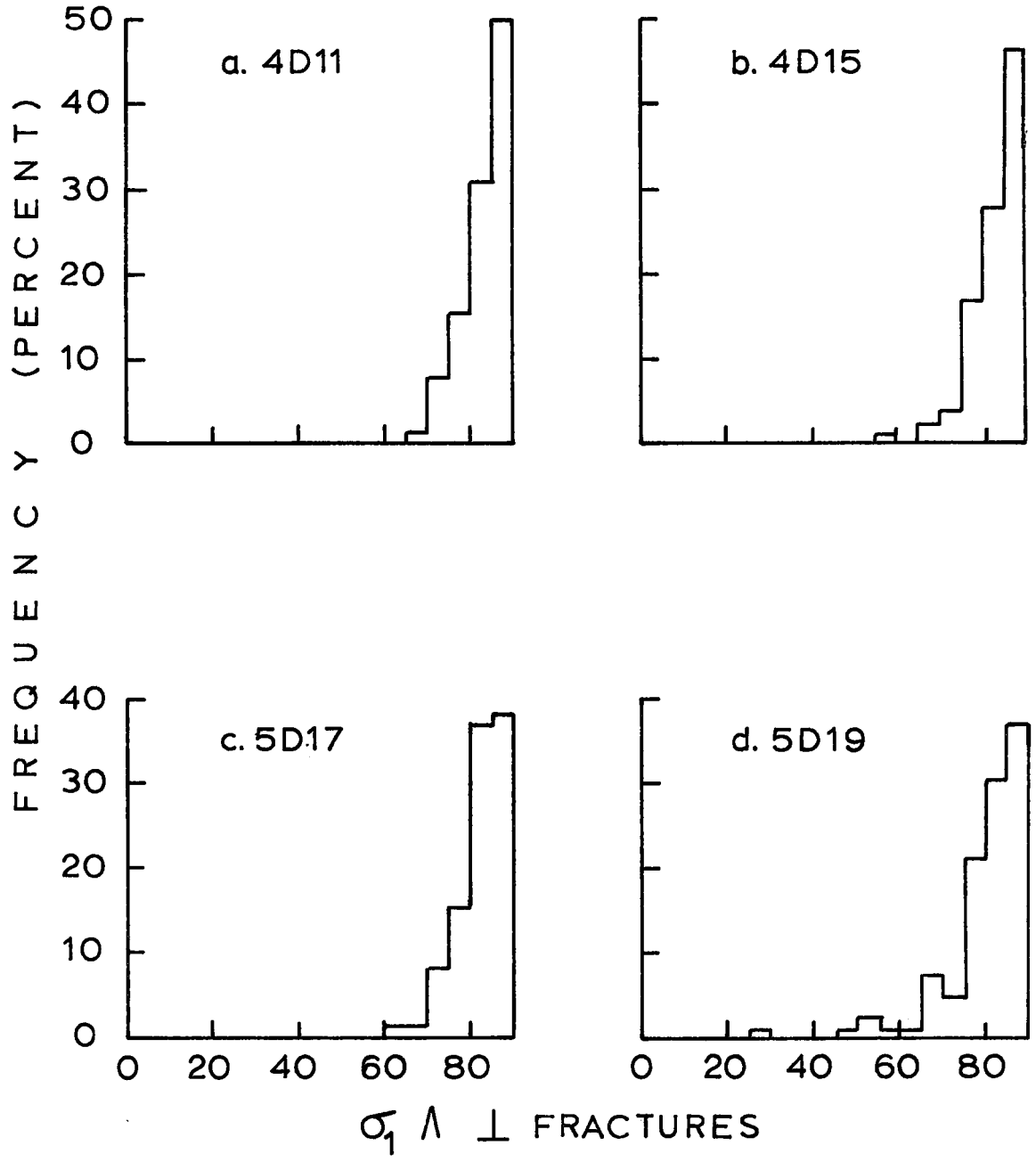

Fig. 18 Histograms showing the orientation of poles of sets, consisting of two or more microfractures, within quartz grains with respect to σ_1. a. poles to 61 sets in specimen 4D11; b. poles to 73 sets in specimen 4D15; c. poles to 69 sets in specimen 5D17; d. poles to 75 sets in specimen 5D19.

effect is not great.

In order to test the possibility that the orientations of sets consisting of 2 or more fractures may give a significantly different pattern than the orientations of individual fractures, the orientation of 184 single fractures in 64 grains of specimen 5D17 were measured with the universal stage. A stereogram showing the orientation of the fractures is shown in Fig. 19. A histogram showing the angular relation between σ_1 and the poles to the individual microfractures is also given in the same figure.

The results indicate that 82.5 percent of the individual microfractures are inclined at less than 20 degrees to σ_1, and that 60.5 percent are inclined at less than 10 degrees. Although these values are lower than the respective values of 97 and 85 percent for sets of 2 or more fractures in the same specimen, the dominant pattern of microfracture development nearly parallel to σ_1 is still very highly developed. There is clearly a strong preference for microfractures in detrital quartz grains to develop nearly parallel to σ_1. Although similar measurements of microfracture orientations in detrital grains other than quartz were not made, the pattern of microfracture development is apparently similar for all detrital grains.

(e) Summary of Quartz Grain Behavior

1. Microfractures develop within detrital grains distributed throughout specimens subjected to shortening under confining pressure.

2. The microfractures develop within a majority of grains in specimens which have been shortened between 2 and 5 percent.

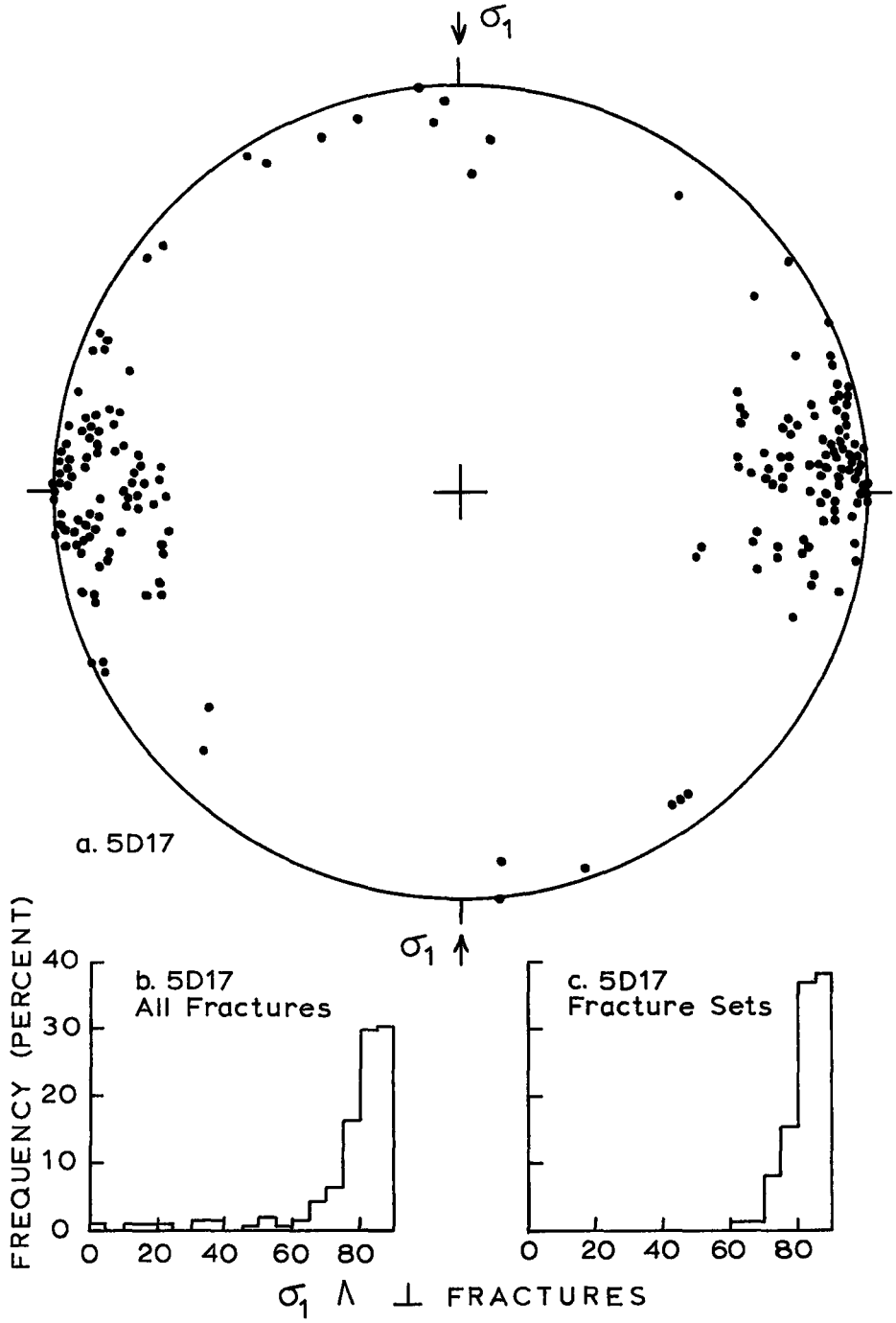

FIG. 19. DIAGRAMS SHOWING THE ORIENTATION OF INDIVIDUAL MICROFRACTURES AND SETS OF PARALLEL MICROFRACTURES WITHIN SPEC. 5D17. a. STEREOGRAM ORIENTED PARALLEL TO THE CORE AXIS SHOWING POLES TO 184 INDIVIDUAL MICROFRACTURES IN 61 QUARTZ GRAINS; b. HISTOGRAM SHOWING THE ANGULAR RELATION OF THE POLES SHOWN IN a. WITH RESPECT TO σ_1; c. HISTOGRAM SHOWING THE ANGULAR RELATION BETWEEN THE POLES TO 69 SETS OF PARALLEL MICROFRACTURES AND σ_1.

3. The development of microfractures is most clearly related to the amount of shortening which the specimen sustains. The number of fractures increases linearly up to between 5 and 10 percent shortening, and then the rate of fracture generation decreases.

4. For equivalent amounts of shortening, there is an increase in the frequency of fracture development up to about 1.0 kb confining pressure. Above 1.0 kb, there is little difference in the number of fractures at equivalent shortening.

5. Nearly all of the fractures, both individual and sets consisting of 2 or more parallel fractures, develop in an orientation which is inclined at less than 20 degrees to σ_1.

(f) Deformation of the Calcite Matrix

The calcite matrix of the starting material shows relatively few signs of deformation. Sixty-seven percent of the grains examined contain no visible twin lamellae. Furthermore, the twin lamellae spacing index of the most intensely developed set of lamellae within twinned grains is 32, which is quite low.

In contrast, the calcite grains of the deformed specimens commonly contain several different deformation features. Twin lamellae of the non-twinned or microtwinned type(Conel, 1962) are profusely developed. Calcite grains within shear zones are finely granulated and/or fractured, and slip surfaces mark the shear fractures. In some cases, microfractures developed within detrital grains extend into the adjacent calcite cement grains. Calcite grains exhibit bent lamellae and undulatory extinction.

The twin lamellae, fault surfaces, microfractures and granulated grains are the most widespread and obvious signs of deformation within the calcite matrix. It is known that these features also characteristically develop in other deformed limestones(Tobin, 1966). This is not to say that other modes of deformation such as translation gliding do not contribute to the strain, but rather that twin lamellae development, fault surface development, fracturing and granulation are the most significant features which may be readily studied under the microscope.

The low value of the shear stress required for the development of twins parallel to e$\{01\bar{1}2\}$ makes it probable that this mechanism accounts for a significant portion of plastic deformation. The near random orientation of the calcite grains assures that a significant portion of the grains will be favorably oriented for twin development. It is also apparent that under brittle conditions a major part of the shortening is taken up through shear displacements associated with shear fractures and/or restricted shear zones. This behavior is accompanied by the fracturing and granulation of the calcite matrix.

The study, therefore, involves the systematic census of the calcite grains in order to determine the presence or absence of lamellae, slip surfaces, major fractures and/or granulation as described on page 79. Minor fractures which cut only part way across grains have been ignored because of the uncertainity of recognizing them.

The results of the microscopic study are summarized in histograms

which indicate the relative number each of (1) undeformed grains, (2) grains containing twin lamellae and (3) fractured or granulated grains(shown as the left-hand, center and right-hand columns respectively) shown in Fig. 20. Grains containing fractures and lamellae are included only within the fracture mode. Each histogram is positioned on a stress-shortening grid near a point which corresponds to the confining pressure of the experiment and the amount of shortening.

(i) Shortening of between 2 and 4 percent -- Compared with the starting material, in all specimens deformed over the range of confining pressures between .25 and 2.60 kb, there is an increase in both the number of calcite grains which contain visible twin lamellae and the relative number of lamellae within twinned grains. (Specimens deformed under atmospheric confining pressure are not included in this portion of the study.) In contrast to the starting material in which 67 percent of the calcite grains contain no lamellae, the number of lamellae-free grains is between 3 and 15 percent in all specimens with the sole exception of 5D3. Furthermore, the degree of lamellae development within individual grains is high. (See discussion of twin lamellae spacing index within this section.) Specimen 5D3 was deformed at .25 kb confining pressure and contains 39 percent undeformed calcite grains. In general, not more than 10 to 20 percent of the grains have more than one set of lamellae developed.

At 2.20 and 2.60 kb confining pressure, no calcite grains show more than a minor development of microfractures. At lower confining pressures, between 5 and 15 percent of the calcite grains are cut by

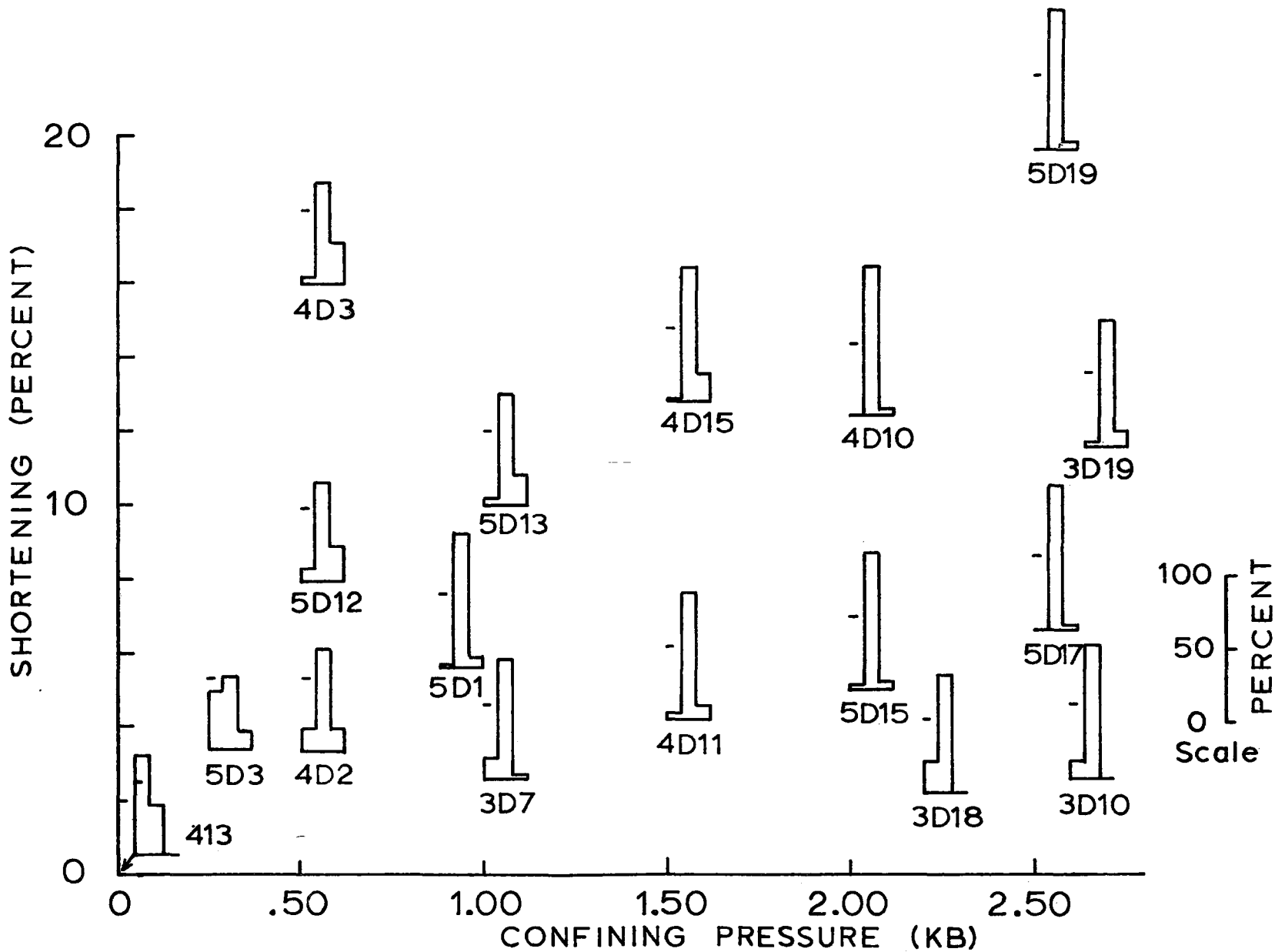

Fig. 20 Histograms showing the deformation state of calcite grains(undeformed, lamellae bearing and fracture modes from left to right) in specimens deformed to different amounts of permanent shortening at confining pressures between .25 and 2.60 kilobars.

faults or fractures.

(ii) Shortening of between 4 and 6.5 percent -- Increasing the shortening to between 4 and 6.5 percent results in the development of twin lamellae within nearly all grains(i.e. less than 4 percent of the grains remain undeformed) and an increase in the number of fractured grains(up to 11 percent).

(iii) Shortening of greater than 6.5 percent -- Essentially no calcite grains remain undeformed in specimens shortened more than 6.5 percent. The increase in the amount of shortening is accompanied by an increase in the number of grains in the fracture mode. The increase is greatest at low confining pressures where as many as 27 percent of the grains occur in the fracture mode as in speciemn 4D3, shortened 15.95 percent at .25 kb. In contrast, specimen 5D19, shortened 17.57 percent at 2.50 kb, has 5 percent of the calcite grains in the fracture mode.

(g) Orientation of Lamellae in Calcite

In order to determine the characteristic orientation of lamellae development, thin sections of specimens 5D15 and 3D18 were studied with the aid of the universal stage. Stereograms showing the lamellae orientation are shown in Fig. 21.

A consistent pattern of orientation is observed within the two specimens. Not more than 5 percent of the lamellae are inclined at less than 30 degrees to σ_1. Otherwise, the lamellae have a more or less uniform distribution of orientations.

(h) Intensity of Lamellae Development

In order to determine the relative intensity of lamellae develop-

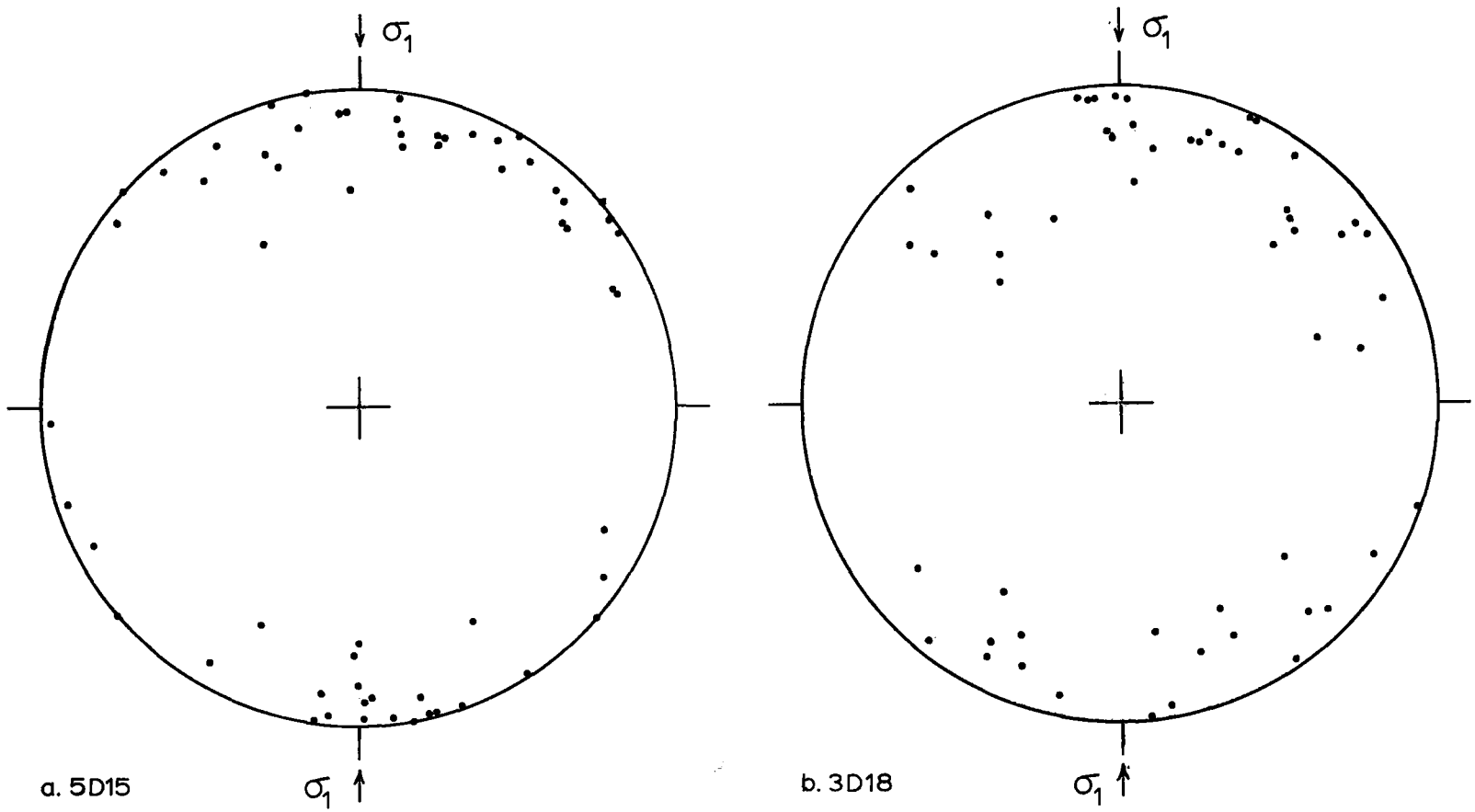

FIG. 21 STEREOGRAMS SHOWING THE ORIENTATION OF POLES TO CALCITE TWIN LAMELLAE IN DEFORMED SPECIMENS OF THE CALCAREOUS BLAIRMORE SANDSTONE. a. 55 POLES FROM SPECIMEN 3D18; b. 54 POLES FROM SPECIMEN 5D15.

ment, the lamellae spacing index was determined for 50 calcite grains, for each of three specimens(5D15, 5D17 and 3D18). These specimens were deformed at or above 2.0 kb confining pressure within the macroscopic field of homogeneous flow. Although the initial program of study called for the determination of the lamellae spacing index within a greater number of specimens, it was found that lamellae were so profusely developed within specimens shortened more than about 6.5 percent, that accurate determinations of the index could not be made. In fact, some difficulty was encountered even at lower strains, as the intensity of lamellae development makes accurate counting difficult. For this reason, the lamellae spacing index may not be as accurate as would be desired.

The average spacing index for the best developed set of lamellae (i.e. designated e_1) increases from 188 to 225 to 323 for relative shortening of 2.14, 5.09 and 6.50 percent respectively. The increase is approximately linear. Furthermore, not more than 25 percent of the grains exhibit more than one orientation of lamellae development. In general, the second orientation has a much lower lamellae index (e.g. 90 or less).

(h) Summary of Calcite Behavior

1. Calcite clearly deforms by both twinning and brittle fracture. The presence of bent twin lamellae and the development of undulatory extinction within some of the calcite grains indicates that translation gliding also contributes to the deformation.

2. Fracturing of calcite occurs commonly at low confining pressures, but is essentially absent at high confining pressures.

3. Twin lamellae are developed within all specimens deformed under confining pressures between .25 and 2.60 kb.

4. The relative number of calcite grains containing twin lamellae increases with increased shortening to 6 percent. At this level, essentially all grains show profuse lamellae development in specimens deformed under 1.00 kb confining pressure or more.

5. Determination of the twin lamellae spacing index within three specimens deformed between 2.00 and 2.60 kb confining pressure, indicates that the number of lamellae increases with increased shortening up to at least 6.5 percent.

6. Thin section study of two specimens indicates that the lamellae are more or less uniformly distributed over the orientation between 30 and 90 degrees to σ_1.

Discussion

(1) Strength and Macroscopic Deformational Behavior

The macroscopic deformational behavior of the calcareous Blairmore sandstone can be expressed in terms of the four fundamental modes of deformation -- longitudinal fracture, brittle faulting, ductile faulting and homogeneous flow. The transition takes place over the range of confining pressure between atmospheric and 2.00 kb.

Comparison of the experimental results from Friedman(1963) for the calcite-cemented Tensleep sandstone deformed under somewhat similar conditions to some of the tests of the present study indicates that the two rocks have comparable strengths and show similar deformational behavior under 1.00 kb confining pressure. Therefore, the

results of this study may provide a basis for understanding the deformational behavior of other calcite-cemented sandstones.

Although deformed specimens of the calcareous Blairmore sandstone have an appearance similar to deformed specimens of orthocalcite rocks(e.g. Paterson, 1958; Donath, 1964), comparison of the experimental results indicate there are some significant differences in behavior. In the first case, the uniaxial compressive strength is 2.30 kb. This is greater than the published strengths of most limestones and marbles, with the exception of the extremely fine-grained Solenhofen limestone(i.e. .008 to .0145 mm(Brace, 1961)). If the strengths of limestones with a grain size comparable to the dimensions of the calcite grain size in the Blairmore sandstone are compared, the Blairmore sandstone is found to be 3 to 4 times as strong as the orthocalcite rocks(Handin, 1966; and see p. 38).

Further contrasts in behavior under confining pressure may be defined with the aid of Fig. 22. The hatched area shows the field which defines the range of most published stress-shortening curves for limestones and marbles. The upper limit is defined by stress-shortening curves for the high strength Solenhofen limestone, while the lower limit is defined by curves for the Marianas limestone. Most other records plot within the double hatched portion of the field(Handin, 1966; Donath, 1964). Comparison of the deformation records show the following contrasts. During the initial stage of deformation(i.e. 1.7 percent at 1.0 kb and 5 percent at 2.5 kb confining pressure), the strengths are considerably higher for the sandstone(e.g. as great as 4 times). This contrast is greatest at the

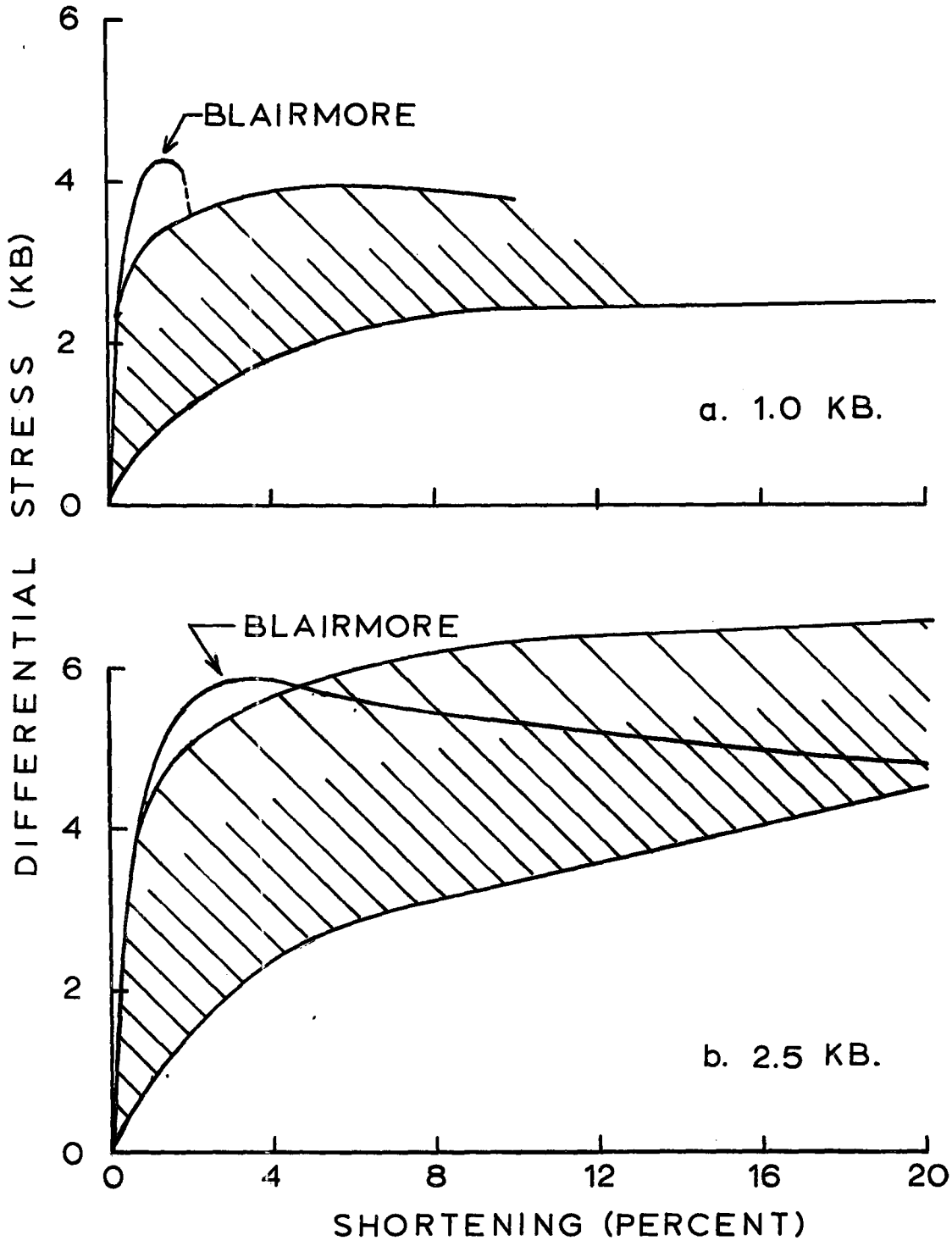

Fig. 22. Average stress-shortening curves for the calcite-cemented Blairmore sandstone at (a) 1.00 kb, and (b) 2.50 kb confining pressure. The hatched area covers the field of published curves for most orthocalcite rocks deformed under comparable conditions. The uppermost curve is for the very fine grained Solenhofen limestone, and the lowermost curve is for the Marianna limestone. Published curves most commonly fall within the double hatched area(Summary of data from: Handin, 1966; Donath, 1964).

level of the ultimate strength of the sandstone. The ductility or the strain before faulting is much greater in the orthocalcite rocks. Such rocks normally have ductilities in excess of 10 percent at 1.0 kb confining pressure(Handin, 1966). In contrast, the Blairmore sandstone has a ductility of about 1.5 percent under the same conditions. Homogeneous flow, marked by uniform deformation of the specimen and accompanied by a rising stress-strain record is characterisitc of most orthocalcite rocks at confining pressures in excess of .50 to 1.00 kb. In contrast, the Blairmore shows only limited homogeneous deformation at a confining pressure of 2.60 kb.

Further evidence of the strengthening effect of strong inclusions upon the strength of calcite is given in Figure 23. Comparison of published deformation records indicates that calcite single crystals containing sand grains may support a differential stress which is as great as one to two orders of magnitude greater than the stress which inclusion-free calcite single crystals may support under similar conditions.

In summary, it is apparent that a similar transition in deformational behavior related to increasing confining pressure is observed in both orthocalcite rocks and calcite-cemented sandstone. However, comparison of experimental results from tests performed at the same confining pressure indicates that the sandstone has greater strength and much less ductility than orthocalcite rocks. Furthermore, the brittle-ductile transition occurs at much higher confining pressures in the sandstone than in the marbles and limestones.

(2) Fracturing of Quartz Grains

The microscopic study of deformed specimens of the Blairmore sand-

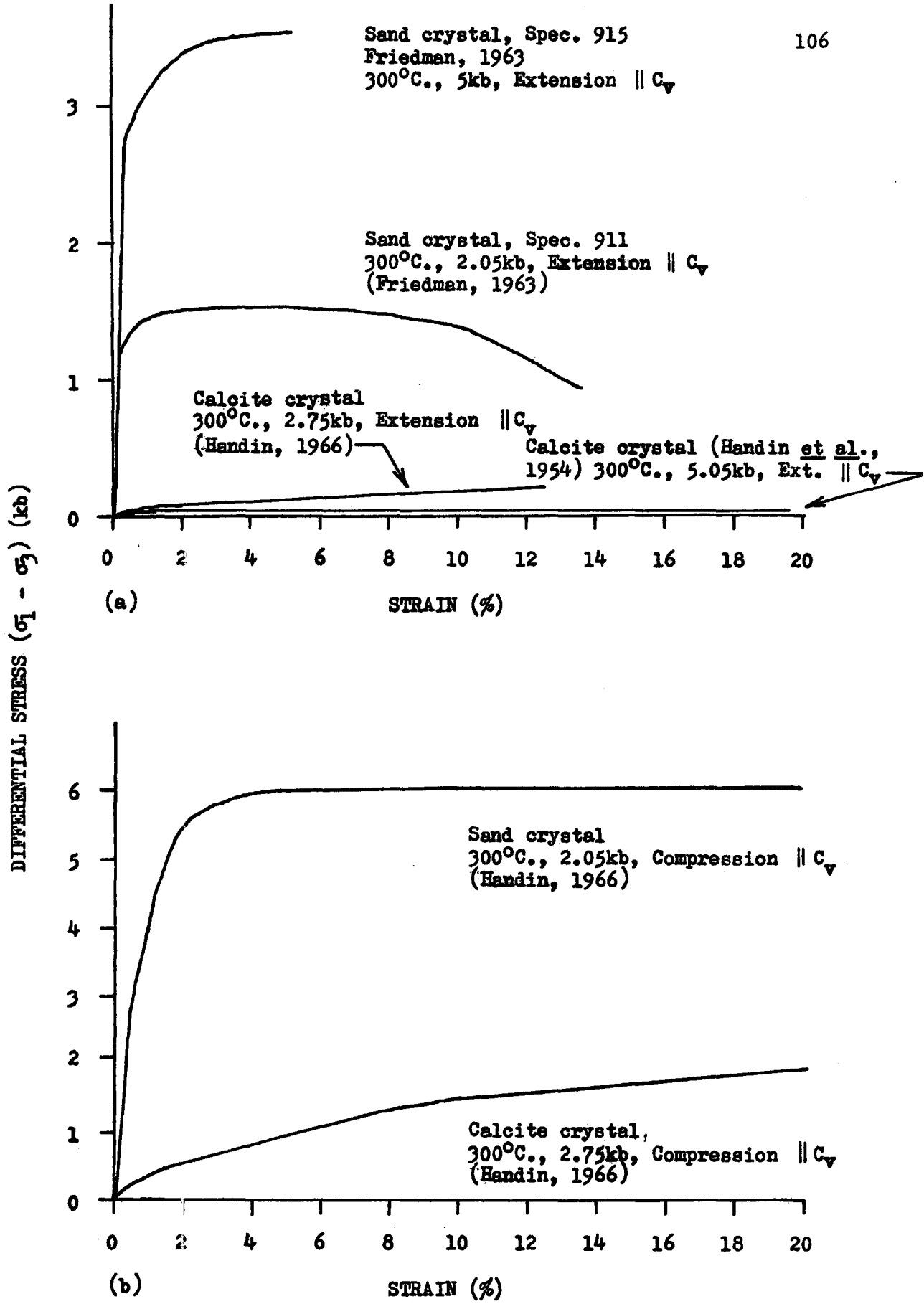

Fig. 23. Stress-strain curves for calcite single crystals and sand crystals under approximately the same conditions; (a) tests at 300°C., in extension ‖ C_v, (b) tests in compression ‖ C_v.

stone indicates that a majority of detrital quartz grains are cut by microfractures. These fractures show a high degree of preferred orientation which is nearly parallel to the direction σ_1.

The pattern and intensity of development of microfractures within quartz grains of the Blairmore sandstone is comparable to the development of microfractures within calcite-cemented sands previously studied by Friedman(1963). For example, two specimens of the Tensleep sandstone shortened 3.9 and 5.9 percent under conditions of 1.00 kb confining pressure and 150° C. have fracture indices of 169 and 184 respectively. Specimens of the Blairmore sandstone shortened 2.6 and 5.5 percent under 1.00 kb confining pressure gave indices of 168 and 190.

Furthermore, the pattern of development of microfractures with a preferred orientation nearly parallel to σ_1 is common to both(See below).

Similar behavior is observed in other calcite-cemented rocks deformed by Friedman even though his experimental conditions include both triaxial compression and extension, and span a greater range of temperature and pressure than the present study.

Results of this study indicate that the shape of the detrital grains apparently has little influence on the development of microfractures, as the Blairmore contains a high proportion of angular grains which exhibit low sphericity.

Microfracture development within non-cemented sands provides some interesting contrasts to cemented sands. The application of confining pressure to non-cemented quartz sands results in the development of numerous fractures within the quartz grains(Borg, et al., 1960). In contrast, Friedman(1963) found that the application of

confining pressure does not result in the development of fractures in calcite-cemented sands. Furthermore, the fracture indices for the sands are in most cases much higher than the indices of cemented sands which have been subjected to equivalent amounts of deformation(i.e. range of 262 to 382 for sands as compared with 152 to 275 for cemented sands).

There are several other differences between the fractures which develop within the grains of calcite-cemented and non-cemented sands and they are summarized in Table 7.

One of the most significant differences is that microfractures of detrital grains of cemented sands may develop within grains which apparently do not make contact with other detrital grains. This is the case for some fractured quartz grains of the Blairmore sandstone. Further evidence is given by Friedman(1963, p. 25 and Plate 3), who gives a photo and a sketch of fractured detrital grains which "float" within the calcite matrix of sand crystals and have no obvious contacts with other detrital grains.

Additional evidence that the individual quartz grains in a calcite-cemented sandstone may be subjected to a significant differential stress even though the deformed grains do not touch other strong detrital grains is found in the work of Carter and Friedman(1965). Microfabric analysis of the naturally deformed calcite-cemented Swift formation indicates the presence of deformation lamellae within quartz grains of this rock. The common occurrence of deformation lamellae within quartz grains of a rock consisting of 50 percent calcite, and with no touching grains led Carter and Friedman to conclude that the quartz was not deformed

	NON-CEMENTED SANDS	CALCITE-CEMENTED SANDS
Nature of microfractures	Fractures are conjugate or consist of a series of parallel planar breaks which join to form a single discontinuity.	Commonly planar or slightly curving.
	They radiate and curve away from point-to-point grain contacts, and are clearly related to the contacts.	Fractures develop both at point-to-point contacts and in portions of grains with no adjacent contacts.
	Sets of parallel trending fractures are rare.	Sets consisting of two or more nearly parallel fractures are common
Conditions of formation	Numerous fractures form upon application of confining pressure. Additional fractures form when differential stress is applied.	No fractures form upon application of confining pressure alone. Application of differential stress in excess of the yield stress(*sensu stricto*) results in the development of fractures.
Orientation of microfractures with respect to the applied stress field.	Fractures develop at essentially all orientations, but there is a tendency for the fractures to be inclined at less than 45 degrees to σ_1.	Fractures show a very high degree of preferred orientation nearly parallel to σ_1. Essentially all of the microfractures are inclined at less than 30 degrees to σ_1.

Table 7. A comparative summary of the characteristics of microfracture development within sand grains of non-cemented and calcite-cemented sands. (Observations on non-cemented sands from Borg & Maxwell, 1956; Borg, *et al.*, 1960).

solely by stresses transmitted across quartz-quartz contacts.

A further contrast between the development of microfractures in quartz grains of various materials may be observed with the aid of

Fig. 24. Histograms of this figure show the relative degree of preferred orientation of microfractures within detrital grains of calcite-cemented and non-cemented sands with respect to the imposed stress system. The summary includes results from four specimens of this study as well as published data for other materials. The specimen number, conditions of deformation, and the amount of strain are specified for each diagram.

The compilation has the following short-comings. The histograms for the non-cemented sands were derived from stereograms showing the orientations of the poles to individual microfractures, while the histograms for cemented sands show the relative orientation of poles to sets of 2 or more microfractures. Furthermore, although the histograms for cemented sands were constructed from stereograms giving orientation of individual poles, the published stereograms for the microfractures in non-cemented sands are contoured. Histograms for non-cemented sands therefore reflect the averages of the contoured diagrams and are somewhat less exact than the other data.

These short-comings are not thought to be too serious, however. It has been shown that the pattern of preferred orientation of individual microfractures and sets of microfractures does not differ significantly for specimen 5D17(Fig. 19). This suggests that the pattern of orientation of sets of fractures is reasonably representative of the orientation of all fractures.

Although the construction of histograms from contoured diagrams undoubtedly masks the orientation of particular zones of concentration, it does not significantly alter the major trends. The fact that less

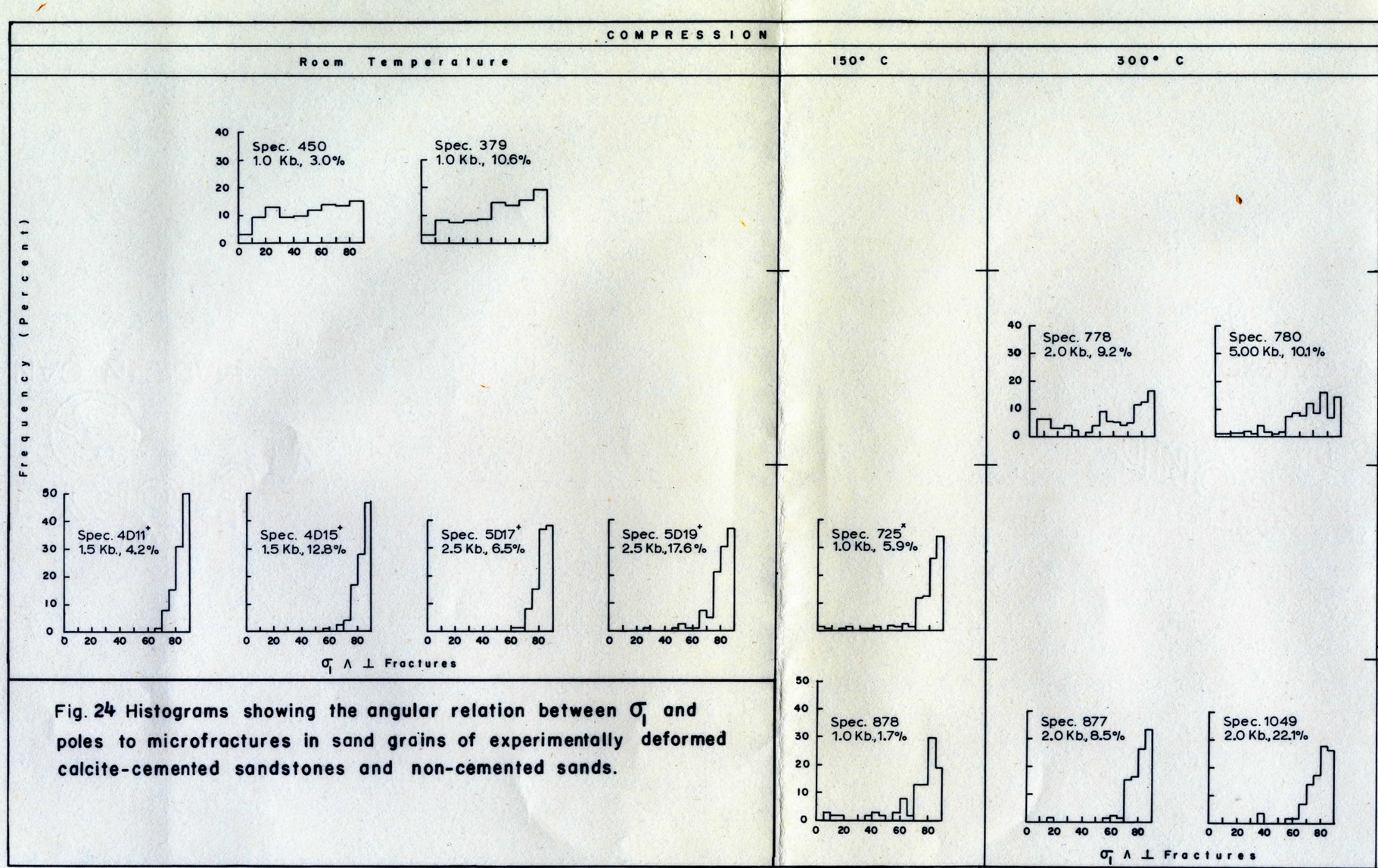

Fig. 24 Histograms showing the angular relation between σ_1 and poles to microfractures in sand grains of experimentally deformed calcite-cemented sandstones and non-cemented sands.

than 10 to 15 percent of the microfractures within sand grains of calcite-cemented sands of low porosity are inclined at more than 60 degrees to σ_1 is in marked contrast with the non-cemented sands where about 50 percent of the fractures are inclined at more than 60 degrees to σ_1.

Comparison of the various histograms indicates that the patterns of preferred orientation do have some common features. In all cases under a rather wide variety of experimental conditions, there is a marked tendency for microfractures to be oriented nearly parallel to σ_1. However, this tendency is much more well developed for cemented sands and sand crystals.

It is evident that the degree of preferred orientation of fractures in the deformed Supai sandstone(Friedman, 1963) is less well developed than in cemented sands of low porosity or for sand crystals, although the degree of preferred orientation is more highly developed than in non-cemented sands.

Friedman(p. 28-30) suggests that the observed spread of poles in specimen 780 of the Supai sandstone can be accounted for by rotation of the fracture planes away from their initial positions.

Consideration of the orientation of microfractures within specimens 1049, 4D15 and 5D19 shortened 22.1, 12.8 and 17.6 percent respectively, indicates that even though all of these specimens have been subjected to greater amounts of shortening than were either of the Supai specimens, they do not show the lower degree of preferred orientation which Friedman suggests is caused by rotation during shortening. It is therefore proposed that the greater variation in the orientation

of microfractures in the deformed Supai sandstone specimens must be accounted for in another way.

Ideally, it should be possible to account for all of the differences in microfracture development in non-cemented and calcite-cemented sands. The major differences are the conditions of formation, character of the microfractures and the orientation of the microfractures with respect to the imposed stress system.

Chapter 5

GENERAL DISCUSSION AND THEORY

Introduction

The deformational behavior of the calcite-cemented Blairmore sandstone can be understood in terms of the competition between brittle processes which result in fracture and ductile processes which are responsible for shape change. The mechanical behavior of the rock depends on the mechanical properties of the individual phases. It is also necessary, however, to consider the differential behavior and interaction of the relatively weak, ductile calcite matrix and the strong "rigid" detrital grains. An understanding of the micromechanics should provide an explanation for the development of the microscopic fabric, as well as accounting for the strength and ductility of the rock as a whole.

In the first part of the discussion, we will look at the macroscopic behavior and the stress-shortening records for the rock. Particular attention will be paid to how confining pressure affects the behavior. We will then turn attention to the development of the microscopic fabric.

Macroscopic Behavior and the Stress-Shortening Records

The stress-shortening records reflect the ability of the rock to sustain load under the experimental conditions, while at the same time they indicate the amount of deformation which the specimens undergo as

the load is applied. The appearance and shape of the specimen shows how the deformation takes place and how it is distributed over the specimen.

The record reflects both the inherent behavior of the rock and the mechanical restraint of the test apparatus. It is therefore necessary to consider the experimental effects in order to determine what part of the behavior is intrinsic to the rock itself.

(1) Experimental Effects

In the present study, the test apparatus is thought to influence the deformational behavior as a result of the (1) relatively low stiffness of the pressure vessel and loading system, and (2) through end effects resulting from interaction of the test specimen and the hard steel anvils through which the load is applied to the specimen. Jacketing is thought to have had little effect on the tests. A majority of the tests were carried out in light-weight polyethylene jackets which have little strength, yet provide a moisture-proof seal. Tests carried out in copper jackets were predominately within the brittle range and gave results which were similar to those of tests carried out in the light-weight jackets.

The elastic recovery of the test apparatus is most significant to the tests carried out under confining pressures up to 1.00 kb. In this range characterized by brittle failure and slip on shear surfaces, post-failure stress-shortening curves reflect the recovery of the machine as much as the intrinsic behavior of the rock(See p. 22 for discussion).

End effects are known to be responsible for (1) the development

of the barrel-shaped specimen during tests run under ductile conditions and (2) the development of symmetrical deformation(e.g. symmetrical faults) in tests carried out under more brittle conditions. It has also been proposed that the anvils may be responsible for the development of longitudinal fractures which develop in uniaxial compressive tests carried out at atmospheric confining pressure(Jaeger & Cook, 1969, p. 139), or that the behavior results from the geometry of the triaxial test(Jaeger & Cook, 1969, p. 148).

Lateral constraint resulting from frictional resistance at the specimen-anvil interface is responsible for barreling of ductile specimens and is a well-known phenomenon(Jaeger & Cook, 1969). A somewhat similar effect is observed in relatively brittle specimens deformed within the type of test apparatus where the anvils are not free to move laterally. Under these conditions, the ends of the test cylinder remain nearly coaxial and symmetrical features such as conjugate faults are observed to form(Donath, 1968). Such behavior occurs in the present study as specimens shortened more than four to five percent at confining pressures below about 1.00 kb develop conjugate faults. The second peak in the stress-shortening record reflects this aspect of machine restraint.

In contrast, deformation under otherwise similar conditions but in apparatus in which the apecimen is free to move laterally results in the formation of only a single fault or ductile zone. Furthermore, the stress-shortening record follows a downslopeing path terminating at rupture at smaller amounts of total shortening than is observed in the present study.

(2) Intrinsic Rock Behavior

(a) Behavior and strength in the uniaxial compression test

Stress-strain curves for the Blairmore sandstone(Fig. 25)deformed under atmospheric confining pressure have the characteristic S-shape associated with limestones and sandstones deformed under similar conditions(Miller, 1965; Friedman, et al., 1970). This curve reflects the normal elastic response of the rock and is expressed by the effective Young's modulus. Because of the rather large corrections necessary to account for the elastic distortion of the test apparatus, the experimentally determined value to the Young's modulus may not be very accurate. However, the values of the order of 0.2 to 0.5 x 10^6 bars are in agreement with published values for limestones and sandstones(Birch,1966).

It is readily apparent that these values are well below either the intrinsic Young's moduli of the individual phases or a composite value based on a simple rule of mixtures calculation. The low value is thought to be caused by the presence of porosity and cracks. Both types of imperfections act to reduce the effective elastic constants to values which are markedly less than the level of the intrinsic elastic constants for material free from imperfections(Jaeger & Cook, 1969, p. 313-321; Brace, 1964).

Under atmospheric confining pressure, the rising curve is terminated by brittle fracture at about .65 percent shortening. The sudden drop of the record reflects the elastic recovery of the apparatus as discussed earlier. Upon removel from the test chamber, the specimens are found to be divided by two or more irregular to planar surfaces oriented at a small angle(i.e. 4 to 20 degrees) to the core axis.

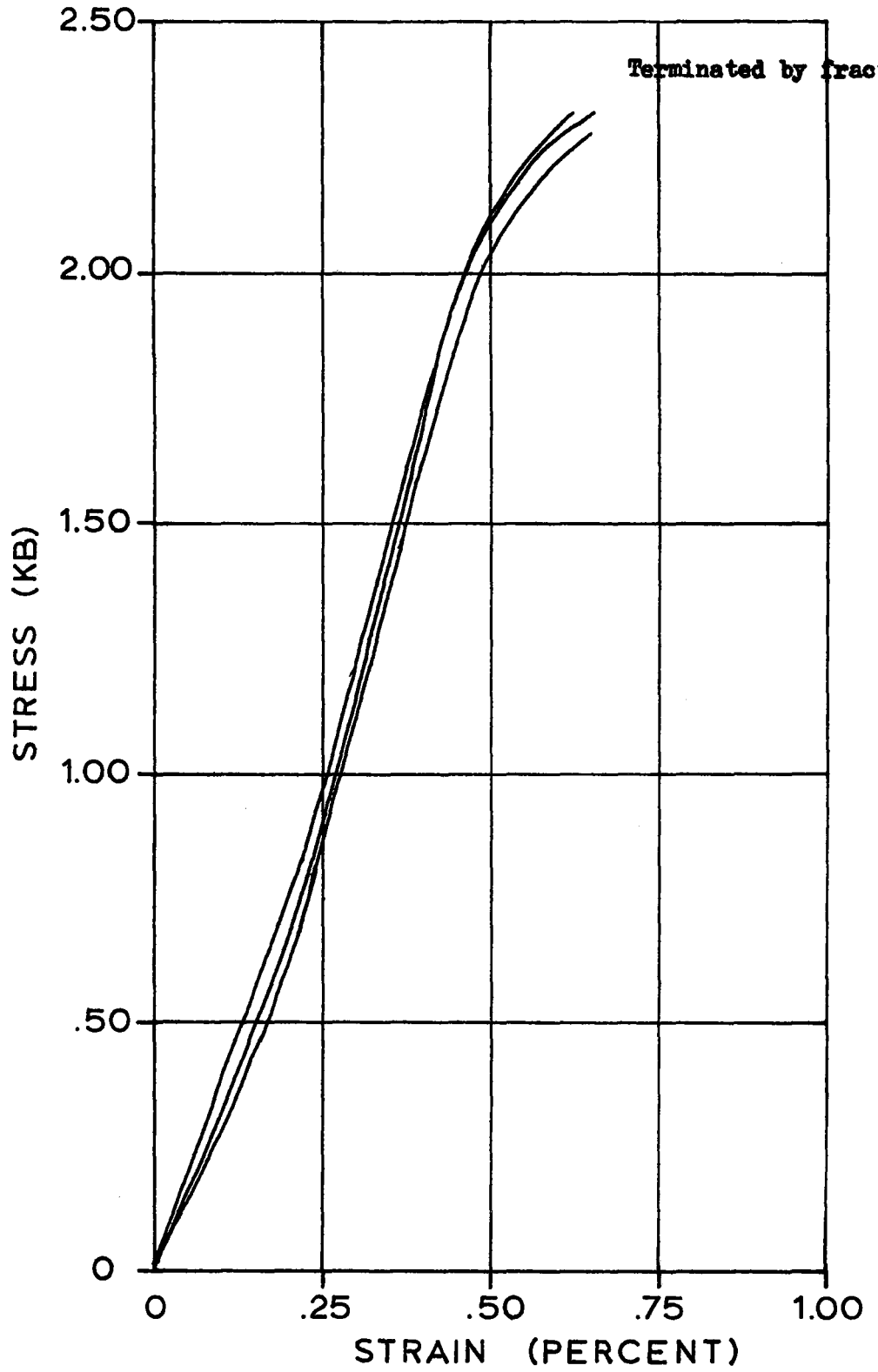

Fig. 25. Stress-strain curves for the calcite-cemented Blairmore sandstone deformed at room temperature, atmospheric confining pressure and a strain rate on the order of 10^{-5} per second.

The experiments indicate that the rock tested can sustain an axial load of 2.31 kb(mean of three tests--2.28, 2.34 and 2.32 kb) under the test conditions. This puts the rock within the "very high strength" class of Deere's classification system(1966) indicating that the rock has a high strength as compared with many rocks.

b. Griffith Theory and the uniaxial compressive strength

Discussions of the ultimate factors controlling brittle rock strength have been limited in number. The only commonly considered mechanistic theory of rock strength is the Griffith Theory.

The Griffith Theory assumes the pre-existence of small flaws or cracks within the material. These cracks act to produce stress concentrations of sufficient magnitude so that the theoretical cohesive strength is reached in localized regions at an average applied stress which is well below the theoretical value. For the uniaxial compressive condition, the Griffith Theory predicts a strength which is eight times the tensile strength, and the Griffith equation is then $\sigma_{compressive} = 8(2E\gamma/\pi c)^{\frac{1}{2}}$.

Brace(1961;1964) has demonstrated that the Griffith Theory apparently accounts for the failure strength of monomineralic rocks such as limestone and quartzite, and that the flaw size, 2c is equivalent to the grain size in these rocks. A similar relation has been shown for anhydrite(Skinner, 1959). With the exception of Houpert(1966), who found a grain size-strength dependence for granite which he related to Griffith Theory, little consideration has been given to the determining factors of the strength of rocks consisting of more than one mineral phase.

Work of Hasselman, Fulrath and other investigators(Hasselman & Fulrath, 1966; 1967; Nivas & Fulrath, 1970; Tummala & Friedberg, 1970) in ceramic systems, however, suggests an approach whereby the Griffith Theory may be applied to give an understanding of the brittle behavior of some polymineralic rock materials(See discussion on p. 53).

Experiments performed by these investigators involved the determination of the strength of two phase ceramic materials consisting of strong inclusions within a brittle glass matrix. The inclusions act to limit the size of potential Griffith flaws by limiting the mean free path within the glass matrix. The strengths of the ceramic materials can be accounted for if the Griffith flaw size is considered to be equivalent to the mean free path within the brittle glass matrix.

The investigation of uniaxial compressive strength of the calcareous Blairmore sandstone focuses on the determination of the potential size of Griffith flaws. It is also necessary to consider other factors which are thought to affect the brittle strength of two phase materials.

Griffith flaws are most commonly thought to be situated at grain boundaries or to lie along planes of weakness within individual grains. The dimensions of the detrital grains and the calcite grains were determined during the petrographic study of undeformed material. In addition, the mean free path within the calcite matrix was determined. These values are plotted versus strength in Fig. 26. Comparison of the strength of the Blairmore sandstone with the experimentally determined uniaxial strength curve of limestones(Brace, 1964) indicates that the strength is more than four times as great as the strengths of

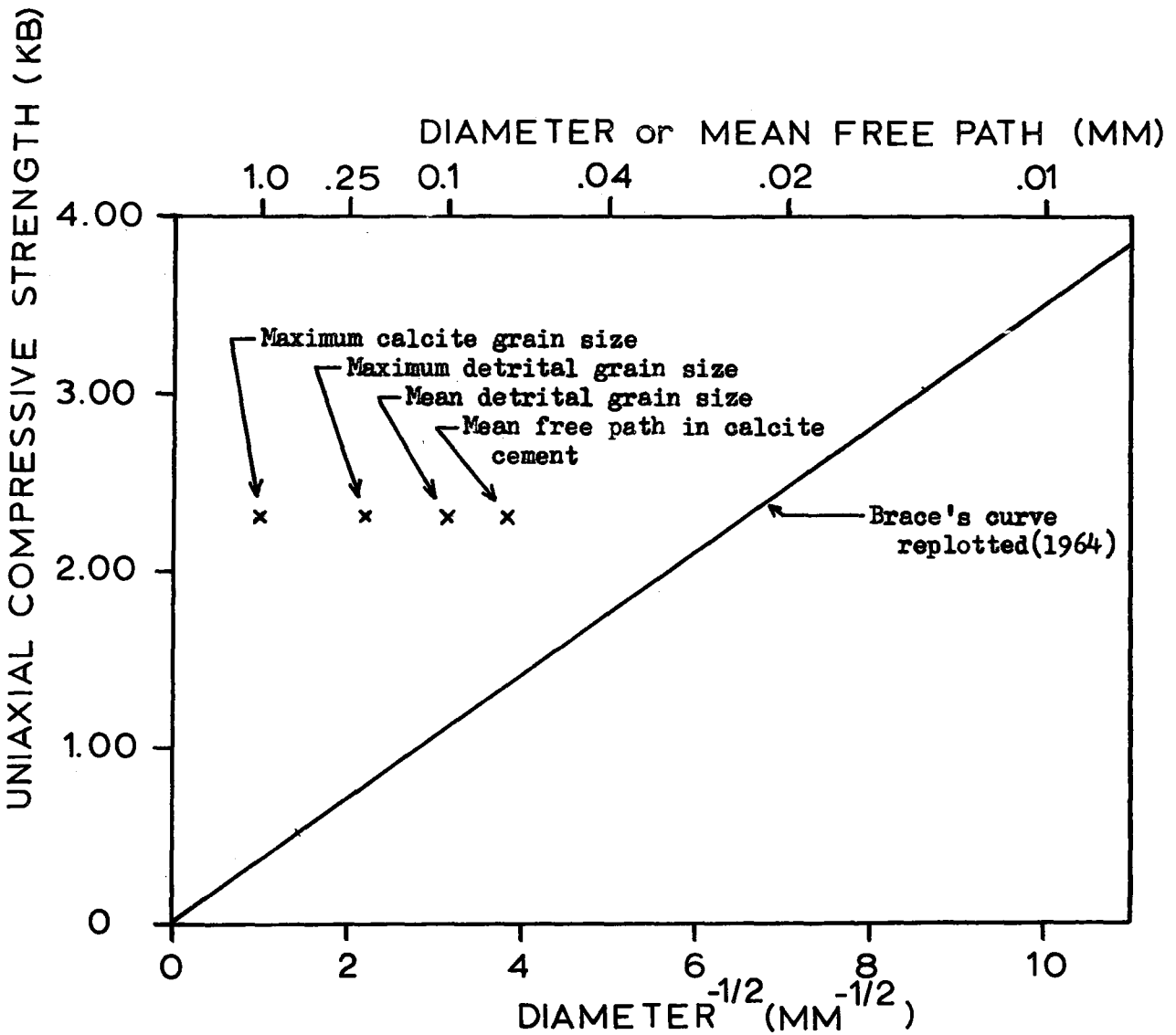

Figure 26. Graph showing the relation between grain size(or mean free path) and uniaxial compressive strength for orthocalcite rocks(curve from Brace, 1964), and for dimensions of the detrital and cement phases of the calcareous Blairmore sandstone.

limestones of equivalent grain size.

It is also found that the uniaxial compressive strength is seventy percent higher than would be expected if the flaw size responsible for failure is equivalent to the mean free path within the calcite matrix(found to be 0.068 mm.).

The lack of agreement between the predicted and experimentally determined strengths indicates that either other factors must influence the strength, or the Griffith Theory does not account for the strength of this rock. Re-examination of the Griffith equation shows that, with the exception of the numerical terms, the only other variables are E and γ. The Young's modulus, E, is a material constant which cannot increase significantly over the value for the individual phases. However, the effective surface energy, γ, has been shown to increase by as much as 100 percent within glass systems when a dispersion of particles consisting of a second phase is added(Lange, 1970).

In the Griffith equation, the strength is dependent upon the square root of γ. It would therefore be necessary to increase the value of γ to about 435 ergs/cm^2, which is an increase of 190 percent over the value of calcite alone(i.e. 230 ergs/cm^2(Brace, 1961)). It is not known whether such a large increase in γ does occur.

Other factors which have been found to effect the strength of two-phase brittle ceramics are stress concentrations associated with porosity, regular and irregular shaped inclusions(Hasselman & Fulrath, 1967; Tummala & Friedberg, 1970). Porosity has also been shown to decrease strengths in various rock materials including sandstones

(Balakrishma, 1963; Rector, 1970). In general, all of these factors act to reduce the strength as compared with the matrix alone. They do not therefore provide any insight into the high strength of the rock under study.

(c) Behavior and Strength Under Confining Pressure

(i) Macroscopic behavior -- The initial portion of each stress-shortening record has a steeply rising nearly linear elastic segment. However, records of experiments carried out under confining pressure differ from the uniaxial tests. After initial elastic deformation, the record deviates from the linear portion and follows a path of diminishing slope which is concave downward. This yielding results in a marked increase in the deformation prior to reaching the ultimate strength.

The Young's moduli of quartz and calcite differ only slightly. Therefore under elastic conditions, the intensity of stress and amount of strain are essentially equal in the two phases. The rock strength(i.e. in this case, the yield stress or onset of plastic deformation) is controlled by the mineral with the lowest critical stress(Kartesz, 1968). In fact, the yield stress of favorably oriented single crystals of calcite is far exceeded in the macroscopic range of the polycrystalline specimens as the critical resolved shear stress for e-twinning is only 50 bars. Calcite is therefore the first mineral to deform in a non-elastic manner.

Once the ultimate strength is achieved, the record marks a sudden and precipitous drop in stress with accompanying shortening of about two to three percent. Specimens from these tests are offset along a

shear surface oriented at an average of 30 degrees to the core axis. Shortening is primarily taken up by sliding along the shear fracture and the shape of the specimen is otherwise little changed from the original.

The stress difference falls to some level which is significantly less than the ultimate strength(e.g. from 2.75 to 1.25 kb at .25 kb confining pressure or from 4.25 to about 3.0 kb at 1.00 kb confining pressure). It then rises to form the second fault as discussed above, and then falls to a somewhat lower level where it remains more or less constant with further shortening. Most of the shortening is taken up by sliding along the shear fractures. The observed stress is then the stress necessary to cause sliding along the fracture surface and is expressed as $\tau = S_o + u\sigma_n$, where τ = shear stress to produce sliding, u = coefficient of sliding friction, S_o = a constant and σ_n = the normal stress on the surface upon which sliding occurs(Jaeger and Cook, 1969, p. 56).

At 1.25 and 1.50 kb confinihg pressure, the stress-shortening record indicates that there (1) is an increase in the amount of yielding prior to attaining the ultimate strength, and (2) the rock strength does not undergo a sudden drop once the ultimate strength is reached. Instead, the record follows a gradually falling path which levels off with increased shortening.

Although discrete fractures inclined at about 35 degrees to the core axis mark the specimen surface, these failure surfaces diminish as they pass into specimens which have been shortened only a few percent. Within the specimen shortening is taken up by a more general deformation

within a zone parallel to the fractures. Shape change occurs; however, barreling is restricted to the central portion of the specimen.

At confining pressures of 2.0 kb and above, the specimen may undergo 2.0 to 3.5 percent shortening before reaching the ultimate strength. Under these conditions, the specimen reflects a more ductile behavior and deforms through general barreling.

It should be noted, however, that within the range of experimental conditions, we do not see completely homogeneous or fully ductile behavior which is associated with a continually rising stress-strain curve. Furthermore, local shear surfaces do develop within specimens deformed more than about 5 percent at 2.0 kb and 12 percent at 2.5 kb confining pressure.

(ii) Microscopic behavior -- Examination under the microscope revealed that in all specimens deformed between .25 kb and 2.60 kb confining pressure, (1) twin lamellae developed within calcite grains and (2) microfractures developed within detrital grains with a preferred orientation nearly parallel to the core axis. These features are distributed more or less uniformly over the specimens.

The microfabric is found to be related to (1) the confining pressure of the experiment and (2) the amount of shortening which the specimen undergoes. Increasing the confining pressure to .50 kb results in an increase in the amount of calcite which exhibits twin lamellae up to .50 kb where a majority of the grains contain lamellae. This is accompanied by an increase in the number of microfractures within detrital grains. Further increases in confining pressure are accompanied by a reduction of fractured calcite grains and there is more

evidence of intense plastic deformation of calcite grains through other mechanisms(probably r- or f-translation) which produce bent lamellae and undulatory extinction.

Increasing the amount of shortening results in (1) more calcite grains becoming twinned, (2) the number of twin lamellae increase with shortening(at least at confining pressures greater than about 2.0 kb), and (3) the number of microfractures within detrital grains increase, with a continued preference for development nearly parallel to the core axis.

Friedman(1963) has shown for similar rocks that the application of confining pressure alone does not result in the development of either twin lamellae or microfractures. Furthermore, he found that twin lamellae and microfractures do not form during triaxial extension tests carried out at 1.0 kb confining pressure and 150°C. on the calcite-cemented Tensleep sandstone, even though the rock was deformed to rupture. This is thought by the writer to reflect the very high confining pressures required to obtain ductile deformation(in this case, e-twinning) of rocks under extension conditions in general as compared with compressive testing(as demonstrated by Heard, 1960).

It is therefore apparent that the presence of twin lamellae and microfractures are indicative of tectonism(as noted by Friedman,1963). Furthermore, the development of lamellae and fractures develop simultaneously and it is this general distributed deformation which is responsible for the yielding which occurs prior to achieving the ultimate strength in the present study. There is a threshold confining pressure below which failure by fracture may occur without the develop-

ment of twin lamellae or fractured grains.

The increase in the number of microfractures with increased shortening is greatest at confining pressures above 1.0 kb. This is attributed to the fact that deformation is much more generally distributed at these higher confining pressures. In contrast, at lower confining pressures much of the shortening is taken up through displacement along shear fractures or zones and there is relatively little yielding and distributed general deformation. This is shown diagrammatically in Fig. 27.

There is also an observed decrease in the rate of fracture development with increased shortening in excess of about 5 to 6 percent. This is thought to reflect (1) the increasing importance of shortening through shear displacement observed at higher levels of shortening and (2) the general decrease in the number of detrital grains which are favorably disposed to develop fractures. In the second case, there is a decrease in the number of touching unfractured grains as more and more grains are fractured. Also as detrital grains are fractured as the result of interaction with the matrix, the length to width ratio decreases and the grains are no longer stressed to failure(to be discussed in a following section).

(iii) Summary of the effects of confining pressure -- Confining pressure is shown to affect the strength, ductility and the orientation of macroscopic fracture development. In the brittle range, the fracture stress increases rapidly with $(\sigma_1 - \sigma_3)$ rising from 2.31 kb at atmospheric to 3.50 kb at .50 kb confining pressure(an increase of 240 bars for every 100 bars increase in confining pressure). The magni-

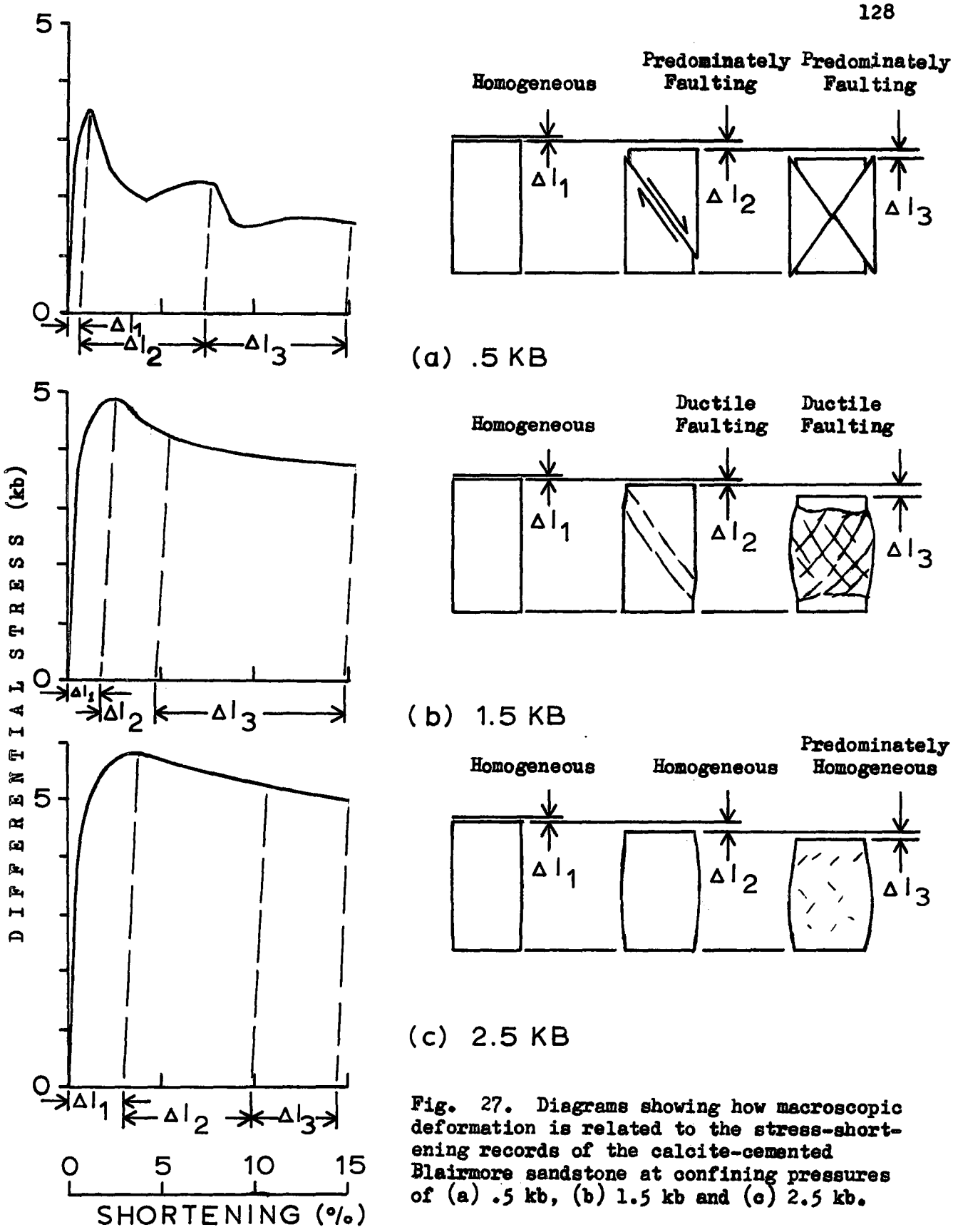

Fig. 27. Diagrams showing how macroscopic deformation is related to the stress-shortening records of the calcite-cemented Blairmore sandstone at confining pressures of (a) .5 kb, (b) 1.5 kb and (c) 2.5 kb.

tude of this effect becomes less with increasing pressure and the strength increases from 5.50 to 5.90 kb over the range from 2.00 kb to 2.50 kb confining pressure(an increase of about 90 bars for 100 bars increase in confining pressure).

With increasing confining pressure, there is a transition from brittle behavior below 1.0 kb to ductile behavior above 2.0 kb. Specimens sustain less than 1.50 percent shortening(elastic plus plastic) below 1.00 kb confining pressure, while this increase to about 3.50 percent at 2.50 kb confining pressure. Furthermore, while the specimens deformed at pressures below 1.00 kb confining pressure deform predominately by shear fracture, and undergo little shape change; specimens deformed at confining pressures above 2.00 kb deform through a general change in shape. A similar transition is observed microscopically where increasing confining pressure results in the suppression of fracturing of calcite grains. The onset of predominately plastic deformation of the calcite is accompanied by the more general development of microfractures in the detrital grains.

The orientation of macroscopic fractures and shear surfaces changes from longitudinal at atmospheric to an average of 30 degrees to σ_1 at low to moderate confining pressures increasing to nearly 40 degrees at 1.50 kb.

Confining pressure acts to increase the ultimate strength while at the same time it promotes more general plastic behavior.

(3) Theory of the Effect of Confining Pressure on Brittle Deformation Processes

Although the effect of confining pressure in increasing strength and ductility has been well known since the earliest investigations of rock behavior, little consideration has been given to the theoretical basis for this observation. We will therefore consider how confining pressure acts to suppress brittle behavior while at the same time promoting ductile deformation. Brittle failure results from the development of macroscopic fractures. We will first consider the initiation and propagation of cracks.

(a) Griffith Theory

We have already noted in an earlier section that the Griffith theory assumes the pre-existence of small flaws or cracks within the material. Under compressive conditions, it has been shown both theoretically and experimentally that the most critically oriented cracks within a biaxial stress field are inclined at between 20 and 40 degrees to σ_1. These flaws may initiate fractures near the ends. However, the fractures propagate less than one or two crack lengths following a curved path into a position parallel to σ_1 which is then stable. It is then necessary to increase the applied load to several times the load at primary initiation in order to continue propagation.

This led to the conclusion that shear fractures most probably develop from an overlapping array of closely spaced, en echelon cracks which could coalesce to form the macroscopic shear fracture(Bombolakis,

1964; Hoek & Bieniawski, 1965).

The stress to initiate fracture, σ_1, from the end of pre-existing flaws can be shown to be dependent upon the confining pressure, σ_3, where

$$\sigma_1 = \sigma_3 + \sigma_c(2\sigma_3/\sigma_c + 1)^{\frac{1}{2}} + \tfrac{1}{2}\sigma_c \qquad (5\text{-}1)$$

and σ_c = uniaxial compressive strength of the rock(Hoek & Bieniawski, 1965).

(b) McClintock-Walsh Theory

The Griffith Theory assumes no forces are carried across the faces of the crack. But McClintock and Walsh(1963) argue that cracks can close and carry normal and shear stresses due to friction. These stresses will tend to increase the strength of the rock by reducing the stress concentration at the ends of the crack from the value it would have been in the absence of the friction stress which resists the deformation of the crack. If the friction is taken into consideration, the stress to initiate fracture, σ_1, is shown to be

$$\sigma_1 = \sigma_3 \frac{(1 + u^2)^{\frac{1}{2}} + u}{(1 + u^2)^{\frac{1}{2}} - u} + \sigma_c \qquad (5\text{-}2)$$

where u is the coefficient of friction between crack faces(Hoek & Bieniawski, 1965). It has been found that this equation gives a much better agreement with experimentally determined strengths than the original Griffith equation. Values of u are found to most commonly lie between .5 and 1.0.

(c) The Effect of Confining Pressure on Crack Formation Resulting From Plastic Deformation

Most discussions of rock strength have been based on the consideration of strictly brittle materials. The ductile behavior of calcite under confining pressure makes it necessary, however, to consider the possibility of fracture being initiated as a result of plastic deformation.

Microyielding within individual grains of a polycrystalline material is thought to lead to fracture development in a variety of metallic and ceramic materials(McClintock & Argon, 1966). In such case, stress concentrations result where translation slip(i.e. dislocation pile-up) is blocked by some strong obstacle. This may occur where slip in one grain intersects a grain boundary. If the stress concentration is not relaxed through further slip in the adjacent grain, crack initiation and propagation may occur.

Dower(1967) considers the effect of confining pressure on fracture development resulting from this process and we will follow his discussion. Dower assumes that the propagation of a crack requires more energy than its initiation. This was subsequently shown to be true under conditions of high pressure(Francois & Wilshaw, 1968).

Consider a crack of length c at an angle θ to the slip plane, wedged open by n dislocations of Burger vector b, under the action of the applied tensile stress σ at an angle 45 degrees to the slip plane.

Let the applied hydrostatic pressure be p. The assumption is made that the hydrostatic pressure only affects the work done in opening the crack, the energy W, of the crack under the stress system, is comprised of:

(1) The elastic energy of the stress field set up by the crack; this has been calculated by Stroh(1954) to be $[n^2b^2G/\{4\pi(1 - \nu)\}] \ln 4r/c$, (5-3) where G is the rigidity modulus, ν the Poisson's ratio and r the effective radius of the stress field.

(2) The surface energy of the crack; this is given by $2c\gamma'$, where γ' is the effective surface energy of the crack. This effective surface energy term includes the plastic work associated with the growth of the crack, and may be much greater than the true surface energy.

(3) The elastic energy of the crack in the applied stress field; Stroh(1955) calculates this to be

$$-\frac{\pi(1 - \nu)\sigma^2c^2}{8G}. \qquad (5-4)$$

The work of Sack(1946) suggests that no great error results in ignoring the effect of the hydrostatic pressure.

(4) The energy due to the increase in volume on opening the crack; this consists of two parts, namely (a) the work done by the component of compressive stress normal to the crack, $(-nbc/2)\sigma \sin(\theta - \frac{1}{4}\pi)$, and (b) the work done against the hydrostatic pressure $(nbc/2)p$.

The total energy of the crack is thus

$$W = \frac{n^2b^2G}{4\pi(1 - \nu)} \ln \frac{4r}{c} + 2c\gamma' - \frac{\pi(1 - \nu)\sigma^2c^2}{8G} - \frac{nbc}{2}\sigma \sin\left(\theta - \frac{\pi}{4}\right) + \frac{nbc}{2}p. \qquad (5-5)$$

Strictly, this equation applies only to a two-dimensional model but Sack(1946), who extended the argument to a penny-shaped crack, showed that the difference will be a numerical factor only.

For the crack to spread under the appled stress, W must decrease as c increases, and the length of the crack at equilibrium will be given by $dW/dc = 0$. Thus

$$\frac{dW}{dc} = 0 = -\frac{n^2b^2G}{4\pi(1-\nu)}\frac{1}{c} + \frac{nb}{2}\left\{\frac{4\gamma'}{nb} + p - \sigma\sin\left(\theta - \frac{\pi}{4}\right)\right\} - \frac{\pi c}{4G}(1-\nu)\sigma^2. \quad (5\text{-}6)$$

Rearranging equation 5-6 we get

$$\frac{\pi}{4G}(1-\nu)\sigma^2c^2 - \frac{nb}{2}\left\{\frac{4\gamma'}{nb} + p - \sigma\sin\left(\theta - \frac{\pi}{4}\right)\right\}c + \frac{n^2b^2G}{4\pi(1-\nu)} = 0. \quad (5\text{-}7)$$

The critical length of crack will occur when the roots of equation 5-7 are equal, and this will happen when

$$\frac{4\gamma'}{nb} + p_c - \sigma\sin\left(0 - \frac{\pi}{4}\right) = 0 \quad (5\text{-}8)$$

where p_c is now the critical hydrostatic pressure for the transition from brittle to ductile fracture. Rearranging equation 5-8 we get as the critical condition

$$nb\left\{\sigma + \sigma\sin\left(\theta - \frac{\pi}{4}\right) - p_c\right\} = 4\gamma'. \quad (5\text{-}9)$$

Under tensile conditions, the crack will spread catastrophically if the left-hand side of equation 5-9 exceeds $4\gamma'$. Under confining pressure, the crack will not spread catastrophically. Failure may result from the linking up of many small cracks.

The increased ductility associated with higher confining pressures may act to increase the plastic work associated with γ'. This acts to increase σ, the stress required to propagate a crack at confining pressure, p.

(d) Summary of the Effect of Confining Pressure on Crack Propagation

In all cases considered, whether fracture is initiated

from pre-existing cracks, or whether cracks are nucleated as a result of stress concentrations generated by plastic deformation, confining pressure acts to suppress crack propagation. In each case, σ_1 increases more rapidly than σ_3, and therefore the differential stress, $\sigma_1 - \sigma_3$ increases. The shear stress $(\sigma_1 - \sigma_3)/2$ also increases.

(4) Confining Pressure, Ductile Deformation and the Brittle-Ductile Transition

In contrast to crack propagation which has been shown to be pressure sensitive, the ductile processes of twinning and translation gliding are generally insensitive to hydrostatic pressure(Paterson, 1967). Instead, they depend on some critical resolved shear stress (c.r.s.s.) which remains essentially constant under different conditions of hydrostatic pressure. This has been shown to be true for calcite(Turner, et al., 1954, p. 889).

In the present case, the increasing shear stress associated with rising confining pressure may serve to activate a previously inoperative slip system as the c.r.s.s. for the slip system is surpassed. In the case of calcite, either r-translation, with a c.r.s.s. of 1.50 kb, or f-translation with a c.r.s.s. of about 2.20 kb, may be activated(Borg & Turner, 1967). With increasing confining pressure, shear stresses with these magnitudes are first developed in regions of stress concentration, and then more generally as the differential stress is further increased.

Although translation gliding leaves no visible evidence of having

occurred, the development of bent lamellae and undulatory extinction within calcite grains are evidence that plastic mechanisms other than twinning have contributed to the deformation.

The activation of either system provides a contribution to the five independent slip systems which are necessary(but not necessarily sufficient) for general homogeneous strain to occur as required by the von Mises criteria(1928). Paterson(1969) has indicated that e-twinning plus either r- or f-translation give five independent slip systems so that von Mises criteria are satisfied. Additional deformation through minor fracture or kinking may act to relax the criteria somewhat.

An analogous case is seen for polycrystalline magnesium oxide where slip occurs only on (110) at low confining pressures and brittle failure predominates. At higher confining pressures, more widespread plastic deformation involving (112) and (100) slip systems become operative and fully ductile deformation occurs as von Mises criteria are satisfied(Paterson & Weaver, 1970).

(5) The Effect of Confining Pressure on Strength

The general argument developed within this section provides a basis to understand how confining pressure controls the strength of the Blairmore sandstone. Under confining pressures at which deformation proceeds primarily by brittle processes(up to 1.00 kb in the present study) increased confining pressure results in a rapid rise in ultimate strength because the propagation of fractures from flaws

is highly pressure dependent.

At higher confining pressures where high shear stresses activate more general ductile behavior of the calcite, the strength(at equivalent amounts of shortening) increases less rapidly because of the relative insensitivity of twinning and translation gliding to confining pressure(Paterson, 1967).

Micromechanics and the Microscopic Deformational Behavior

(1) The Role of Detrital Grains

Under confining pressure, the detrital grains act as rigid inclusions within the ductile calcite matrix. In general, these grains have a high strength and may sustain only small amounts of elastic strain(i.e. less than .5 percent) before brittle fracture occurs. In this section, we will consider the behavior of quartz and use it as a guide to understanding the behavior of the other detrital grains.

(2) The Role of Quartz

Within the present study, quartz is observed to deform only by fracture. Recrystallization or deformation by intracrystalline mechanisms would not be expected to take place under the conditions of the experiments, and no evidence of this behavior was observed.

Natural quartz is one of the strongest common substances and all attempts to render quartz ductile by high confining pressure at

room temperature have failed(Griggs & Blacic, 1965). Single crystal quartz has a compressive strength of 20 to 30 kb even at atmospheric confining pressure. The strength(defined by differential stress) increases to between 36 and 55 kb under 2.5 kb confining pressure. Under confining pressure, quartz fails by shear fracture along a plane oriented at an angle of 35 degrees to σ_1(Griggs et al., 1960).

Relatively less is known about the strength of quartz under conditions of the uniaxial tensile or triaxial extension test. Sosman(1927) found that the tensile strength of quartz is between 0.8 and 1.1 kb. If the behavior of single crystals is similar to the behavior of polycrystalline quartzite(and many other brittle materials), the strength under extension conditions would be expected to be between one-twenty-fifth and one-tenth of the compressive strength. The strength would then be between 1.4 and 5.5 kb under 2.5 kb confining pressure.

All of the principal stresses were compressive in the present study with the exception of the tests run under atmospheric confining pressure. At no time, however, did the differential stress approach the compressive strength of single crystal quartz. Furthermore, essentially all of the microfractures within detrital grains develop nearly parallel to σ_1, and nearly all are inclined at less than 30 degrees. This contrasts sharply with the 30 to 40 degree inclination which is characteristic of shear fractures in quartz and other brittle materials. In fact, it has been generally argued that in order for fractures to form parallel to σ_1, the minimum principal

stress, σ_3, must be zero or tensile. This conclusion has been reached on the basis of uniaxial and triaxial testing(Brace, 1964; Jaeger & Cook, 1969) and from theoretical and model studies of crack propagation(Bombolakis, 1964; Hoek & Bieniawski, 1965).

The two important observations are (1) that quartz undergoes fracture at applied loads which are much below its normal compressive strength and (2) the fractures have the characteristic orientation of tensile, rather than shear fractures, as would normally be expected under triaxial compressive conditions. The implication of these factors is that significant stress concentrations act on the individual grains and the stress concentrations have a significant tensile component which controls the propagation of the microfractures.

It should be noted that although there is considerable evidence that the orientation of fracture in quartz is in part crystallographically controlled, investigation of deformed non-cemented(Borg et al., 1960) and calcite-cemented quartz sands(Friedman, 1963) indicate that this possible crystallographic control is greatly overshadowed by the marked relation between the microfractures and principal stresses across the boundaries of each specimen.

(a) The Development of Stress Concentrations Associated with Detrital Grains

Discontinuities within a solid material, such as pores, cracks or hard inclusions, result in enhancement of the stress over and above the stress applied at the margin of the solid under consideration. Stress concentrations may arise from either differential

elastic properties or as a result of differential plastic behavior (McClintock & Argon, 1966).

(i) Elastic stress concentrations -- The Herzian solution for the stress distributions in two spherical bodies in contact has previously been used to provide an understanding of the nature of stress concentration of two sand grains in contact(Borg et al., 1960; Friedman, 1963). We will review this solution in order to have a basis to understand its relevance to the present study.

Following Timoshenko and Goodier(1951, p. 372-377), the maximum pressure σ_{max} occurs at the center of the circular contact surface and is given by

$$\sigma_{max} = 0.6(QE^2/R^2)^{1/3} \qquad (5\text{-}10)$$

where Q = compressive force, E = Young's modulus, and R = radius of two spheres of equal size. This formulation is valid for Poisson's ratio between .1 and .3 with only a five percent variation of σ_{max} resulting from this range.

The maximum tensile stress occurs at the circular boundary of the surface of contact. This stress acts in a radial direction with respect to the surface of contact and has the magnitude

$$\sigma_{tensile} = \frac{(1 - 2v)}{3} \sigma_{max} \qquad (5\text{-}11)$$

where v is the Poisson ratio. The Poisson ratio of quartz is about 0.1(Birch, 1966). The maximum tensile stress for quartz is therefore about 0.27 σ_{max}. It should be noted that this is a 100 percent increase

over the previously recognized value of 0.13 σ_{max} which was obtained by using a Poisson ratio of 0.3(Borg et al., 1960).

Therefore, as previously noted, for a radius of 10^{-2}cm. and a Young's modulus of 10^6 bars, a force of only 13 gm would produce a maximum stress of 30,000 bars. The tensile stress associated with this would be 7,500 bars. Significantly, the stress concentration is very localized and falls off rapidly within the spheres. At distances of three to four times the radius of contact, the stress decreases to one-tenth or less of the maximum values. However, the stress at the surface is sufficient to exceed the tensile strength, which is the most critical strength in brittle materials like quartz which fail in tension.

Although the above solution is well-suited to the analysis of non-cemented sands, its application is not thought to apply to calcite-cemented sands under elastic loading. In these materials, the quartz grains are dispersed within a matrix which has nearly identical elastic properties to those of quartz. The Young's moduli of quartz and calcite are 1.00×10^6 bars and $.85 \times 10^6$ bars respectively(Brace, 1961). Therefore, during loading where only elastic strains occur, no significant stress concentrations develop at the quartz grain-grain contacts.

This difference between calcite-cemented and non-cemented sands accounts for the difference in behavior of the two materials under hydrostatic loading conditions. While non-cemented sands sustain considerable fracturing when confining pressure is applied(Borg et al., 1960), calcite-cemented sands, in contrast, show no signs of deformation

(Friedman, 1963).

The similarity of Young's modulus for calcite and quartz(and the other detrital grains) in fact eliminates the potential for any significant elastic stress concentrations which may develop when an inclusion of high Young's modulus is surrounded by a matrix of lower Young's modulus. Investigations showing the relative magnitude of stress concentrations arising from differential elastic properties indicate that minor differences in Young's modulus comparable to the difference between calcite and quartz will not give rise to significant stress concentrations(Edmonds & Beevers, 1968; Jaeger & Cook, 1969, p. 250).

(ii) Stress concentrations arising from plastic deformation -- While the differential behavior between calcite and quartz may be insignificant under elastic conditions, the onset of plastic behavior in calcite may give rise to more signifcant differential behavior.

Consideration of an analysis by Ashby(1966) to explain the deformation of dispersion hardened metal crystals may provide some insight into the phenomenon. We may consider a hard spherical particle within a plastic matrix as shown in Fig. 28. Consider what happens when the matrix undergoes a shear. A shear stress τ, is applied to the specimen causing a homogeneous plastic shear a, in the matrix in the x_1 direction on the family of planes normal to x_2, which we call the primary slip planes of the matrix. The displacement within the matrix is then $u_1 = ax_2$. In the present case, all of the deformation within the particle is elastic. Within the matrix, the plastic strain

Fig. 28. (a) A hard particle in a plastic matrix. (b) When the particle is removed form its hole, and the matrix undergoes a uniform primary shear displacement $u_1 = ax_2$, the hole is distorted as shown. (c) To replace the particle in its hole, a secondary shear displacement $u_2 = cx_1$ at the particle-matrix interface is first needed if the particle is to be elastically distorted only. (d) Alternatively, the matrix can be displaced by prismatic punching to give displacements u_1' and u_2' parallel to new axes x_1' and x_2'. (e) One alternative for accomodation occurs through cavity formation along the x_1' axis. (f) Another alternative is for the particle to fracture. (For clarity, diagram (b) shows a large shear strain of 0.5. In consequence, a subsequent uniform secondary shear $u_2 = cx_1$ would not restore the hole to a sphere. When strains are small, or are applied simultaneously, a uniform shear u_2 restores the ellipsoid to a sphere). (After Ashby, 1966).

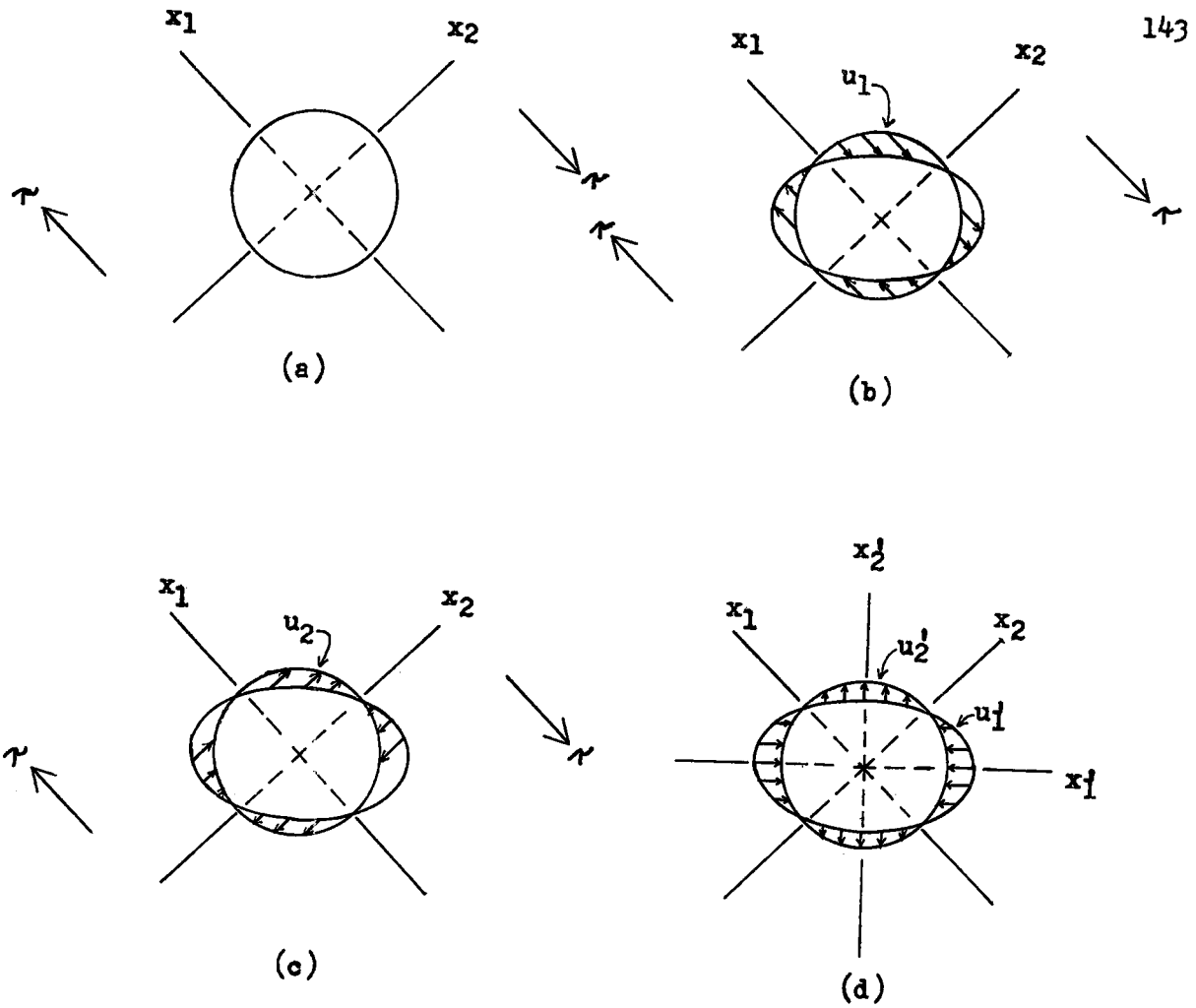
x1
x2
(a)
x1
x2
u1
(b)
x1
x2
u2
(c)
x2'
x1
x2
u2'
u1'
x1'
(d)
cavity
(e)
(f)

is much greater than the elastic strain. If the particle is removed from the hole in matrix, the hole is free to deform, and takes up the shape in (b), Fig. 28. Suppose we replace the hard particle in its hole. In order to do this, it will either be necessary to (1) displace the surface of the hole until the remaining deviation from the spherical shape can be carried elasticly by the particle, or (2) the particle can be deformed until it assumes the shape of the hole, or (3) both mechanisms can contribute to accomodation.

There are basically three ways in which this accomodation can occur: (1) The matrix may undergo slip on one or more additional slip systems in order to displace the matrix-inclusion interface; (2) Shearing may occur at the matrix-inclusion interface with the simultaneous development of voids at the x'_1 poles of the particles; or (3) The particle is strained to a level where the strength is exceeded and fracture occurs.

An important aspect of the strain is shown in Fig. 28 as the shear strain is accompanied by maximum compression at 45 degrees to the primary slip planes and maximum tension at 90 degrees to the compression axis(as is the case for infinitisimal analysis of any simple shear). The strain results in stress on the inclusion and the stress is transferred to the particle through shear stresses exerted on the particle by the matrix. As the stress is developed through the shear stress at the interface, the shape of the particle is important. More elongate particles will be more highly stressed.

The critical factor is probably the elongation and associated

tensile stress to which the particle is subjected. For most common brittle rock materials, including quartz, elongation of as little as 0.1 to 0.2 percent with accompanying tensile stresses of 1.0 to 2.0 kb would result in tensile failure. Stresses and strains with this order of magnitude could be achieved with the development of very little shear strain on the primary slip planes of the matrix.

(iii) The fiber model -- Kelly(1967) discusses a model which is used to understand the nature of fiber reinforced materials. Consider a strong rod of radius r embedded to a depth ℓ in a matrix as in Fig. 29. Suppose that the sliding friction between the rod and matrix produces a shear force τ per unit area. For the case where no matrix is present at the end of the rod, the total load necessary to pull the rod out is

$$P = 2\pi r \ell \tau \qquad (5\text{-}12)$$

This will increase without limit as we increase ℓ. Assuming that the rod has a breaking strength σ_f, then the maximum load which can be applied to the rod in terms of σ_f can be written

$$\frac{\sigma_f}{4\tau} = \frac{\ell}{2r} = \frac{\ell}{d}, \text{ where d is the diameter} \qquad (5\text{-}13)$$

The ratio ℓ/d is the aspect ratio of the fiber. When the expression is rewritten as $\ell = \frac{\sigma_f d}{2\tau}$ the so-called critical length is obtained. (5-14) This is the length of fiber for which the tensile strength of the fiber is just equivalent to the shear stress exerted on the fiber. For any length greater than $\ell_{critical}$, the fiber will fail rather than pull out. For shorter lengths, the fiber remains intact and

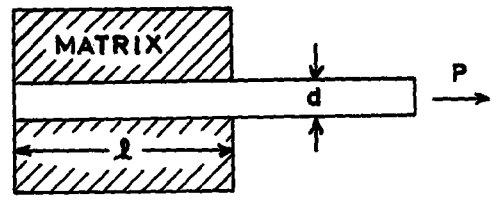

Fig. 29. Model used to determine the critical aspect ratio for fracture of a brittle fiber embedded within a matrix.

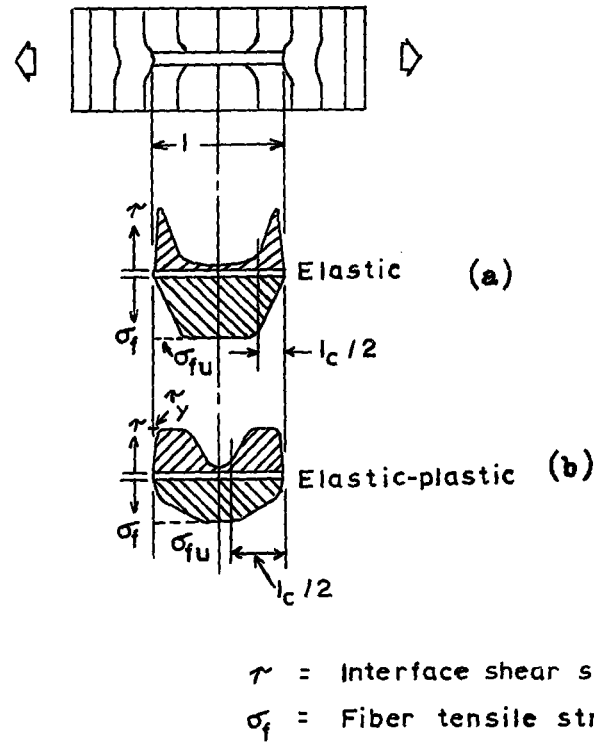

Fig. 30. Schematic representation of interfacial shear stress (τ) and fiber tensile stress (σ_f) when matrix exhibits (a) elastic and (b) elastic-plastic deformation (After Krock & Broutman, 1967).

shears by the matrix.

This rather simple model has been tested in tension for a composite material consisting of tungsten fibers within a copper matrix. Using appropriate values of tensile strength, σ_f, for tungsten and shear strength, τ, for copper, a critical length of 5 was predicted. Experimental verification of the model was carried out by pulling out embedded fibers as described above. End bonded fibers were found to have a critical length of about 2; while for fibers without the end bond, the critical length was found to be about 4(Kelly & Tyson, 1965a).

Further verification through experimental analysis was carried out by subjecting a composite consisting of a tungsten wire within a copper matrix to tensile deformation(Kelly & Tyson, 1965b). Upon completion of the test during which the copper was observed to deform through plastic deformation, the tungsten wire was found to have broken into short segments. The segments were extracted and measured and most of the fragments were found to have ℓ/d ratios between 1.5 and 3.5.

It has been suggested that this model is valid for two different cases. If the fiber-matrix interface is strong, then the value of τ may represent the shear strength of the matrix material. If the matrix does not shear or the interface is weak, then the transfer of stress may be accomplished by frictional forces at the interface, and the equation becomes $\ell_c = \frac{r\sigma_f}{u\sigma_n}$, where u = coefficient of friction between the two surfaces and σ_n = normal stress at the fiber-matrix (5-15)

interface(Outwater, 1956).

Now, if a similar model consisting of a quartz fiber within a calcite matrix is considered what critical length would be expected? For a triaxial extension test executed at about 2.5 kb confining pressure, the strength of quartz might be expected to be about 2.0 kb which is then taken as σ_f. The value of τ for calcite is less certain, but a value of 1.0 kb is not out of line for the observed shear strength in many triaxial tests on calcite rocks. This is also the approximate critical resolved shear stress for r-translation. For these values, ℓ/d, the critical aspect ratio equals 2.0 kb/(2 x 1.0 kb), which is equal to one.

If the model for slip at the interface is taken instead, then the value of the coefficient of friction between calcite and quartz would have to be used. Although this is not known, recent work on the friction between faces of sandstone and limestone suggest a coefficient of .5 or more(Logan et al., 1970). For equation (5-15), the critical aspect ratio is again about one.

Although this fiber model may not be directly applicable to the present study because of the idealized grain shape and the assumed stress state, it does serve to demonstrate the probable nature of stresses which act on particles within a matrix deforming by ductile flow. Furthermore, if appropriate values for a quartz fiber within calcite matrix are assumed, the results indicate that nearly equant grains of quartz may be subjected to sufficient stress concentration to cause tensile failure. Because of the high proportion of elongate

grains in the Blairmore sandstone, the fiber model analysis may be more relevent than for a rock in which the detrital grains are all well rounded and have high sphericity.

(iv) Summary and discussion -- Ashby's model indicates one way in which tensile stresses may develop in an inclusion which is in a matrix undergoing plastic deformation by simple shear. The fiber model shows more generally how elastic stress concentrations develop as a result of shear stresses being exerted at the margins of the inclusion. The stress concentration within the inclusion has certain characteristics which should be considered further.

The stress within the inclusion is elastic. Because the stress concentration is the product of interaction with a plastically deforming medium, the greatest force is exerted near the midpoint of the inclusion. If the inclusion has the shape of an elongate fiber with a uniform cross sectional area, the stress will also be at a maximum near the center. In addition, the stress will be proportional to the length of the grain and therefore, the greatest stress will develop in the most elongate grains. As long as the shear stresses at the margins are uniform or vary in a uniform manner, the stress concentration will affect the entire inclusion. This is in marked contrast to the stress concentrations resulting from grain to grain contacts which affect only the immediate vicinity of the point of contact.

We should consider the more general case of what happens in a calcite-cemented sandstone which is undergoing shortening through homogeneous flow. Friedman(1963) has shown that the majority of the

calcite grains deform statistically in response to the principal stresses across the boundaries of the specimen as a whole. As a result of the nature of the relations between stress and strain in the technique involved in Friedman's study(the Turner technique), it may be inferred from the results that maximum elongation of the calcite grains(at least the component resulting from e_1 twinning) is statistically parallel to σ_3, or for triaxial compression parallel to the radius of the core axis.

If this strain of the calcite matrix is effective in causing tensile stresses within the detrital grains as proposed in this section, then the maximum tensile stresses will reflect the statistical nature of strain of the calcite matrix. That is to say that a majority of the detrital grains will be subjected to tensile stresses which are oriented more or less parallel to the radius of the specimen core and therefore nearly parallel to σ_3. Therefore, the microfractures have a symmetrical relation to the principal stresses applied at the margins of the specimen.

The writer feels that this may be one of the reasons that the significance of stress concentrations may have been overlooked in the past. In fact, they have been explicitly excluded by Friedman(1963, p. 34) who wrote "...both the calcite cement and the detrital grains deform in response to the principal stresses across the boundaries of the specimen as a whole rather than to local stress concentrations at grain contacts".

Recognition of the fact that the symmetry of the strains

associated with stress concentrations may reflect the symmetry of the applied stresses accounts for the apparent relation between the orientation of the microfractures and applied stresses. It only becomes clear that the stress concentrations are a very necessary part of the system if we recall that the tensile stresses are necessary for the development of extension fractures which form the vast majority of the microfractures within the detrital grains, and that without the concentrations the applied stresses could not be expected to cause extension fracture. Furthermore, this mechanism can account for failure of quartz and other detrital grains under applied stresses which are well below the compressive strengths of these materials.

The following sequence is visualized to account for the deformation of a calcite-cemented sandstone. The first inelastic strain occurs by twinning of favorably oriented calcite grains. The detrital grains are affected in two ways at this point. The grains are subjected to an elastic strain by the deforming calcite. In addition, previously touching detrital grains are pressed together. Fractures are initiated at the touching contacts after very little strain occurs as a result of the tensile component of the contact stress concentration. Once the fracture is initiated further propagation is caused by the tensile stress exerted by the deforming calcite on the grain margins. The non-localized nature of the stress(in contrast to the contact stresses) and the nearly uniform orientation of the stresses are responsible for the very systematic orientation of the microfractures.

In addition, individual detrital grains and parts of grains which do not touch other detrital grains are subjected to tensile stresses by the deforming calcite. These stresses are of sufficient magnitude to initiate fractures. Very little plastic strain is necessary if the strain is efficiently transmitted to the detrital grains. Propagation and orientation of these fractures is effected by the same forces.

The effectiveness of the calcite matrix in controlling the orientation of the fracture propagation accounts for the difference in orientation pattern between fractures formed in calcite-cemented and non-cemented sands. In non-cemented sands, the initiation and orientation of fractures depends upon stress concentrations developed at the site of grain to grain contacts(as proposed by Borg et al., 1960; Gallagher et al., 1970). The locallized and non-uniform distribution of the stress concentrations accounts for the irregular character and variable orientation of the fractures in non-cemented sands. The pre-eminence of the development of the much more pervasive and uniform stress concentrations caused by the plastically deforming matrix accounts for the more regular character of the microfractures in the detrital grains of calcite-cemented sandstones.

It would be expected that both mechanisms may act to control the development of fractures in poorly cemented sandstones which have a high porosity. The change in orientation pattern with porosity or conversely cement content is shown in Fig. 24 (p. 111). In the opinion of the writer, the less well-developed pattern of fracture

NON-CEMENTED SANDS

Fractures initiated by elastic stress concentrations at grain-grain contacts. Stress concentration is very localized and orientation of the developed stresses have only a statistical relation to the applied stresses, σ_1 and σ_3.

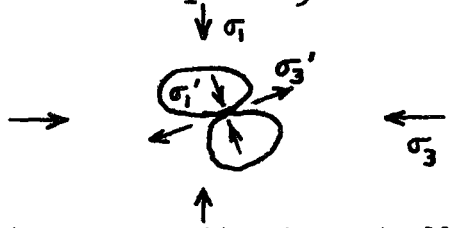

Fracture propagation is controlled by the same stress concentrations. Fractures propagate parallel to σ_1', whose orientation is determined by the local nature of the stress concentraction. Other factors such as wedging or bending may also contribute, but these factors are primarily related to the point of contact stresses.

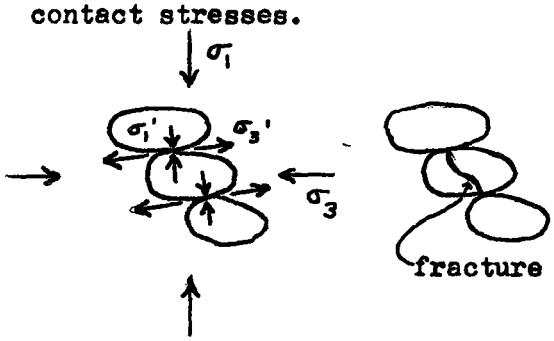

The result is that each of the fractures has an orientation which is controlled by local stress concentrations. The overall pattern is only statistically related to the applied stress system.

CALCITE-CEMENTED SANDS

Fractures initiated by both grain-grain contact stress concentrations, and by shear stresses exerted on the detrital grains by the plasticly deforming calcite matrix. These stresses, σ_1'', σ_3'', affect the entire grain and have an orientation which is closely related to the applied stress.

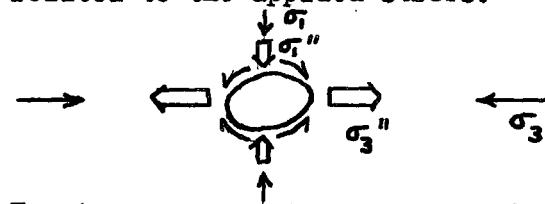

Fracture propagation is controlled by by stress concentractions resulting from the ductilely deforming matrix. Fractures propagate parallel to σ_1'', which is generally parallel to σ_1. Fractures initiated by stresses at grain-grain contacts propagate under the influence of σ_1'', which has a more pervasive influence.

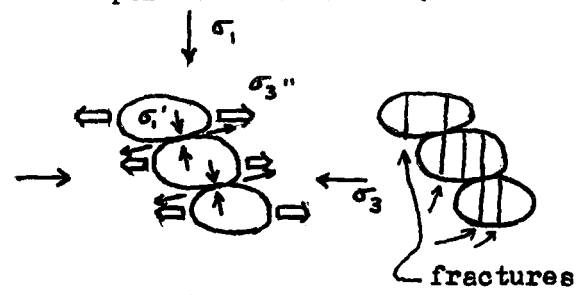

The orientations of the effective stress concentrations are closely related to the orientation of the applied stress system. Therefore, a majority of the fractures lie nearly parallel to σ_1.

Fig. 30. Comparison of the factors which control the initiation and propagation of fractures within detrital grains of non-cemented and calcite-cemented sands. Comparison of the resultant fracture pattern.

orientation observed in the porous(17.5 percent porosity)Supai sandstone is caused by the development of some fractures by the contact stress mechanism in that part of the rock where the calcite cement is absent. This explanation is preferred over Friedman's(1963, p. 28)suggestion that the fracture planes were rotated away from their original positions.

(3) Deformational Behavior of the Calcite Matrix

During plastic deformation of a polycrystalline aggregate, the need to maintain continuity at the boundary between a grain and its neighboring grains determines the deformation processes within the grain and so determines the stress required for deformation(Taylor, 1938). It has been shown that the flow stress of ductile metals follows the Hall-Petch relation, i.e., $\sigma_{flow} = \sigma_o + kl^{-\frac{1}{2}}$ (5-16) where σ_{flow} is the stress required for flow at some constant strain, σ_o and k are material constants and l is the grain diameter (Armstrong et al., 1962). The explanation for this effect is thought to lie in the difference in slip band formation in the single crystal and in a polycrystal. In a single crystal, dislocations arriving at a free surface can emerge there, but, in a polycrystal, dislocations arriving at a grain boundary cannot freely cross the boundary. When the concentrated stress at the end is sufficiently high, a new dislocation source will be unlocked and plastic deformation initiated in the next grain. The reason that the flow stress is dependent upon the grain size is that the stress concentration at the end of a slip band is also dependent upon the slip band length. The stress concen-

tration factor at a short distance r, ahead of a slip band of length l is $(l/4r)^{\frac{1}{2}}$(Eshelby et al., 1951).

Although the writer is unaware of a specific solution for the stress concentration associated with twinning, the yield stress for a polycrystalline material deforming by twinning has also been shown to follow a grain size dependence expressed by 5-16 (Tetelman & McEvily, 1967, p. 252).

The relation of 5-16 can only be expected to apply once the limiting grain boundary resistance has been reached. During plastic deformation of a polycrystalline aggregate, the critical resistance is the stress necessary to initiate plastic deformation within the adjacent grain.

This relationship has been demonstrated to hold for several metals(Armstrong et al., 1962; Tetelman & McEvily, 1967). Although no quantitative analysis has been carried out for limestones and marbles, there is qualitative evidence that a similar relation does hold(compare the high flow stress of the very fine-grained Solenhofen limestone with the much lower values associated with equivalent strain in more coarse-grained marbles).

It is therefore not unreasonable to expect that any reduction in grain size will result in an increased resistance to flow. As the detrital grains in the Blairmore sandstone effectively reduce the calcite grain size, this factor probably accounts for at least part of the high strength of the rock under ductile conditions.

In a polycrystalline calcite aggregate, stress concentration within a grain is normally relieved by plastic deformation within

adjacent grains as the limiting boundary resistance is reached. However, if the adjacent grain is high strength quartz(or some other strong rigid mineral) which is incapable of plastic deformation under the prevailing conditions, then the stress within the initial grain may reach much higher values that it would in a material bearing no inclusions.

In the last section, it was argued that stress could be relieved by either fracture and shape change of the hard inclusion or by additional deformation within the plastically deforming matrix. Although it is clear in the present study that the inclusions do fracture, this permits only limited stress relief, as most of the grain boundaries are still formed by rigid quartz grains. Therefore, if the material is to undergo additional ductile deformation, the matrix must undergo general deformation particularly in the vicinity of the grain boundaries. In the present case, the calcite must deform on less favorably oriented systems which may have large critical resolved shear stresses.

In fact, there is good evidence that the calcite does undergo more general deformation especially in the immediate vicinity of grain contacts with detrital grains. The development of bent lamellae near grain boundaries was observed in this study and is noted by Friedman(1963, p. 19, 24 and 25). Even single calcite crystals containing sand grains favorably oriented for e-twinning were found to deform by additional mechanisms(Friedman, 1963).

Friedman also notes that single crystals of calcite containing sand grains which were not favorably oriented for e-twinning developed e-twins which tend to die out away from the sand grains(1963).

Development of general strain on less favorably oriented, more resistant slip systems will affect both the strength and ductility of the rock. In the first place, high stresses are required for even small amounts of macroscopic strain to occur as the rigid inclusions make it necessary that nearly all of the accomodation at the grain boundaries occurs within the calcite itself. This also affects the general ductility as large strains may only be accomodated once the calcite can readily deform on five independent slip systems.

In summary, the strength is thought to increase as a result of both a grain size effect and the constraint on deformation which is offered by the rigid inclusions. The ductility is decreased and therefore, the brittle-ductile transition is suppressed because of the constraint of the inclusions. Macroscopic shear fractures form at much higher confining pressures than in orthocalcite rocks because the stress required to develop shear fracture is much less than that required for general deformation of the calcite.

Applications of Composite Material Theory

The behavior of the calcite-cemented Blairmore sandstone follows the general pattern of behavior which is expected for a particulate reinforced composite material with a non-deforming dispersed phase. That is, as compared with the matrix, the strength is considerably

increased and the ductility is markedly reduced. If this is in fact a valid analogy, it should be possible to define which variables will have the greatest effect on the deformational behavior of calcite-cemented rocks. It should also be possible to predict how changes in these variables will affect the deformational behavior of the rock.

Engineering composites with a non-deforming dispersed phase show a yield strength, tensile strength and fracture elongation which is dependent upon the mean free matrix separation and therefore volume fraction of the dispersed phase(Krock, 1967). Normally the strengths increase and the ductility decreases with increasing volume fraction. Although there is insufficient available data to definitively test this hypothesis, recent work by Rector(1970) gives some supporting evidence.

The arenaceous and dolomitic Columbus limestone containing 21 percent quartz, 17 percent dolomite and 62 percent calcite was found to behave much like a pure limestone. Strengths were relatively low, and ductility was high. Microscopic examination indicated that the quartz and dolomite grains showed only very limited development of microfractures in specimens shortened up to 10 percent. These results indicate that there is little or no change in deformational behavior at the volume fraction level of this rock. The reinforcing effect must become effective between 40 and 60 percent volume fraction of sand-sized detrital grains. Further work will be required in order to fully define the volume fraction effect in these rocks.

An important consideration of any experimental study of rock

deformation is what effect increasing temperature will have on the deformational behavior. Although the present study did not carry the investigation into higher temperatures, it should be possible to predict the effect of increasing temperature on the behavior of calcite-cemented sandstones based on the principles of composite material behavior.

The primary advantage of composite materials is not their ability to improve the room temperature strength, but rather their ability to maintain the attendant yield strength increase and creep resistance over a wide temperature range - up to 80 percent of the melting point of the matrix. The effectiveness of the dispersion is determined by its insensitivity to temperature increase(Krock & Broutman, 1967).

With this in mind, we can predict that the behavior of calcite-cemented sandstones will depend primarily upon the behavior of the detrital grains. Even though the deformational behavior of calcite is quite sensitive to temperature changes, strengths will remain high as long as the detrital grains remain strong and rigid.

A similar dependence may be expected for changes of strain-rate. As long as the detrital grains are deforming predominately by brittle fracture, it is probable that reduction of strain rate will have little effect on the deformational behavior of calcite-cemented sandstones.

In summary, the known behavior of particulate reinforced composite engineering materials supported by available data on the behavior of calcite-cemented rocks provides the basis for a general understanding of the deformational behavior of these rocks. The strength

and behavior primarily depend on the relative volume fraction of the sand components(the greatest effect will be observed over the range of 40 to 60 percent detrital grains) and the operative confining pressure. It is probable, however, that the strength will remain high even when the rock is deformed under increased temperatures and under decreased strain rates.

Chapter 6

SUMMARY AND CONCLUSIONS

General Statement

The calcite-cemented Blairmore sandstone has been subjected to shortening of up to 20 percent in a triaxial test apparatus at an approximate shortening rate of 10^{-4}/second, at room temperature and dry. The variation in macroscopic and microscopic deformational behavior has been defined over the range of confining pressure between 1 and 2600 bars. The behavior may be compared and contrasted with the well known behavior of the constituent phases.

The deformational behavior of the calcite-cemented Blairmore sandstone may be summarized as follows:

(1) The Blairmore sandstone undergoes a transition in deformational behavior from longitudinal fracture at atmospheric confining pressure, to brittle shear fracture up to 1.00 kb. Ductile faulting predominates at intermediate pressures and limited homogeneous flow occurs above 2.00 kb.

(2) The rock has a uniaxial compressive strength of 2.31 kb. The strength rises rapidly with increasing confining pressure up to 1.00 kb, and less rapidly above this.

(3) As compared with calcite rocks the strengths are very high, the ductility is greatly reduced and the brittle-ductile transition is suppressed to much higher confining pressures.

(4) At low confining pressures the calcite deforms through both fracture and ductile processes. With increasing confining pressure fracture is suppressed. Under these conditions calcite deforms primarily through twinning. However, additional plastic mechanisms (probably translation gliding) is responsible for the development of

bent twin lamellae and undulatory extinction. The twin lamellae show a considerable variation in orientation, but nearly all of the lamellae form at an inclination which is greater than 30 degrees to σ_1. The number of lamellae increase with increased shortening.

(5) The detrital grains deform by brittle fracture. Nearly all of the microfractures which develop are oriented more or less parallel to σ_1(inclined less than 15 to 20 degrees). Although microfractured detrital grains occur within all specimens deformed under confining pressure(the minimum confining pressure employed was 250 bars), fracturing is more pervasive above 1.00 kb, where a majority of the detrital grains are fractured. Numerous fractures are present within specimens which have sustained as little as 2.14 percent permanent shortening. The number of fractures increases rapidly with increased shortening up to about 5 percent, and then increases less rapidly.

Conclusions

The deformational behavior of the Blairmore sandstone can be understood in terms of the competition between the various modes of local fracture and of shape change. At low confining pressures fracture and brittle behavior predominate, while at high confining pressures plastic processes and shape change predominate.

The rapid increase in fracture strength in the brittle range associated with rising confining pressure occurs because the process of fracture propagation responsible for failure is very sensitive to changes in hydrostatic pressure. This is found to be true for all of the theoretical models of fracture propagation(Griffith and

McClintock-Walsh for brittle behavior; Dower and Francois-Wilshaw for initiation by plastic processes).

Significantly, this accounts for the fact that σ_1 increases much more rapidly than σ_3, which provides an increasing shear stress, $(\sigma_1 - \sigma_3)/2$. The increasing shear stress resulting from increased confining pressure serves to activate additional slip systems within calcite which have a high critical resolved shear stress. This forms the basis for the brittle-ductile transition of calcite. Activation of one or more additional slip systems provides the five independent slip systems which are required by the von Mises criteria in order for any solid to undergo homogeneous ductile flow.

With the onset of general ductile deformation of the calcite, fracture of the calcite contributes very little to the deformation. In fact, the transition from brittle-ductile occurs over a range of confining pressures, and increased confining pressure is accompanied by increased ductility. Once ductile processes make a significant contribution to the deformation, further increases in confining pressure are accompanied by only moderate increases in strength because the pressure sensitivity of the plastic processes of ductile flow is not great.

The behavior of the rock is determined by the mechanical behavior of the individual phases and their interactions. The interactions (which imply the homogeneous hypothesis of deformation of Taylor) profoundly affect the microscopic behavior of the individual phases. They, in turn, account for the differences in behavior between this

rock and the behavior of rocks consisting of the individual phases such as limestones and quartzites.

Although it may appear that the deformation mechanisms of calcite and quartz are the same in calcite-cemented sandstones as in the monomineralic aggregates, such as marbles and quartz sands, the writer proposes that it is necessary to consider the interaction of the different phases for the following reasons: (a) The strength and macroscopic deformational behavior of the rock is much different than would be expected based on the properties of orthocalcite rocks; (b) In general, the detrital grains fracture at applied stresses much below their normal confined compressive strengths; (c) The detrital grains do not fail by shear fracture as would be expected under triaxial compressive conditions, but rather by extension fracture.

Consideration of the differential mechanical properties between the ductile matrix and the rigid detrital grains and their interaction provides a basis to understand the development of the microfabric as well as the macroscopic behavior and strength. Contrasting mechanical properties such as differential ductility may give rise to stress concentrations. The effect of stress concentrations is to significantly alter the state of stress within, and in the immediate vicinity of, the detrital grains. Both the absolute magnitudes and the relative ratios of the effective stresses may change. By considering the effect of stress concentrations, it is possible to rationalize the observed behavior of the detrital grains(failure at relatively small applied stresses through the mechanism of extensional failure) with the stresses applied at the margins of the specimen.

In the present case, the most significant stress concentration is thought to develop as a result of the differential ductility between the calcite matrix and the rigid detrital grains. The plastic deforming calcite exerts shear stresses on the surface of the detrital grains. The shear stresses in turn generate tensile stresses within the detrital grains. The symmetry of the stress concentration(and of the orientation of the resultant fractures which it produces) reflects the symmetry of both the applied stress and the material being acted upon. It is for this reason, that the fractures are oriented parallel to the maximum principal stress of the applied system, not as a direct response to the applied system.

The interaction also has an effect on the deformation of the plastically deforming calcite. The forces exerted on the calcite serve to restrain deformation. Furthermore, the boundaries of the rigid grains serve to block deformation within the calcite and essentially all accomodation and shape change must therefore occur solely within the calcite grains themselves. In order for this to occur, slip or twinning must take place on the less favorably oriented systems, and/or on systems which have large critical resolved shear stresses. These factors, coupled with the small effective calcite grain size(determined by the distance between the detrital grains), are responsible for the high strength and low ductility of this rock. Because the calcite is not as free to deform ductilely as when detrital grains are not present, the rock deforms by shear fracture under conditions where limestone and marble normally deform by homogeneous flow.

The deformational behavior of this rock has much in common with the behavior of particulate reinforced composite engineering materials. Because of this similarity, it should be possible to predict what effect changes in other variables may have on the deformational behavior of this rock based on the well-known behavior of composite engineering materials.

The following sequence of events is visualized for ductile deformation:

(1) Yielding first develops by e-twinning in favorably oriented calcite grains in response to shear stresses directly related to the stresses applied to the margins of the specimen.

(2) With the onset of yielding, transverse tensile stresses are generated within the detrital grains by the plastically deforming calcite. Detrital grains previously touching each other, but previously "cushioned" by calcite, are forced together.

(3) Fractures are initiated by (a) the tensile component of elastic stress concentrations which develop at the site of detrital grain to grain contacts, and by (b) elastic tensile stresses generated within the detrital grains by the shear stresses exerted by the plastically deforming calcite.

(4) The propagation and orientation of the fractures is controlled by the tensile stresses exerted by the calcite. Evidence for the importance of this mechanism comes from two observations. Fractures are frequently developed within detrital grains which do not make contact with other detrital grains. The fractures are systematically oriented

and reflect the control of a pervasive stress which is not localized, as is the case for stress concentrations generated at detrital grain to grain contacts.

(5) The development of microfractures within the detrital grains does not significantly affect the deformational behavior of the calcite. This is because much of the grain boundary between the calcite and the detrital grains is unchanged, but retains the character of a rigid non-yielding interface. Further deformation requires that calcite deform by slip or twinning on the less favorably oriented and highly resistant systems. The need for additional mechanisms of accommodation is particularly acute near the grain boundary interface where bent lamellae and undulatory extinction is observed to be most intensely developed.

(6) Much of the increased strain is accomplished by the development of additional twin lamellae.

(7) At low to moderate confining pressures, the ultimate strength is reached once the favorably oriented twin and slip systems have been exhausted. A point is reached at which the increased differential stress required for further ductile deformation reaches the level where shear fractures are propageted and failure occurs.

(8) At high confining pressures, similar behavior is observed. However, considerably more plastic deformation may occur because of the higher prevailing shear stresses. Strain hardening occurs with increased shortening until the onset of incipient shear fractures is observed once the ultimate strength is achieved. Continued deformation

is accomplished through a combination of additional plastic deformation in the calcite and by displacement on shear surfaces.

Geological Implications

It is proposed that the results of this study may provide the basis of understanding the deformation of several geological materials which are similar or have analogous properties to the calcite-cemented sandstone investigated in this study.

The direct application to the reinterpretation of work by Friedman(1963) on calcite-cemented rocks is readily apparent. In fact, the similarity of such features as grain size and calcite content between the Blairmore sandstone and some of the rocks investigated by Friedman indicate that these rocks have many properties in common. While the results of the present study confirm many of the observations made by Friedman, the writer thinks that the interpretation developed in the present investigation provides a much more thorough understanding of the deformational processes involved, and also accounts for some previously unexplained features and relations. In particular, it accounts for the general macroscopic behavior of the rocks, while at the same time it resolves the general problem of the development of microfractures within the detrital grains.

One of the most important contributions to the understanding of deformational processes of rock materials resulting from this work, is the recognition of the role which stress concentrations play in the development of extension fractures. Differential ductility of a

deforming material may be responsible for the development of localized states of stress within the material which are much different from the stress applied at the margins of the rock as a whole. Because the state of stress is one of the most powerful variables in controlling the deformational behavior of rock materials, recognition that stress concentrations may develop is fundamental to understanding the deformation of these materials.

The natural occurrence of such features as extension fractures, tension fractures, "microboudinage" etc. which occur within relatively strong, rigid mineral grains is well documented in the literature. Such features have been shown to form normal to the axis of principal elongation within many deformed rocks and are known to occur within quartz(Carter & Friedman, 1965; Stauffer, 1970), feldspar(Dalziel & Bailey, 1968; Stauffer, 1970), garnet(Harker, 1932, p. 195, 308; de Sitter, 1956; Naha, 1959; Ramsay, 1967, p. 182; Dalziel & Bailey, 1968), and pyrite(Spry, 1969, p. 242). They are also found under similar conditions within pebbles and boulders of deformed conglomerates(Stauffer, 1970; Ramsay & Sturt, 1970; Hsu, 1971).

However, nowhere(to the writer's knowledge) is there any consideration given to the mechanism and stresses responsible for the development of this fundamental deformational feature. The mechanism of stress concentration associated with rigid inclusions within a ductilely deforming matrix provides a rational explanation of how tensile stresses may develop locally within a material which is subjected to compressive stresses. This mechanism provides a fundamental understanding of the development of such features based on rational mechanics.

Another contribution of this study is laying of the groundwork for attacking the general problem of how rocks consisting of more than one mineral phase which normally have highly contrasting mechanical properties will deform. The understanding provided through the investigation of the calcite-cemented Blairmore sandstone, considered together with the known behavior of engineering composite materials, provides a basis for such a study.

Recommendations for Future Work

Several experiments may be formulated in order to further evaluate the factors which control the deformational behavior of calcite-cemented sandstones. A series of experiments may be carried out using the apparatus and techniques which were developed during the present study, and this could be extended by employing model studies and theoretical analysis.

The effect of volume fraction on the behavior of calcite-cemented sandstones over the range between 40 and 60 percent sand fraction is of particular interest. Experimental deformation of sandstones within this volume fraction range would not only define the effect of this variable on macroscopic behavior and strength, but would also allow detailed verification of the nature of microfracture development in those cases where the detrital grain to grain contacts do not occur.

A statistical study could be carried out which relates microfracture development to such factors as the axial ratio of the detrital grains, or to mineralogy(elongate grains or relatively weak minerals should show the development of more fractures).

The hypothesis proposed to explain the high strength of the Blairmore sandstone has several implications for the behavior of calcite. The effect of grain size on the flow stress of limestone should be evaluated by deforming several limestones of known grain size and otherwise uniform properties in order to test the general applicability of the Hall-Petch relation to this rock type.

By comparing the nature of strain development within orthocalcite rocks and calcite-cemented sandstones, it should be possible to determine how strain development differs within the two rock types. Attention should focus on the general intensity such as comparing twin lamellae indices for the two rocks deformed under comparable conditions. This could be of particular interest if a more precise definition of the thickness of twins could be better determined.

The high strength and diminished ductility is thought to be primarily related to the need for relatively great amounts of general strain to develop in the immediate vicinity of the interface between the calcite and the detrital grains. It may be possible to compare the development of strain at grain boundaries in orthocalcite rocks and calcite-cemented sandstones in order to determine whether such a difference does in fact exist.

The proposed mechanism of interaction of the calcite and detrital grains is thought to be responsible for the fracture development within the detrital grains. Comparison of the orientation of individual microfractures with the strain of the surrounding calcite grains(for instance, using the Turner technique through which the principal

strains in the calcite may be defined) should serve to test the validity of this relationship.

More generally, tests of the predictions made with the aid of composite material theory(which indicate that the behavior of the composite will be primarily controlled by the properties of the strong dispersed phase) may be made by performing experiments over a range of temperature and strain rates. This should be useful as calcite behavior is very sensitive to changes in both temperature and strain rate, while quartz and other common constituents of sand grains are quite insensitive except at high temperatures and very low strain rates.

A model or theoretical study should be devised which better defines stress concentrations resulting from plastic or ductile flow around rigid inclusions, particularly for inclusions which have a shape characteristic of sand grains(spherical to ellipsoidal).

BIBLIOGRAPHY

Armstrong, R., Codd, I., Douthwaite, R.M. & Petch, 1962, The plastic deformation of polycrystalline aggregates. Phil. Mag., 7:45-58.

Ashby, M.F., 1966, Work hardening of dispersion-hardened crystals. Phil. Mag., 14:1157-1178.

Balakrishma, S., 1963, Experimental study of fracture mechanisms in sandstones. Geophys. Jour., 14:119-128.

Birch, F., 1966, Compressibility; Elastic constants: in Handbook of Physical Constants, editor S.P. Clark, Jr., Geol. Soc. Amer., Memoir 97, 97-173.

Bombolakis, E.G., 1964, Photoelastic investigation of brittle crack growth within a field of uniaxial compression. Tectonophysics, 1:343-351.

Borg, I.Y. & Handin, J., 1967, Torsion of calcite single crystals. Jour. Geophys. Res., 72:641-669.

_____ and Maxwell, J.C., 1956, Interpretation of fabrics of experimentally deformed sands. Amer. Jour. Sci., 254:71-81.

_____ and Turner, F.J., 1953, Deformation of Yule Marble: Part VI - Identity and significance of deformation lamellae and partings in calcite grains. Bull. Geol. Soc. Amer., 64:1343-1352.

_____ and _____, 1967, Torsion of calcite single crystals. Jour. Geophys. Res., 72:641-691.

Borg, I.Y., Friedman, M., Handin, J. & Higgs, D.V., 1960, Experimental deformation of St. Peter sand: A study of cataclastic flow: in Rock Deformation, editors D. Griggs and J. Handin, Geol. Soc. Amer. Memoir 79, 133-191.

Boyd, J.M. & Currie, J.B., 1969, Fracture porosity in alabaster; an experimental model of rock deformation. Bull. Can. Pet. Geol., 17:117-132.

Brace, W.F., 1961, Dependence of fracture strength of rocks on grain size. Penn. State Univ. Mineral Industries Experimental Station Bull., 76:99-103.

_____, 1964, Brittle fracture of rocks: in Proc. Internat. Conf. on State of Stress in the Earth's Crust, editor W.R. Judd, American Elsevier, N.Y., 110-178.

_____, 1968, The mechanical effects of pore pressure on fracturing of rocks: in Pro. Conf. on Research in Tectonics, editors A.J. Baer and D.K. Norris, Geol. Sur. of Canada, G.S.C. Paper 68-52, p. 113-123.

Carniglia, S.C., 1966, Grain boundary and surface influence on mechanical behavior of refractory oxides: in Materials Science Research, editors Kriegel and Palmour, Plenum Press, N.Y., 3:425-471.

Carter, N.L. & Friedman, M., 1965, Dynamic analysis of deformed quartz and calcite from the Dry Creek Ridge Anticline, Montana. Amer. Jour. Sci., 263:747-785.

_____ and Raleigh, C.B., 1969, Principal stress directions from plastic flow in crystals. Geol. Soc. Amer. Bull., 80:1231-1264.

Colback, P.S.B. & Wild, B.L., 1965, The influence of moisture content on the compressive strength of rock. Proc. Symp. Rock Mech., 3rd, Toronto.

Conel, J.E., 1962, Studies of the development of fabrics in some naturally deformed limestones. Ph.D. thesis, Calif. Inst. Tech., Pasadina, Calif., 257 p.

Dalziel, I.W.D., & S.W. Bailey, 1968, Deformed garnets in a mylonitic rock from the Grenville Front and their significance. Amer. Jour. Sci., 266:542-562.

Deer, W.A., Howie, R.A. & Zussman, J., 1962. Rock-forming Minerals. J. Wiley & Sons, Inc., N.Y., 5, 371 p.

Deere, D.U., 1966, Discussion on rock classification; Proc. Cong. Intern. Soc. Rock Mech., 1st Lisbon, 5:156-158.

de Sitter, L.U., 1956, The strain on rock in mountain building processes. Amer. Jour. Sci., 254:586-604.

Donath, F.A., 1961, Experimental study of shear failure in anisotropic rocks. Geol. Soc. Amer. Bull., 72:985-990.

_____, 1964, Strength variation and deformational behavior in anisotropic rock: in State of Stress in the Earth's Crust, editor W.R. Judd, American Elsevier, N.Y., 281-297.

_____, 1968, Experimental rock deformation in dynamic structural geology. Rock Mechanics Seminar, editor R.E. Riecker. Air Force Cambridge Res. Lab., 2:355-437.

_____, 1970, Some information squeezed out of rock. Amer. Sci., 58:54-72.

_____, 1970a, Rock deformation apparatus and experiments for dynamic structural geology. Jour. Geol. Educ., 18:3-12.

_____ and Parker, R.B., 1964, Folds and folding. Geol. Soc. Amer. Bull., 75:48.

Dower, R.J., 1967, On the brittle-ductile transition pressure. Acta. Metall., 15:497-500.

Drucker, D.C., 1966, The continuum theory of plasticity on the macroscale and the microscale. Jour. of Materials, 1:873-910.

Edelson, B.I. & Baldwin, W.M., Jr., 1962, The effect of second phases on the mechanical properties of alloys. Trans. Quar., Amer. Soc. Metals, 55:230-250.

Edmonds, D.V. & Beevers, C.J., 1968, The effects of inclusions on the stress distribution in solids. Jour. of Mater. Sci., 3:457-463.

Eshelby, J.K., Frank, F.C. & Nabarro, F.R.N., 1951, The equilibrium of linear arrays of dislocations. Phil. Mag., 42:351-364.

Folk, R.L., 1961, Petrology of Sedimentary Rocks. Hemphills, Austin, Texas, 154 p.

Francois, D. & Wilshaw, T.R., 1968, The effect of hydrostatic pressure on the cleavage fracture of polycrystalline materials. Jour. of App. Physics, 39:4170-4177.

Friedman, M., 1963, Petrofabric analysis of experimentally deformed calcite-cemented sandstones. Jour. Geol., 71:12-37.

_____, Perkins, R.D. & Green, S.J., 1970, Observation of brittle-

deformation features at the maximum stress of Westerly granite and Solenhofen limestone. Int. Jour. Rock Mech. Min. Sci., 7:297-306.

Gallagher, J.J., Sower, G.M. & Friedman, M., 1970, Photomechanical model studies relating to fracture in granular rock aggregates. Abstract, Geol. Soc. of Amer.; South-Central Section Fourth Annual Meeting, April 2-4, 1910 Ramada Inn College Stations, Texas, 2:285.

Gangulee, A. & Gurland, J., 1967, On the fracture of silicon particles in aluminum-silicon alloys. Trans. of Metal. Soc. of AIME, 239:269-272.

Garber, R.I., 1947, The mechanism of calcite and nitre twinning under plastic deformation. Jour. Phys. USSR, 11:55-66.

Griffith, A.A., 1921, The phenomena of rupture and flow in solids. Phil. Trans. Roy. Soc., A, 221:163-198.

Griggs, D.T., 1938, Deformation of single calcite crystals under high confining pressures. Amer. Mineralogist, 23:27-33.

_____ and Bell, J.F., 1938, Experiments bearing on the orientation of quartz in deformed rocks. B.G.S.A., 49:1732-1746.

_____ and Blacic, J.D., 1965, Quartz: Anomalous weakness of synthetic crystals. Science, 147:292-295.

_____ and Handin, J., 1960, Observations on fracture and a hypothesis of earthquakes, in Rock Deformation, editors D. Griggs and J. Handin, Geol. Soc. Amer. Mem. 79, 347-364.

_____, Turner, F.J. and Heard, H.C., 1960, Deformation of rocks at 500° to 800°C, in Rock Deformation, editors D. Griggs

and J. Handin, Geol. Soc. Amer. Mem. 79, 39-104.

Gurland, J. & Plateau, J., 1963, The mechanisms of ductile rupture of metals containing inclusions. Trans. for Amer. Soc. of Metals, 56:442-454.

Handin, J., 1966, Strength and ductility, in Handbook of Physical Constants, editor S.P. Clark, Rev. Ed., Geol. Soc. Amer. Mem. 97, 223-289.

_____, 1969, On the Coulomb-Mohr failure criterion. Jour. Geophys. Res., 74:5343-5348.

_____ and Griggs, D., 1951, Deformation of Yule Marble: Part II - Predicted fabric changes. Bull. G.S.A., 62:863-886.

_____ and Hager, R.V., Jr., 1957, Experimental deformation of sedimentary rocks under confining pressure: Tests at room temperature on dry samples. Amer. Assoc. Petr. Geologists Bull., 41:1-50.

_____ and _____, 1958, Experimental deformation of sedimentary rocks under confining pressure; Tests at high temperature. Amer. Assoc. Petr. Geologists Bull., 42:2892-2934.

_____, Heard, H.C., & Magouirk, J.N., 1967, Effects of the intermediate principal stress on the failure of limestone, dolomite and glass at different temperatures and strain rates. Jour. Geophys. Res., 72:611-640.

Hardy, H.R., Jr., Kim, R.Y., Stefanko, F. & Wang, Y.J., 1970, Creep and microseismic activity in geologic materials, in Rock Mechanics - Theory and Practice, editor W.H. Somerton. Amer. Inst. Min. Met. and Petr. Eng., Inc., N.Y., p. 377-413.

Harker, A., 1932, Metamorphism, Methuen & Co., London, 362 p.

Hasselman, D.P.H. & Fulrath, R.M. 1966, Proposed fracture theory of a dispersion-strengthened glass matrix. Jour. Amer. Cer. Soc., 49:68-72.

_____ and _____, 1967, Micromechanical stress concentrations in two-phase brittle-matrix ceramic composites. Jour. Amer. Cer. Soc., 50:399-404.

Hawkes, I. & Mellor, M., 1970, Uniaxial testing in rock mechanics laboratories. Eng. Geol., 4:177-285.

Heard, H.C., 1960, Transition from brittle fracture to ductile flow in the Solenhofen limestone as a function of temperature, confining pressure and interstitial fluid pressure, in Rock Deformation, editors D. Griggs and J. Handin, Geol. Soc. Amer. Mem. 79, 193-226.

_____, 1963, The effect of large changes in strain rate in the experimental deformation of Yule marble. Jour. Geol., 71: 162-195.

_____ and Carter, N.L., 1968, Experimentally induced "Natural" intergranular flow in quartz and quartzite. Amer. Jour. Sci., 266:1-42.

Hoek, E., 1965, Rock fracture under static stress conditions. Mech. Eng. Res. Inst., C.S.I.R. Pretoria, Report MEG 383.

_____ and Bieniawski, Z.T., 1965, Brittle fracture propagation in rock under compression. Jour. Fract. Mech., 1:137-155.

Hoskins, J.R. & Horino, F.G., 1968, Effect of end conditions on determining compressive strength of rock samples. U.S. Dept.

Interior Rept., RI 7171, 22 p.

Houpert, R., 1966, Relation entre la résistance à la rupture des roches et la dimension de leurs minéraux. C.R. Acad. Sci. Paris, t. 263:516-519.

Hsu, M.Y., 1971, Analysis of strain, shape and orientation of the deformed pebbles in the Seine River Area, Ontario. Ph.D. thesis, McMaster Univ., Hamilton, Ontario, 179 p.

Inglis, C.E., 1913, The stresses in a plate due to the presence of cracks and sharp corners. Trans. Inst. Naval Architects, 55:219-230.

Jaeger, J.C., 1960, Shear fracture of anisotropic rocks. Geol. Mag., 97:65-72.

_____, 1967, Brittle fracture of rocks; in Failure and Breakage of Rock, editor C. Fairhurst, Proc. 8th Symp. on Rock Mech., Univ. of Miss., Amer. Inst. Min. Metal. and Petrol. Eng., Inc., N.Y., p. 1-57.

_____ and Cook, N.G.W., 1969, Fundamentals of Rock Mechanics. Methuen & Co. Ltd., London, 513 p.

Jaswon, M.A. & Dove, D.B., 1960, The crystallography of deformation twinning. Acta Cryst., 13:232-240.

Kartesz, P., 1968, A static rock model based on petrological properties(Abstract). Proc. 3rd Budapest Conf. on Soil Mech. Found. Eng., Sect. 4, 101-110.

Keith, R.E. & Gilman, J.J., 1960, Dislocation etch pits and plastic deformation in calcite. Acta Metall., 8:1-10.

Kelly, A., 1966, Strong Solids. Clarendon Press, Oxford, 212 p.

_____ and Tyson, W.R., 1965a, Tensile properties of fiber-reinforced metals: Copper/tungsten and copper/molybdenum. Jour. Mech. Phys. Solids, 13:329-350.

_____ and _____, 1965b. Fiber-strengthened materials; in High Strength Materials, editor V.F. Zackey, J. Wiley & Sons Inc., N.Y., 578-602.

Krock, R.H., 1967, Inorganic particulate composites; in Modern Composite Materials, editors L.J. Broutman & R.H. Krock, Addison-Wesley, Reading, Mass., p. 455-478.

_____ and Broutman, L.J., 1967, Principles of composites and composite reinforcement; in Modern Composite Materials, editors L.J. Broutman and R.H. Krock, Addison-Wesley, Reading, Mass., 3-26.

_____ and Shepard, L.A., 1963, Mechanical behavior of the two-phase composite, Tengsten-Nickel-Iron. Trans. Met. Soc. of AIME, 227:1127-1134.

Lange, F.F., 1970, Fracture energy measurements of Glass-Al_2O_3. Abstract, Bull. Amer. Cer. Soc., 49:390.

Logan, J.M., Iwasaki, M.T., & Friedman, M., 1970, Experimental investigation of sliding friction in multi-lithologic specimens. Geol. Soc. Amer. Abstracts, Milwaukee, Wisconsin, p. 608-609.

McClintock, F.A., 1968, On the mechanics of fracture from inclusions, in Ductility, ASM Seminar, Metals Park, Ohio, 255-277.

_____ and Argon, A.S., 1966, Mechanical Behavior of Materials. Addison-Wesley, Reading, Mass., 770 p.

_____ and Walsh, J.B., 1963, Friction on Griffith cracks in rocks

under pressure. Proc. Fourth U.S. Congress on Appl. Mech., ASME, N.Y., 1015-1021.

McLamore, R. & Gray, K.E., 1967, The mechanical behavior of anisotropic sedimentary rocks. Trans. ASME Jour. of Engin. for Industry, 89, Ser. B, 62-73.

Middleton, G.V., 1962, Size and sphericity of quartz grains in two turbidity formations. Jour. Sed. Petrol., 32:725-742.

Miller, R.P., 1965, Engineering classification and index properties for intact rock, Ph..D. thesis, Univ. of Illinois, Urbana, Illinois.

Mogi, K., 1966, Some precise measurements of fracture strength of rocks under uniform compressive stress. Rock Mech. Eng. Geol., 4:41-55.

_____, 1971a, Fracture and flow of rocks under high triaxial compression. Jour. Geophys. Res., 76:1255-1269.

_____, 1971b, Effect of the triaxial stress system on the failure of dolomite and limestone. Tectonophysics, 11:111-127.

Nadai, A., 1950, Theory of flow and fracture of solids. McGraw-Hill Book Co. Inc., N.Y., 572 p.

Naha, K., 1959, Time of formation and kinematic significance of deformation lamellae in quartz. Jour. Geol., 67:120-124.

Nivas, Y. & Fulrath, R.M., 1970, Limitations of Griffith flaws in glass-matrix composites. Jour. Amer. Cer. Soc., 53:188-191.

Orowan, E., 1950, Fatigue and fracture of Metals. Symposium at M.I.T., Wiley & Sons., Inc., N.Y.

Outwater, J.O., Jr., 1956, The mechanics of plastics reinforcement in

tension. Modern Plastics, 33, no. 7, p. 156.

Parkash, B., 1968, A Fortran IV program for grain size data from thin sections. Tech. Memo. 68-2, Geology Dept., McMaster University, Hamilton, Ontario, 9 p.

Paterson, M.S., 1958, Experimenatl deformation and faulting in the Wombeyan marble. Geol. Soc. Amer. Bull., 69:465-475.

_____, 1967, Effect of pressure on stress-strain properties of materials. Geophys. Jour. Royal Soc., 14:13-17.

_____, 1969, The ductility of rocks, in Physics of Strength and Plasticity, editor, A.S. Argon, M.I.T. Press, Cambridge, Mass., 377-392.

_____ and Weaver, C.W., 1970, Deformation of polycrystalline MgO under pressure. Jour. Amer. Cer. Soc., 53:463-471.

Perkins, R.D., Green, S.J., & Friedman, M., 1970, Uniaxial stress behavior of porphyritic toanlite at strain rates to 10^3/second. Int. Jour. Rock Mech. Min. Sci., 7:527-535.

Price, N.J., 1966, Fault and Joint Development in Brittle and Semi-brittle Rock. Pergamon Press, Toronto, 176 p.

_____, 1970, Laws of rock behavior in the earth's crust, in Rock Mechanics -- Theory and practice, editor, W.H. Somerton, Amer. Inst. Min. Met. and Petr. Eng., Inc., N.Y., 3-23.

Ramsay, J.G., 1967, Folding and Fracturing of Rocks. McGraw-Hill Book Co., Toronto, 568 p.

Ramsay, D.M. & Sturt, B.A., 1970, Polyphase deformation of a polymict Silurian conglomerate from Mageroy, Norway. Jour. Geol., 78:264-280.

Rector, R.J., 1970, An experimental investigation into the influence of environmental and fabric parameters on the deformational behavior of sandstones. Ph.D. thesis, McMaster Univ., Hamilton, Ontario, 179 p.

Sack, R.A., 1946, Extension of Griffith Theory of rupture to three dimensions. Pro. Phys. Soc. London, 58:729-736.

Skinner, W.J., 1959, Experiments on the compressive strength of anhydrite. Engineer, 207:255-259; 288-292.

Sosman, R.R., 1927, Properties of Silica. Chemical Catalog Co., N.Y., 856 p.

Spry, A., 1969, Metamorphic Textures. Pergamon Press, Toronto, 350 p.

Stauffer, M.R., 1970, Deformation textures in tectonites. Can. Jour. Earth Sci., 7:498-511.

Stroh, A.N., 1954, The formation of cracks as a result of plastic flow. Proc. Roy. Soc., 223:404-414.

_____, 1955, The formation of cracks in plastic flow II. Proc. Roy. Soc., 232:548-560.

Swolfs, H. & Logan, J., 1970, Experimental evidence of the role of pore fluid chemistry on the mechanism of fracture in sandstones. Abstract, Geol. Soc. Amer., Annual Meeting, Milwaukee, Wisconsin.

Taylor, G.I., 1938, Plastic strain in metals. Jour. Inst. Metals, 62:307-324.

Tetelman, A.S., & McEvily, A.J., 1967, Fracture of Structural Materials. J. Wiley & Sons., Inc., N.Y., 697 p.

Timoshenko, S. & Goodier, J.N., 1951, Theory of Elasticity. McGraw-Hill Book Co., Toronto, 506 p.

Tobin, D.G., 1966, Microscopic criteria for defining macroscopic modes

of deformation in experimentally deformed oolitic limestone. Ph.D. thesis, Columbia Univ., Univ. Microfilms Inc., Ann Arbor, Michigan, 102 p.

Tummala, R.R. & Friedberg, A.L., 1970, Strength of glass-crystal composites. Jour. Amer. Cer. Soc., 52:228-229.

Turner, F.J., 1953, Nature and dynamic interpretation of deformation lamellae in calcite of three marbles. Amer. Jour. Sci., 251:276-298.

_____, and Ch'ih, C.S., 1951, Deformation of Yule marble: Part III - Observed fabric changes due to deformation at 10,000 atmospheres confining pressure, room temperature, dry. Bull. Geol. Soc. Amer., 62:887-906.

_____, and Weiss, L.F., 1963, Structural Analysis of Metamorphic Tectonites. McGraw-Hill Book Co. Inc., N.Y., 545 p.

_____, Griggs, D.T. & Heard, H.C., 1954, Experimental deformation of calcite crystals. Bull. Geol. Soc. Amer., 65:883-934.

Underwood, E.E., Colcord, A.R. & Waugh, R.C., 1968, Quantitative relationships for random microstructures, in Ceramic Microstructures, editors R.M. Fulrath & J.A. Pask, J. Wiley & Sons, N.Y., 25-52.

von Mises, R., 1928, Mechanik der Plastichen Formanderung von Kristallen. A. Agnew. Math. Mech., 8:161.

Van Vlack, L.H., 1968, Introduction: Ceramic microstructures, in Ceramic Microstructures, editors R.M. Fulrath & J.A. Pask, J. Wiley & Sons, N.Y., 1-21.

Watstein, D., 1953, Effect of straining rate on the compression strength

and elastic properties of concrete. Jour. Amer. Concrete Bull., 24:229.

Wawersik, W.R. & Fairhurst, C., 1970, A study of brittle rock fracture in laboratory compression experiments. Int. Jour. Rock Mech. Min. Sci., 7:561-575.

Willard, R.J. & McWilliams, J.R., 1969, Effect of loading rate on trans-grain or intergranular fracture in charcoal gray granite. Int. Jour. Rock Mech. Min. Sci., 6:415-421.

Williams, A.J. & Cahn, R.W., 1964, The dynamics of elastic twinning in calcite, in Deformation Twinning, editors R.E. Reed-Hill, J.P. Hirth & H.C. Rogers, Gordon & Breach Science Publishers, N.Y., 156-176.

Wuerker, R.G., 1956, Annotated tables of strength and elastic properties of rocks. Petroleum Branch, Amer. Inst. Min. & Metal. Engineers.

_____, 1959, Influence of stress rate and other factors on strength and elastic properties of rock. Quart. Colorado Sch. of Mines, 54:5-31.

Appendix A

Test Apparatus and Experimental Techniques

Design of the Triaxial Test Apparatus

(1) General Statement

The experimental equipment used in this study consists of four basic systems;

(1) pressure vessel

(2) confining pressure system

(3) loading ram and loading rate system

(4) instrumentation

A general view of the triaxial test apparatus and a schematic diagram are shown in Plate 3 and Fig. 31 respectively.

(2) Pressure Vessel

A photograph showing the components, and a schematic diagram of the pressure vessel are given in Plate 4 and Fig. 32. The pressure vessel was built at Columbia University, and with the exception of minor alterations, it is the same as described by Donath(1970a).

(3) Confining Pressure System

Kerosene is used as the confining pressure medium. Confining pressures are generated using a manual Enerpac model P228 hydraulic jack rated at 40,000 psi. Movement of the piston into the test chamber causes a decrease in the volume of the test chamber, which would normally result in an increase in the confining pressure. However,

Plate 3

A general view of the triaxial test apparatus.

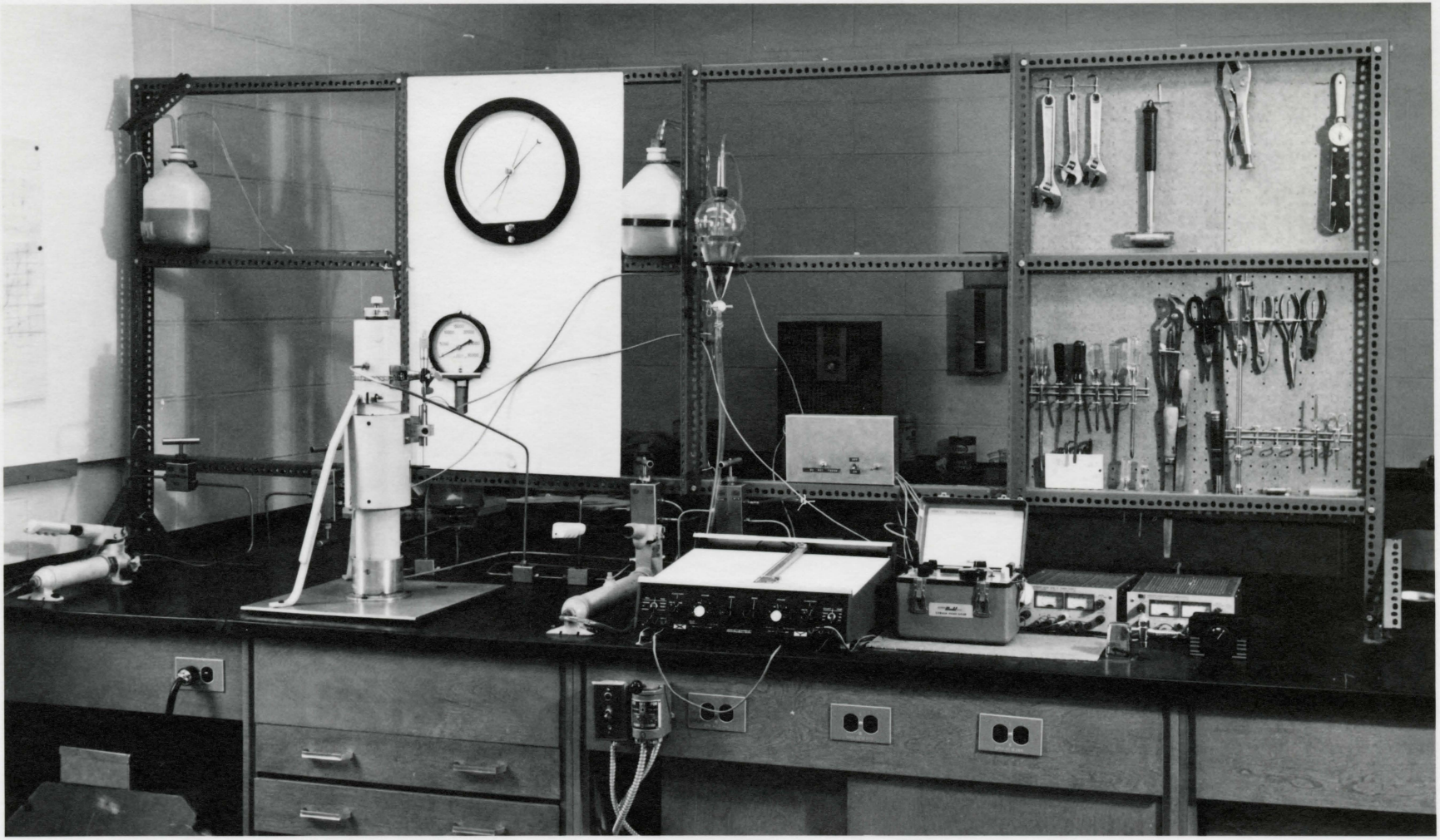

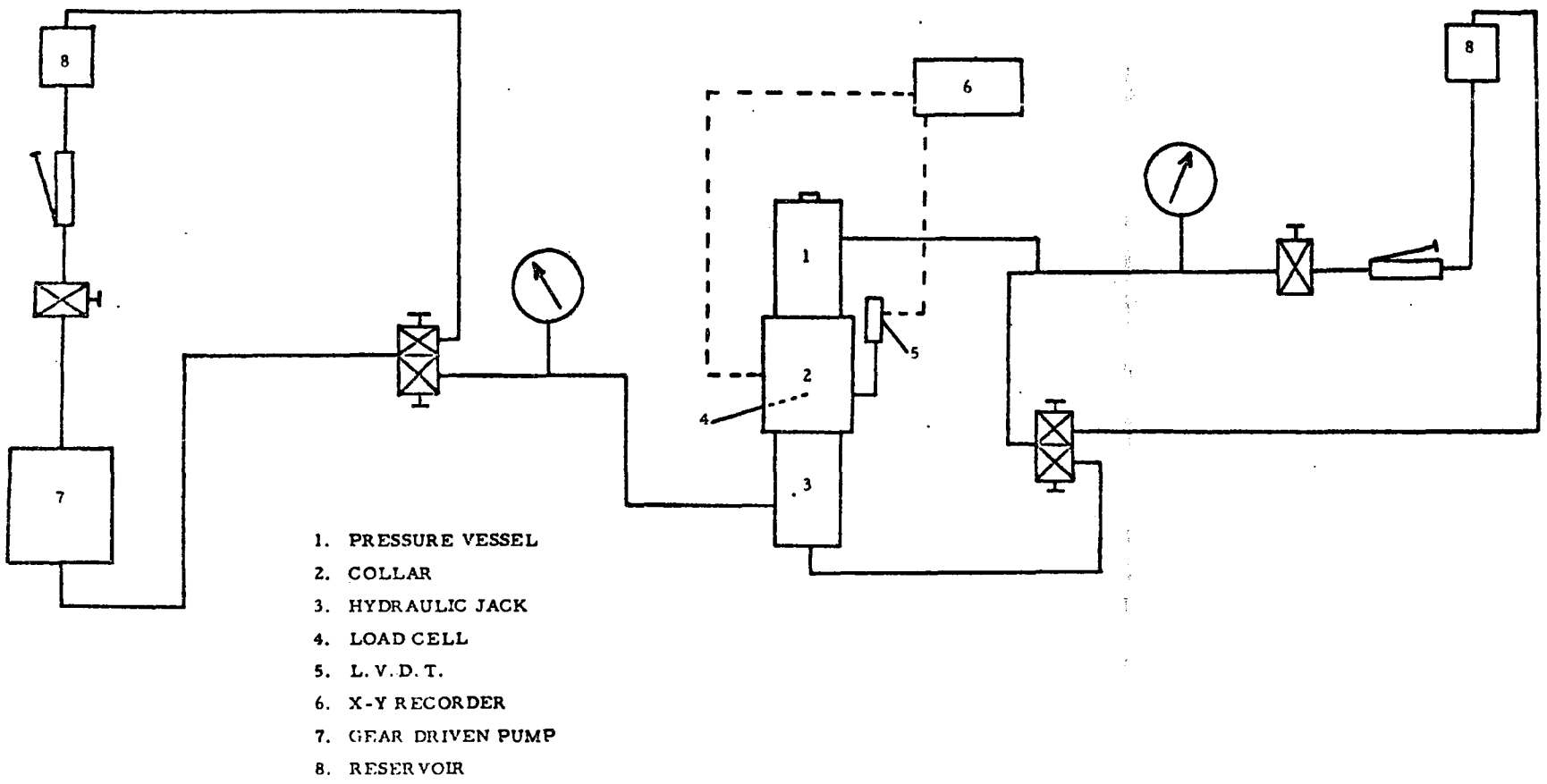

Figure 31 Schematic diagram of triaxial test apparatus.

Plate 4

Exploded photograph of the pressure vessel showing the piston, specimen, anvil, upper and lower retaining plugs, piston rod and the load cell.

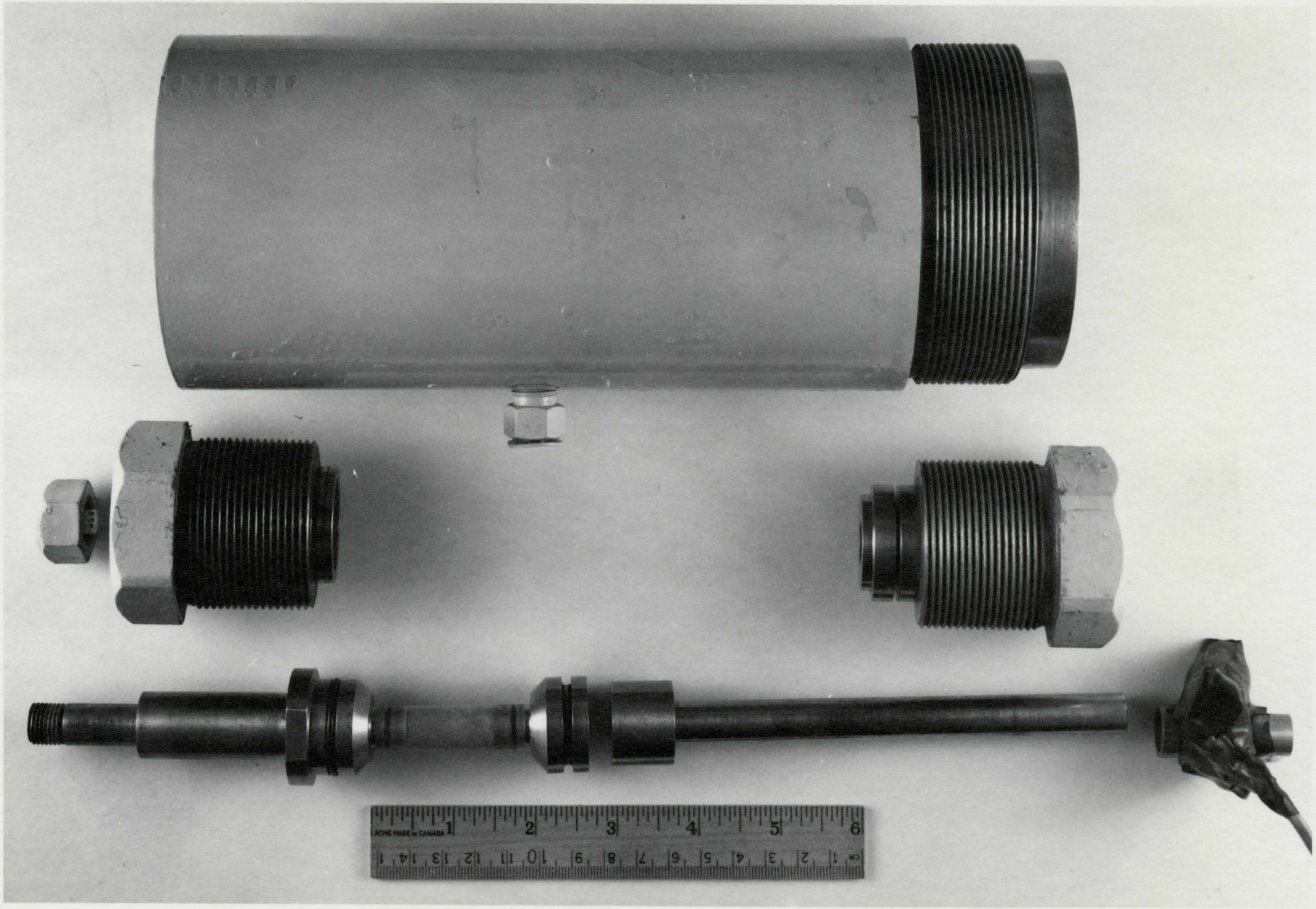
ACME MADE in CANADA
1 2 3 4 5 6
CM 1 2 3 4 5 6 7 8 9 10 11 12 13 14

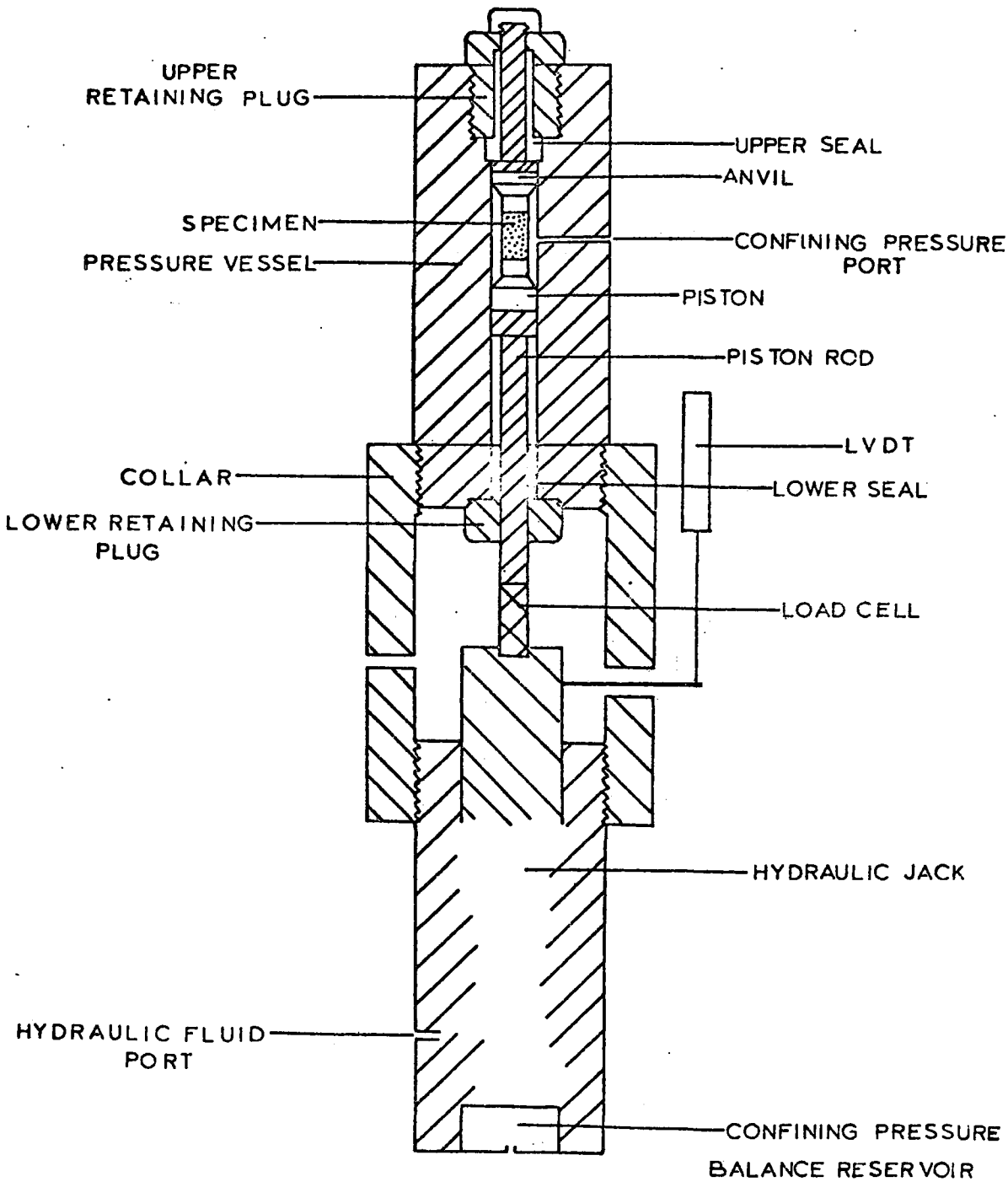

Figure 32 Schematic diagram of pressure vessel-press assembly.

constant confining pressure is maintained through a balance overflow system which allows the excess kerosene to flow into a reservoir in the hydraulic jack behind the advancing ram. A temperature compensated (-25° to 125°F) Heise gage is used to monitor the confining pressure. Confining pressure measurements are accurate to within 10 bars or less.

(4) Loading System

The load is applied through a 20 ton Enerpac hydraulic ram which is connected to the pressure vessel by a cylindrical steel collar. The ram is mechanically linked to the test specimen by a load cell, piston rod and the lower piston. The hydraulic ram is driven by a motor-driven hydraulic pump which was designed and built at McMaster University during the period 1966-1969. This system provides a constant loading rate.

(5) Instrumentation

A Hewlett-Packard model 2D-2A, X-Y recorder is used to record the axial load and the piston displacement. A Cramer electric motor and a switching device interrupts the Y-axis to provide a time signal on the record from which shortening rates may be calculated.

The axial load is measured with the aid of a load cell made by mounting four Budd metal film strain gages(Type C-6-141-B) on 1-½ by ½ inch cylinder of "Ultimo 200" steel. These gages have a high resolution and are virtually temperature insensitive between 62° and 100°F. The load cells are calibrated by applying known loads in a Tinius Olsen testing machine. A Budd P-350 Strain Indicator is used to

calibrate the load cell and to amplify the signal from the load cell to the X-Y recorder.

The axial stress in the specimen can be calculated from the axial load after corrections for confining pressure, frictional contributions of the piston, and changing cross-sectional area of the specimen have been made. The stress is estimated to be accurate within 3 percent.

Displacement of the piston is measured by a Sanborn LVDT which is mechanically linked to the ram. Output from the LVDT is fed to the X-axis of the X-Y recorder. Piston displacement is converted to specimen strain after corrections have been made for the elastic distortion of the apparatus.

The corrections resulting from the elastic distortion of the apparatus is relatively large, as the elastic distortion is 1.3610 x 10^{-5} cm/bar. The relatively large corrections make determination of specimen strain unreliable for small amounts of specimen strain (0.5%). For strains greater than this, the corrections produce errors of no more than about 5 percent of the observed value.

(6) Specimen Preparation

Cylindrical test-pieces one-half inch(1.25 cm) in diameter were cored from the source block with a diamond drill. All of the cores used in this series of experiments came from a volume of rock occurring at the same stratigraphic interval. The source volume is about five inches x five inches x one and one-half inches(12.7 cm x 12.7 cm x 4.3 cm).

The long axes of the cores are oriented normal to the apparent bedding lamination. The ends of the cores were ground flat for form a right cylinder with an overall length between 0.990 and 1.010 inches (2.515 cm and 2.794 cm). Non-parallelism of the ends was kept below .0012 inches(.0030 cm). Results of an investigation of the effects of non-parallelism on rock strength by Hoskins and Horino(1968, p. 6-7) indicate that non-parallelism in excess of this amount resulted in reduced fracture strength.

The finished cores have a true diameter of about 0.490 inches (1.245 cm). The cylindrical surface was given no special treatment. However, normal drilling procedure produced a smooth surface with no marked plucking or grooving. Measurement of the diameter of all cores to within .0001 inch(.00025 cm) indicated that the taper along the length was less than .001 inches(.0025 cm) in all cases.

After fabrication, the cores were placed in a drying oven for a period of one week or longer at an approximate temperature of 90°C. Controlled weighing experiments indicated that the weight loss resulting from drying occurred within the initial week, and the weight remained essentially constant after that.

When the deformation experiments were to be run, the test core was removed from the oven and allowed to cool. The length and diameter were then measured with a vernier micrometer to within .0001 inch(.00025 cm). The cores were jacketed and prepared for the experimental run.

During the initial stages of the study, the test specimens were

jacketed in cylindrical copper jackets one inch in length and .005 inch(.0127 cm) thick. The jacketed speciman was then placed in Tygon tubing of .062 inch(.157 cm) wall thickness which was wired to the end anvils to keep out the kerosene used as a confining pressure medium. During later stages, a jacketing technique was used employing one wrap of .006 inch(.0153 cm) polyethylene film covered by about three wraps of .009 inch(.0228 cm) polyethelene adhesive tape which forms an effective seal on the anvils.

At the completion of the test, the specimen was photographed and then immersed in epoxy resin.

(7) Data Processing

Values of load and displacement are picked from the X-Y recorder record. Care is taken to pick enough points so as to define the curves within close limits. These values and related constants are recorded and later punched on IBM cards.

The stress-strain relations for each test are determined using a computer program which corrects for the elastic distortion of the apparatus and provides true shortening based on an assumption of constant volume, and changing cross sectional area(i.e. that strain is uniformly distributed throughout the specimen).

In order to facilitate interpretation and comparison of several tests, additional subroutines have been added to the main program. One subroutine provides interpolated values of stress at 0.2% increments of strain. These values of stress are used in another program

to compute an average stress-shortening curve for a number of tests run under identical conditions. Values for each test are then compared to the computed average for every 0.2% of shortening and its deviation from the average is calculated and listed. This provides an index of the degree of variation between the tests. In general, all of the tests were found to deviate less than 10% from the average.

A plot program and subroutine plots the corrected stress-shortening curve for individual tests and for the computed average stress-shortening curve.

The programs were written by Mr. R. Rector with assistance from Mr. Julian Coward and are given in Rector(1970).

Appendix B

TABLE 8 SUMMARY OF TRIAXIAL COMPRESSION TESTS ON CALCAREOUS BLAIRMORE SANDSTONE, BLOCK 41, AT ROOM TEMPERATURE AND STRAIN RATES OF THE ORDER OF 10^{-4} PER SECOND.

Experiment Number	Confining Pressure Kb	Ultimate Strength Kb $\sigma_1 - \sigma_3$	Permanent Shortening Percent	Shortening at Ultimate Strength Percent	Total Shortening Percent	Fracture Angle to σ_1 Degrees	Deformational Mode
5D6	Atmospheric	2.28	5.81	.65	5.81	Irregular	Extensional fault
5D8	Atmospheric	2.34	4.44	.63	4.44	16 to 20	Extensional fault
5D9	Atmospheric	2.32	5.96	.62	5.96	4 to 20	Extensional fault
5D3	.25	2.98	3.18	.88	4.07	25 to 35	Brittle fault
5D4	.25	2.79	4.54	1.00	4.88	27 & 36	Brittle fault
5D5	.25	2.83	3.43	.99	3.95	20 & 32	Brittle fault
5D11	.25	2.96	7.64	1.11	8.63	27	Brittle fault
4D1	.50	3.53	3.53	1.09	3.89	30	Brittle fault
4D2	.50	3.69	3.18	1.16	3.92	30 to 35	Brittle fault
4D3	.50	3.42	15.95	1.06	17.06	27 & 27	Brittle fault
5D12	.50	3.45	7.91	1.27	9.01	32 & 33	Brittle fault
3D6	1.00	4.26	2.64	1.13	3.30	34	Brittle fault
3D7	1.00	4.35	2.64	1.13	3.13	38	Brittle fault
3D9	1.00	4.41	3.35	1.19	3.87	33	Brittle fault
4D12	1.00	4.30	2.44	1.72	4.18	38	Brittle fault
4D18	1.00	4.31	14.00	1.45	15.09	N.M.*	Brittle fault
5D1	1.00	4.18	5.54	1.57	6.61	37	Brittle fault
5D13	1.00	4.29	9.90	1.69	11.50	32 & 34	Brittle fault
4D16	1.25	4.70	5.54	1.81	6.98	31	Ductile fault
4D17	1.25	4.69	13.82	1.74	15.55	37 & 39	Ductile fault
4D4	1.50	5.02	13.85	2.46	15.54	-	Ductile fault
4D5	1.50	4.90	3.28	2.24	4.53	28 & 34	Ductile fault
4D6	1.50	5.00	8.74	2.38	10.26	34	Ductile fault
4D11	1.50	4.87	4.22	2.33	6.04	33	Ductile fault
4D13	1.50	5.05	19.82	2.08	22.06	30 & 32	Ductile fault

*N.M. = not measurable

Experiment Number	Confining Pressure Kb	Ultimate Strength Kb $\sigma_1 - \sigma_3$	Permanent Shortening Percent	Shortening at Ultimate Strength Percent	Total Shortening Percent	Fracture Angle to σ_1 Degrees	Deformational Mode
4D15	1.50	5.04	12.83	1.87	14.71	35 to 40	Ductile fault
3D11	2.00	5.28	12.68	2.59	15.02	35 to 38	Ductile fault
3D12	2.00	5.30	12.30	2.21	14.17	35	Ductile fault
3D13	2.00	5.42	13.05	2.41	14.99	37	Ductile fault
4D10	2.00	5.47	12.36	2.97	14.26	38	Ductile fault
4D14	2.00	5.62	11.71	2.42	13.78	40	Ductile fault
5D14	2.00	5.54	9.52	3.21	12.28	37	Ductile fault
5D15	2.00	5.57	5.09	2.54	7.32	-	Ductile fault
3D16	2.20	5.41	12.99	2.84	14.65	36	Ductile fault
3D18	2.20	5.58	2.14	2.73	3.69	-	Homogeneous
4D9	2.20	5.68	7.63	3.31	9.73	-	Homogeneous
5D2	2.40	5.76	11.84	3.14	14.30	35	Ductile fault
3D14	2.50	5.68	12.15	3.20	13.53	26 & 38	Ductile fault
5D16	2.50	5.88	11.81	3.99	14.61	-	Homogeneous
5D17	2.50	5.93	6.50	3.48	9.23	-	Homogeneous
5D19	2.50	5.89	17.57	3.24	20.26	34 & 38	Ductile fault
3D10	2.60	5.95	2.64	3.33	4.44	-	Homogeneous
3D19	2.60	5.55	11.49	3.62	14.12	-	Homogeneous
4D8	2.60	6.14	9.84	3.34	10.93	39	Ductile fault